From Data Integration to Retrofit Strategies: Bridging Urban Climate Models and Urban Building Energy Models

Von der Fakultät für Georessourcen und Materialtechnik der

Rheinisch-Westfälischen Technischen Hochschule Aachen

zur Erlangung des akademischen Grades einer Doktorin der Naturwissenschaften genehmigte Dissertation

vorgelegt von

Qinghua Yu, M.Sc.

Berichter: Univ.-Prof. Dr. rer. nat. Michael Leuchner

Univ.-Prof. Dr. Gerald Mills

Tag der mündlichen Prüfung: 20. Juli 2026

Diese Dissertation ist auf den Internetseiten der Universitätsbibliothek online verfügbar

Abstract

The building sector is a primary driver of global greenhouse gas emissions and a focal point for climate mitigation under the European Green Deal. To design effective decarbonization strategies and assess policy impacts, urban building energy models (UBEMs) have become indispensable tools for predicting energy demand across building stocks. However, traditional UBEMs frequently rely on standardized, non-local weather data, failing to account for the Urban Heat Island (UHI) effect and the localized thermal stress experienced during extreme heat events. Meanwhile, traditional urban climate models (UCMs) usually simplify building section, failing to account for anthropogenic heat emitted by buildings and radiation from building surfaces. This dissertation develops and applies an interdisciplinary and replicable workflow that links high-resolution urban geospatial data, archetype-based building semantics, building energy simulation, and microclimate modelling to address this limitation. The methodological core is a shared urban geographic archetype dataset that integrates GIS-derived urban morphology with TABULA-based building typological attributes and organizes them through a unified building identifier and standardized attribute schema, enabling consistent parameterization across modelling environments.

This dissertation uses a dense perimeter-block neighborhood in Düsseldorf (Germany) as a case study. The workflow links UBEM and UCM as interoperable executed components via the shared database. The urban building energy simulation tool CitySim has been used to quantify archetype-specific retrofit impacts on hourly heating and cooling demand and related performance indicators, while the 3D microclimate model ENVI-met has been used to assess pedestrian-scale summer thermal comfort under alternative building and greening scenarios. Furthermore, ENVI-met provides CitySim high-resolution microclimatic boundary conditions to refine indoor overheating assessments, thereby strengthening the coherence between outdoor and indoor evaluations during heatwave conditions.

The first study (UCM–UBEM integration via shared databases) shows that shared-database integration provides a practical pathway for UCM–UBEM interoperability by harmonizing geospatial data, meteorological inputs, and simulation parameters, particularly the misalignment of Levels of Detail (LoD) between models operating at different spatial scales. The unified identifier and standardized attribute schema enable transparent data exchange between the two modelling domains and improves reproducibility of neighborhood-scale simulations.

The second study (retrofit strategy support from the shared database) shows that the localized database enables consistent, archetype-specific retrofit scenario generation and neighborhood-scale comparison of building performance. Based on CitySim simulations, retrofit strategies can be assessed using indicator-driven evaluation of heating and cooling demand, energy intensity, emissions implications, and economic

metrics (e.g., annual energy costs, payback time, and net present value), supporting prioritization across building types under present and future climate conditions.

The third study (outdoor heat stress and controlling drivers under retrofit and greening) shows that scenario-based ENVI-met simulations quantify how building retrofit measures and neighborhood greening modify the magnitude and spatial difference of outdoor heat stress, evaluated via the Universal Thermal Climate Index (UTCI), during extreme heat conditions. Changes in UTCI are primarily governed by mean radiant temperature patterns (T_{mrt}) shaped by shading and surface radiation interactions, with secondary contributions from wind and humidity, and the local sensitivity depends on neighborhood morphology and ventilation constraints.

Overall, the dissertation provides a transferable integration logic for TABULA-covered contexts with comparable data availability and supports climate-robust retrofit planning that balances decarbonization objectives with heat-risk adaptation in compact urban neighborhoods.

Zusammenfassung

Der Gebäudebereich ist ein Hauptverursacher globaler Treibhausgasemissionen und ein zentraler Ansatzpunkt für den Klimaschutz im Rahmen des Europäischen Grünen Deals. Um wirksame Dekarbonisierungsstrategien zu entwickeln und politische Maßnahmen zu bewerten, sind städtische Gebäudeenergiemodelle (*Urban Building Energy Models*, UBEM) zu unverzichtbaren Werkzeugen für die Prognose des Energiebedarfs von Gebäudebeständen geworden. Traditionelle UBEMs stützen sich jedoch häufig auf standardisierte, nicht-lokale Wetterdaten und berücksichtigen weder den städtischen Hitzeinseleffekt (*Urban Heat Island*, UHI) noch die lokale thermische Belastung während extremer Hitzeereignisse. Gleichzeitig vereinfachen traditionelle Stadtklimamodelle (*Urban Climate Models*, UCM) üblicherweise die Gebäudestruktur und vernachlässigen sowohl die von Gebäuden emittierte anthropogene Wärme als auch die Strahlung von Gebäudeoberflächen. Die vorliegende Dissertation entwickelt und wendet einen interdisziplinären und replizierbaren Arbeitsablauf an, der hochauflösende städtische Geodaten, archetpbasierte Gebäudesemantik, Gebäudeenergiesimulation und Mikroklimamodellierung verknüpft, um diese Einschränkungen zu überwinden. Der methodische Kern ist ein gemeinsamer städtisch-geografischer Archetypen-Datensatz, der GIS-gestützte Stadtmorphologie mit typologischen Gebäudeattributen auf TABULA-Basis integriert und diese über eine einheitliche Gebäude-ID sowie ein standardisiertes Attributschema organisiert, was eine konsistente Parametrisierung über verschiedene Modellierungsumgebungen hinweg ermöglicht.

Als Fallstudie dient ein dicht bebautes Blockrandquartier in Düsseldorf (Deutschland). Der Arbeitsablauf verknüpft UBEM und UCM über die gemeinsame Datenbank als interoperable Komponenten. Das Gebäudeenergiesimulationswerkzeug CitySim wurde verwendet, um die archetypspezifischen Auswirkungen von Sanierungsmaßnahmen auf den stündlichen Heiz- und Kühlbedarf sowie entsprechende Leistungsindikatoren zu quantifizieren. Das 3D-Mikroklimamodell ENVI-met wurde eingesetzt, um den sommerlichen thermischen Komfort auf Fußgängerebene unter verschiedenen Gebäude- und Begrünungsszenarien zu bewerten. Darüber hinaus liefert ENVI-met hochauflösende mikroklimatische Randbedingungen für CitySim, um die Bewertung der indoor-Überhitzung zu verfeinern und dadurch die Kohärenz zwischen Außen- und Innenraumbewertungen während Hitzewellen zu stärken.

Die erste Teilstudie (UCM–UBEM-Integration über gemeinsame Datenbanken) zeigt, dass eine datenbankgestützte Integration einen praktischen Weg für die UCM–UBEM-Interoperabilität bietet, indem sie Geodaten, meteorologische Eingangsdaten und Simulationsparameter harmonisiert – insbesondere im Hinblick auf die Misfits der Detaillierungsgrade (*Levels of Detail*) zwischen Modellen, die auf unterschiedlichen räumlichen Skalen arbeiten. Die einheitliche Kennung und das standardisierte Attributschema ermöglichen einen transparenten Datenaustausch zwischen den beiden

Modellierungsdomänen und verbessern die Reproduzierbarkeit von Simulationen auf Quartiersebene.

Die zweite Teilstudie (Unterstützung von Sanierungsstrategien durch die gemeinsame Datenbank) zeigt, dass die lokalisierte Datenbank eine konsistente, archetypspezifische Generierung von Sanierungsszenarien und einen Vergleich der Gebäudeperformance auf Quartiersebene ermöglicht. Auf der Grundlage von CitySim-Simulationen können Sanierungsstrategien anhand einer indikatorengestützten Evaluierung von Heiz- und Kühlbedarf, Energieintensität, Emissionsauswirkungen und ökonomischen Kennzahlen (z. B. jährliche Energiekosten, Amortisationszeit und Kapitalwert) bewertet werden, was die Priorisierung nach Gebäudepfaden unter gegenwärtigen und zukünftigen Klimabedingungen unterstützt.

Die dritte Teilstudie (äußere Hitzebelastung und steuernde Einflussfaktoren bei Sanierung und Begrünung) zeigt, dass szenarienbasierte ENVI-met-Simulationen quantifizieren, wie Gebäudesanierungsmaßnahmen und Quartiersbegrünungen das Ausmaß und die räumliche Verteilung der äußeren Hitzebelastung – bewertet über den *Universal Thermal Climate Index* (UTCI) – unter extremen Hitzebedingungen verändern. Veränderungen des UTCI werden hauptsächlich durch Muster der mittleren Strahlungstemperatur bestimmt, die durch Verschattung und Strahlungswechselwirkungen der Oberflächen geprägt sind, mit sekundären Beiträgen von Wind und Luftfeuchtigkeit; die lokale Empfindlichkeit hängt dabei von der Morphologie des Quartiers und den Belüftungseinschränkungen ab.

Insgesamt bietet die Dissertation eine übertragbare Integrationslogik für von TABULA abgedeckte Kontexte mit vergleichbarer Datenverfügbarkeit und unterstützt eine klimarobuste Sanierungsplanung, die Dekarbonisierungsziele mit der Anpassung an Hitzerisiken in kompakten städtischen Quartieren in Einklang bringt.

Table of Contents

Abstract ..... **i**
Zusammenfassung ..... **iii**
Table of Contents ..... **v**
List of Figures ..... **ix**
List of Tables ..... **xi**
1. Introduction **1**
1.1 Research background and objectives 1
1.2 Dissertation structure 5
2. Study area **7**
2.1 Building energy and climate adaptation challenges in Germany 7
2.2 City of Düsseldorf 7
2.3 Research area: neighborhoods in Flingern, Düsseldorf 9
3. Methods **11**
3.1 Conceptual framework and workflow 11
3.2 Data sources and shared urban database 11
3.2.1 Building typology framework: TABULA archetypes 12
3.2.2 Spatial integration, unique identifiers, and multi-scale alignment 13
3.3 UBEM: CitySim 13
3.4 UCM: ENVI-met 14
3.5 Linking strategy and analyses 16
3.5.1 Linking strategy (database-centered, one-way/offline) 16
3.5.2 Analytic framework: scenario comparison, driver attribution, and economic indicators 17
4. Exploring the integration of urban climate models and urban building energy models through shared databases: a review **21**
Highlights 22
Abstract 23
Keywords 23
4.1 Introduction 24
4.2 Methodology 28

4.3 Urban building energy modelling approaches 29
4.3.1 UBEM tools and workflow 29
4.3.2 UBEM tools by scale 34
4.4 Urban climate models 35
4.5 Integrating UBEMs and UCMs 39
4.5.1 Exploring applications of UBEMs in climate-responsive urban practices 40
4.5.2 Utilizing shared databases for effective integration of UBEMs and UCMs 40
4.5.3 Challenges in multi-scale model integration 42
4.5.4 Computational trade-offs and scalability 44
4.5.5 Advantages and limitations 44
4.6 Conclusion 45
Declaration of Competing Interest 46
Acknowledgements 46
5. Developing an urban geographic archetype dataset to support energy retrofit strategy on residential buildings in Düsseldorf, Germany 47
Highlights 48
Abstract 49
Keywords 49
5.1 Introduction 51
5.2 Methodology 53
5.2.1 Georeferenced building datasets and study area 54
5.2.2 Construction of a CityGML database for UBEM 58
5.2.3 Climate data and climate indicators for energy demand 59
5.2.4 CitySim experiments 60
5.3 Results and discussion 62
5.3.1 Prioritization of retrofitting efforts 62
5.3.2 Financial and carbon reduction benefits of retrofitting 65
5.3.3 The role of urban effects and climate in retrofitting 69
5.4 Conclusion 70
Declaration of Competing Interest 71

Acknowledgements 71
5.5 Supporting information 72
6. Summer thermal consequences of EU retrofit strategies: an integrated microclimate and indoor comfort study in Düsseldorf 77
Highlights 78
Abstract 79
Keywords 79
6.1 Introduction 81
6.2 Methodology 85
6.2.1 Study area 85
6.2.2 Outdoor microclimate simulation with ENVI-met 86
6.2.3 Scenario design 89
6.2.4 Outdoor–Indoor simulation using a one-way ENVI-met–CitySim integration 89
6.2.5 Analysis methodology 90
6.3 Results and discussion 92
6.3.1 Necessity of realistic building dataset 92
6.3.2 Indoor thermal performance under heatwave conditions 94
6.3.3 Overview of thermal comfort across scenarios 95
6.3.4 Scenario-specific impacts on outdoor thermal comfort 98
6.3.5 Regression analysis of climatic drivers affecting UTCI 99
6.3.6 Localized impacts of microclimate variables on UTCI 100
6.4 Conclusion 102
Declaration of Competing Interest 103
Acknowledgements 103
7. Synthesis and outlook 103
7.1 Synthesis of findings against the research questions 104
7.2 Overall contributions 105
7.3 Limitations 105
7.4 Outlook and future work 107
7.4.1 Towards bidirectional UCM–UBEM coupling 107
7.4.2 Field measurement and validation work 107

7.4.3 Broader scenario space and decision support extensions 108
8. Danksagung/Acknowledgments 109
References 111

List of Figures

Figure 2.1 Administrative Map of Düsseldorf (10 administrative boroughs and their 50 quarters) and Location of Major Rivers. 9
Figure 2.2 Study area overview: city-scale location and neighborhood-scale morphology. 10
Figure 3.1 Database-driven integrated framework for urban climate and energy. 11
Figure 3.2 CitySim workflow. 14
Figure 4.1 Buildings, their structure and influence on urban climate, highlighting the key roles of building geometry and material properties in altering local microclimates. (Futcher et al., 2013; Li et al., 2020; Sadineni et al., 2011; Santamouris et al., 2013; Vahmani et al., 2022). 25
Figure 4.2 The research methodology used in this paper. 28
Figure 4.3 Generalized methodology of the UBEMs workflow based on the existing literature (Hong et al., 2020). 29
Figure 4.4 Five Levels-of-Detail (LoD) provided by CityGML in building modelling illustrated by an example building in the city of Aachen, Germany. Own representation after Löwner et al. (2013). 30
Figure 4.5 Different spatial scales and corresponding models based on Oke et al. 37
Figure 4.6 Shared Database Framework that supports different climate models and UBEMs (Ali et al., 2021; Oke et al., 2017). 42
Figure 5.1 Workflow used in this study. 53
Figure 5.2 The distribution of buildings in the study area. 55
Figure 5.3 Examples of Single-Family House (SFH), Terraced House (TH), Multi Family Houses (MFH), and Apartment Blocks (AB) built in Düsseldorf in different periods (see Table 5.1 for details). 57
Figure 5.4 The building at Ackerstraße 168a. 57
Figure 5.5 Monthly heating degree days (HDD) and cooling degree days (CDD) in 2020, 2050 and 2100 and corresponding monthly mean air temperature data. 60
Figure 5.6 Annual average heating and cooling energy intensity (kWh/m²) for target residential buildings. 63
Figure 5.7 Prioritization map of potential residential retrofit. 68
Figure 6.1 The location of the research area and meteorological station in Düsseldorf (left). Location of the city and North Rhine-Westphalia in Germany (right). 85
Figure 6.2 Different land covers are divided into seven classes, namely, asphalt red pavement, asphalt pavement, single stones pavement, concrete pavement, building, grass and soil. 86
Figure 6.3 Surface Synoptic Weather Map during the July 2022 Heatwave in Europe (00 UTC, July 19). 87
Figure 6.4 The location of six observation points. The land cover map is consistent with **Figure 6.2**. 92

Figure 6.5 UTCI difference map at 14:00 CET, 1.5m height. 93
Figure 6.6 Hourly average indoor temperatures for all buildings in their existing and retrofit states on July 19, 2022. 95
Figure 6.7 Hourly average UTCI values (06:00–22:00 CET). 97
Figure 6.8 The 14:00 CET UTCI map of the study area (1.5m height) of Scenario A (left) and Scenario B (right). 97
Figure 6.9 UTCI values (A) alongside variations in T_{mrt} (B) across four scenarios at 14:00 CET for six observation points within the study area. 101

List of Tables

Table 2.1 Climate normal statistics (1991–2020) and thermal indices for Düsseldorf (Germany). 8
Table 4.1 Weather file sources, building geometry datasets and thermal modelling for common UBEM tools. 31
Table 4.2 Summary of UBEM models' outputs. 33
Table 4.3 Summary of UBEM tool scales and main applications. 35
Table 4.4 Different spatial scales and model input data. 38
Table 4.5 Representative UCMs, their typical outputs and LoD needs. 39
Table 4.6 Applicated LoDs for UBEMs and UCMs. 43
Table 5.1 The number and population distribution of different buildings in the study area are summarized (Düsseldorf Census, 2020). 58
Table 5.2 Total annual heating demand (H in kWh) in original (O) and refurbished (R) buildings under different climate scenarios in 2020 and 2050. 65
Table 5.3 Annual CO_2 emissions (kg/m²·a) total annual CO_2 emission reduction (Mt/a), and the annual energy costs (€/ (m^2. a)) for residential building types in original (O) and refurbished (R) states. 67
Table 5.4 Annual energy savings (€/(m²·a)), annual CO_2 saving, (€/(m²·a)), simple payback time (years), NPV (€/m²), and cumulative CO_2 emissions incurred between 2020 and 2025 as a result of delayed retrofitting for each building type. 69
Table 5.5 Specific constructions of eight common Tabula residential building types and subtypes in the study area according to Tabula WebTool (Tabula WebTool, 2023). 72
Table 5.6 Specific HVAC systems of eight common and refurbished Tabula residential building types and subtypes in the study area according to Tabula WebTool (Tabula WebTool, 2023). 73
Table 5.7 Specific constructions of eight refurbished Tabula residential building types and subtypes in the study area according to Tabula WebTool (Tabula WebTool, 2023). 75
Table 6.1 Thermophysical (λ, ρ, c_p) and radiative (α or albedo A, ε) properties of the main envelope and surface materials. 88
Table 6.2 ENVI-met simulated average values of climatic parameters across four scenarios at 14:00 CET in the study area. 96
Table 6.3 Paired t-Test results for UTCI differences across urban design and retrofit scenarios at 14:00 CET, with BH correction. 98
Table 6.4 Ridge regression analysis of urban design and climatic factors impacting UTCI at 14:00 CET across different scenarios. 99

1. Introduction

1.1 Research background and objectives

Cities are the frontline of global climate action, serving as the key nexus for addressing both energy transition and climate adaptation challenges (Sufyanullah et al., 2022).

As the centers of population and economic activity globally (Esfandi et al., 2024; Goerzen et al., 2024), urban areas are undergoing unprecedented growth. According to the International Energy Agency (International Energy Agency, 2024), more than half of the global population now lives in urban areas, a proportion projected to reach nearly 70% by 2050. This rapid expansion, particularly in emerging markets and developing economies (EMDEs), intensifies global energy demand and carbon mitigation challenges.

Consequently, cities are the hubs of production, transportation, and consumption. They are estimated to consume around 75% of global energy and are responsible for approximately 70% of total greenhouse gas (GHG) emissions (Ullah et al., 2024; International Energy Agency, 2024). Urbanization since 2015 alone has driven urban-related emissions to a record high of nearly 29 billion tons of CO_2 (International Energy Agency, 2024). This trend indicates that any action towards global sustainable development and achieving climate neutrality objectives cannot be separated from cities as the key vehicle.

In Europe, the path toward climate neutrality is guided by the European Green Deal, which legally commits all Member States to achieving net-zero greenhouse gas emissions by 2050 (Fetting, 2020). To support this ambition, the “Fit for 55” package and the recast Energy Performance of Buildings Directive establish stringent interim targets (European Parliament and Council, 2024), such as a 55% reduction in emissions by 2030 compared to 1990 levels and the introduction of Minimum Energy Performance Standards (MEPS) for the existing building stock (European Commission, 2021). Given that buildings account for about 40% of final energy consumption and 36% of CO_2 emissions in the EU, energy retrofitting and urban scale efficiency improvements are central to the European climate agenda (Mondal et al., 2024). These policy frameworks emphasize the integration of energy-efficient renovation, renewable energy deployment, and data-driven urban energy modelling as critical factors for achieving both decarbonization and climate resilience in European cities.

However, this rapid urbanization and high population density simultaneously intensify a wide range of local environmental challenges, demanding urgent climate adaptation strategies.

As cities expand both horizontally and vertically, their growing spatial footprint and built-up density significantly alter surface energy exchanges and disrupt natural ventilation patterns (Oke et al., 2017). Urban areas exhibit highly different surface and

structural characteristics that distinguish them from their rural surroundings (Masson et al., 2020). The complex configuration of buildings, streets, and open spaces forms a three-dimensional urban canopy layer, where variations in height, density, aspect ratio, and street orientation shape the urban geometry (Ching, 2013). This geometry, frequently quantified by the Sky View Factor (SVF), governs solar radiation trapping during the day and restricts longwave radiative cooling at night, while simultaneously altering localized wind flow and shading patterns (Mills, 2014). The predominance of impervious materials with low reflectivity and high heat capacity, such as asphalt and concrete, enhance heat storage during the day and delays nighttime cooling (Mohajerani et al., 2017). In contrast, the limited presence of vegetation and permeable surfaces reduces evapotranspiration, further amplifying sensible heat fluxes (Abdulateef and Al-Alwan, 2022). Together, these morphological and material features determine the energy balance and ventilation efficiency of the city, shaping its distinct microclimatic conditions (Mills, 2014).

These changes have led to an increasing demand for energy, particularly for space cooling in buildings, and have magnified local climate risks, including the urban heat island (UHI) effect (Yang et al., 2016), deteriorating air quality due to pollutant accumulation (Singh et al., 2020), and increased exposure to extreme weather events such as heatwaves and heavy rainfall (Hashemi et al., 2024).

These local environmental challenges do not only represent physical phenomena but also translate directly into a multitude of human living problems that threaten public health, social equity, and economic stability (Jackson, 2003; Shahmohamadi et al., 2011). Specifically, increased temperatures from the UHI effect and frequent heatwaves increase the incidence of heat-related illnesses, hospitalizations, and excess mortality, particularly among vulnerable populations (e.g., the elderly, children, and those with pre-existing conditions) (Cleland et al., 2023). Statistically, Europe as a whole experienced an estimated 61,672 heat-related excess deaths between 30 May and 4 September, with Germany alone accounting for approximately 8,173 excess fatalities during the summer of 2022 (Ballester et al., 2023). Meanwhile, increased ambient temperatures combined with reduced natural ventilation within dense urban canyons impede the dissipation of heat and moisture, severely impairing outdoor and indoor thermal comfort and leading to decreased livability of public spaces (Miao et al., 2023).

Buildings are central to these interactions. They are both the dominant consumers of energy and major sources of anthropogenic heat, forming a critical feedback loop between energy use and urban climate (Hu et al., 2022; Nik et al., 2021). Building geometry (height, density) shapes local airflow and solar trapping, while their operational energy demand directly responds to local climate conditions (Ahmadian et al., 2021; Zhang et al., 2023). Furthermore, the thermal properties of construction materials play a fundamental role in the urban energy balance (Santamouris et al., 2013),

influencing microclimate through their capacity for solar absorption (albedo), heat storage, and re-radiation (thermal mass and emissivity) (Zhong et al., 2021).

To address these interconnected issues, urban researchers and planners rely heavily on simulation tools that capture energy performance and climate dynamics at multiple spatial and temporal scales. Two major strands of modelling have evolved to meet these needs: Urban Building Energy Models (UBEMs) and Urban Climate Models (UCMs) (Yu et al., 2025a). Despite their shared relevance, UBEMs and UCMs have historically developed as complementary yet largely disconnected frameworks for analyzing urban energy use and climate processes (D'Oca et al., 2018).

UBEMs simulate the thermal behavior and energy demand of large groups of buildings by describing their geometry, construction typology, occupancy patterns, HVAC systems, and operational schedules (Worthy et al., 2025). They are widely used to evaluate retrofit measures, quantify energy and emissions savings, and support urban scale decarbonization strategies (Kong et al., 2023). UCMs, in contrast, focus on the physical processes governing urban climates, including radiation exchange, heat fluxes, wind flow, shading, and air temperature (T_a) distributions within the urban canopy layer (Garuma, 2018). These models are fundamental for assessing urban heat island intensity, outdoor thermal comfort, air quality, and exposure to extreme climate events (He et al., 2025).

Although UBEMs primarily serve the urban energy domain and UCMs the meteorological domain, the two frameworks broadly share consistent input data: both depend on weather data and surface parameter information. Yet, this overlap highlights a key methodological gap. UBEMs commonly rely on oversimplified meteorological inputs that do not capture intra-urban climate variability, while UCMs often rely on simplified building representations and may neglect anthropogenic heat emissions altogether (Krelling et al., 2024; Wang et al., 2024). Yet buildings both consume energy and release heat, mediating a critical feedback loop between indoor energy use and outdoor climatic conditions (Yang et al., 2024).

Recognizing the limitations of a siloed approach, the research community has increasingly focused on the integration between UCMs and UBEMs. UCMs require information on anthropogenic heat release from buildings (the output of UBEMs), and UBEMs require realistic, localized climate data (the output of UCMs) for accurate predictions (Yu et al., 2025a). Integrating these models enables more robust and realistic assessments of how climate change influences energy demand and how modifications to the building stock reshape the urban thermal environment. Such integration provides a stronger foundation for climate adaptation planning, decarbonization strategies, and the development of energy-efficient, climate-resilient cities.

Based on those considerations, the general goal of this dissertation is to contribute to the knowledge of model connection by developing a shared database. It harmonizes geometric, semantic, and meteorological information and produces model-ready inputs for both UCMs and UBEMs within the same study area. This dissertation examines how neighborhood-scale microclimate heterogeneity modifies building energy responses under heat stress, and how retrofit decisions alter both indoor conditions and outdoor exposure, using one neighborhood in the city of Düsseldorf, Germany, as a case study. In the present thesis, the integration is implemented as a database-centered, one-way workflow: UCM and UBEM simulations are run using consistent inputs and their outputs are subsequently linked through post-processing and statistical analyses to quantify indoor–outdoor relationships and their spatial variability.

While the current work does not implement an iterative two-way coupling, the proposed database framework provides a clear pathway for future extensions, including through developed shared database, achieve bidirectional coupling between UCMs and UBEMs. Meanwhile, three general research questions are formulated, which are approached in three studies within this dissertation, each with more specific research questions, hypotheses or objectives:

(1) How can urban climate models and urban building energy models integrate through shared databases?

(2) How does the shared database support neighborhood residential building energy retrofit strategy?

(3) To what extent do retrofit measures and neighborhood greening modify outdoor heat stress and its controlling drivers at the neighborhood- scale?

The dissertation highlights that using shared databases is a promising solution. This approach allows for a flexible, scalable, and repeatable data exchange between the models, moving beyond the limitations of traditional direct coupling methods. This represents a fundamental shift toward a structured, data-driven framework for urban modelling.

This dissertation comprises three peer-reviewed studies, each addressing a specific component of the overarching research problem.

The first study establishes the conceptual and methodological foundation by developing a database-centered integration framework between UBEMs and UCMs. Building on this foundation, the second study applies the shared database to evaluate the energy and economic implications of retrofit strategies at the neighborhood- scale. Extending this analysis, the third study investigates how these retrofit strategies interact with urban

microclimate processes and influence outdoor thermal comfort and its controlling drivers. Together, these studies form a coherent progression from methodological development to applied evaluation and process-level understanding, enabling an integrated assessment of indoor–outdoor interactions in urban environments. All these research were partly co-funded under the Excellence Strategy of the Federal Government and the Länder (Project SFBLE003 TRUKLIB).

1.2 Dissertation structure

The remainder of this dissertation is organized into seven chapters. Chapter 2 provides an overview of the case study area (Düsseldorf neighborhood). Chapter 3 provides details of the key modelling and database methodologies employed, such as representative UBEMs and UCMs, and relative mathematical statistical methods.

The core research is presented in three subsequent chapters, each addressing a formulated Research Question (RQ):

Chapter 4: Addresses RQ 1 by proposing a novel framework for integrating UCMs and UBEMs through a shared database. This work has been published in the Journal of Theoretical and Applied Climatology (Yu et al., 2025a).

Chapter 5: Addresses RQ 2 by utilizing the shared database framework to evaluate the impact of EU residential building retrofit strategies on neighborhood-scale energy performance, supporting decarbonization efforts. This work has been published in Energy Reports (Yu et al., 2025b).

Chapter 6: Addresses RQ 3 by quantifying the impact of building retrofits and neighborhood greening on the surrounding microclimate and human thermal comfort, leveraging UCM simulations and offline linkage to UBEM outputs (Yu et al., 2026).

Finally, Chapter 7 provides a synthesis of the findings, discusses the overall contributions, identifies limitations, and offers an outlook for future urban modelling research.

2. Study area

2.1 Building energy and climate adaptation challenges in Germany

The German building sector represents a critical leverage point for national and European climate mitigation goals. In Germany, residential buildings account for nearly 25% of total final energy consumption, with space heating historically dominating domestic energy use (over 65%) (BMWK, n.d.). A central structural challenge of the German housing stock is its age distribution: approximately 70% of all residential buildings were constructed before the implementation of the first thermal insulation ordinance (Wärmeschutzverordnung) in 1977. These uninsulated or minimally insulated structures exhibit high envelope heat losses and rely predominantly on fossil-fuel heating systems (gas and oil boilers) (Loga et al., 2016; TABULA WebTool, 2024). Under the German Federal Climate Change Act (Klimaschutzgesetz) and the recast EU Energy Performance of Buildings Directive (EPBD), Germany is legally committed to achieving a climate-neutral building stock by 2045 (Bundesregierung, 2024; European Parliament and Council, 2024).

Simultaneously, temperate Central European regions like Germany are facing intensifying climate risks (Lee et al., 2023). While winter cold stress has historically dictated building energy standards, recent climate projections and extreme events, such as the severe European heatwaves of summer 2022, highlighting a growing vulnerability to summer heat stress (Kornhuber et al., 2020). Because active air conditioning remains rare in German residential dwellings, standard insulation measures optimized strictly for winter heat retention can trap internal heat gains during extreme hot spells (Porritt et al., 2012; Vellei et al., 2017). Consequently, evaluating neighborhood-scale energy performance and urban microclimate interactions requires integrated assessment frameworks capable of balancing winter decarbonization objectives with summer thermal resilience (Yu er al., 2026).

2.2 City of Düsseldorf

Düsseldorf is situated in western Germany on the Lower Rhine, on the eastern (right) bank of the Rhine River, within the Rhine–Ruhr region. It is the seventh-largest city in Germany (~620,000 inhabitants) with 10 administrative boroughs (Figure 2.1) (City of Düsseldorf, 2023a). The city lies in a lowland setting with generally gentle relief shaped by fluvial processes, where the Rhine floodplain and associated terraces influence local topography, groundwater conditions, and soil moisture (Minister für Umwelt, Raumordnung und Landwirtschaft des Landes Nordrhein-Westfalen, 1989).

Climatically, Düsseldorf is characterized by a temperate oceanic regime with prevailing westerly circulation, relatively mild winters, and moderately warm summers. Seasonal variability is distinct, with a mean annual 2-m T_a of approximately 11 °C during the standard 1991–2020 climate-normal period (City of Düsseldorf, 2022). Table 2.1 shows

the normals for the Düsseldorf–Südfriedhof station (51°18′ N, 06°46′ E; 36.6 m a.s.l.). On average, the city experiences on average around 43 summer days per year ($T_{max} \geq 25$ °C) and about 10 hot days per year ($T_{max} \geq 30$ °C), with most occurrences concentrated in July and August. Cold-season conditions remain relevant, with an average of roughly 52 frost days per year ($T_{min} < 0$ °C), while interannual variability under differing synoptic patterns can lead to substantially higher counts in individual years (DWD, n.d.; NOAA, 2023).

Table 2.1 Climate normal statistics (1991–2020) and thermal indices for Düsseldorf (Germany).

Month	Jan	Feb	Mar	Apr	May	Jun	Jul	Aug	Sep	Oct	Nov	Dec	Year
T_{mean} (°C)	3.5	4.0	6.9	10.5	14.3	17.3	19.4	18.9	15.2	11.2	7.1	4.2	11.0
Precip. (mm)	61.5	56.5	54.1	46.4	61.1	65.7	73.2	77.0	60.3	61.2	63.8	70.0	750.7
RH_avg(%)	81.6	78.6	73.5	68.2	68.5	69.3	68.8	70.8	76.5	80.5	83.6	84.3	75.4
Summer days	0.0	0.0	0.0	1.2	4.3	8.3	13.7	11.5	3.7	0.3	0.0	0.0	43.0
Hot days	0.0	0.0	0.0	0.0	0.4	1.7	4.1	3.6	0.4	0.0	0.0	0.0	10.2
Frost days	12.5	11.2	8.0	3.0	0.2	0.0	0.0	0.0	0.0	1.3	4.9	10.9	52.1
Iced days	2.3	1.5	0.1	0.0	0.0	0.0	0.0	0.0	0.0	0.0	0.3	1.6	5.7

*T_{mean}: Mean temperature at 2 meters above the ground; Precip: Average monthly precipitation; RH_avg: Average monthly relative humidity;
Summer day: Days with a maximum temperature of >= 25 °C;
Hot days: Days with a maximum temperature of >= 30 °C;
Frost days: Days with a minimum temperature of < 0 °C;
Iced days: Days with a maximum temperature of < 0 °C

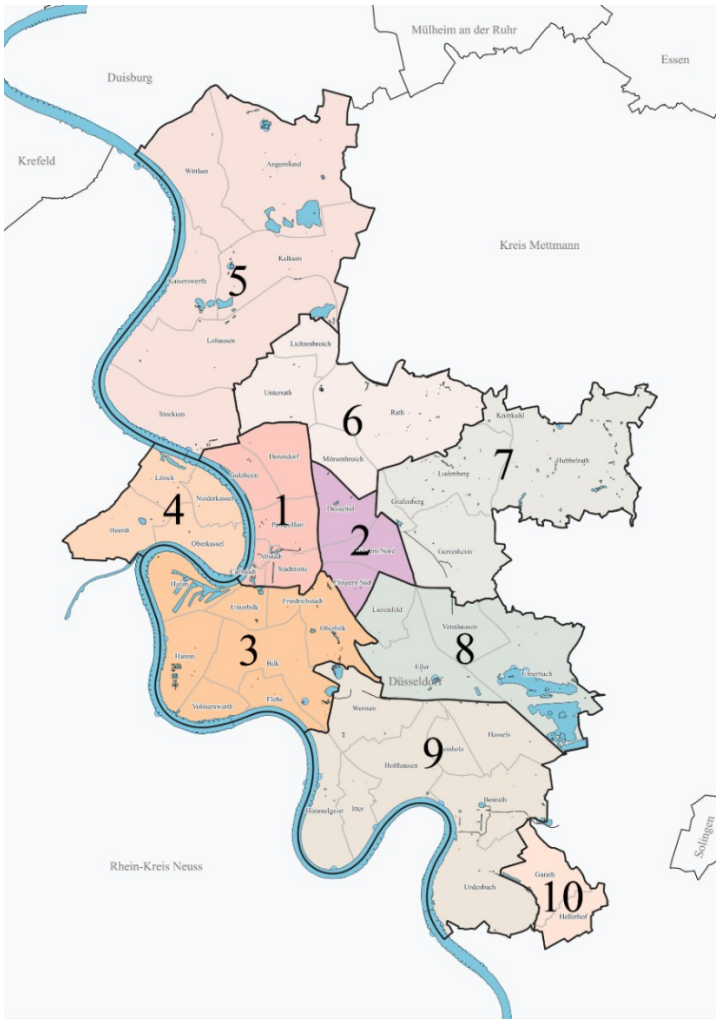


Figure 2.1 Administrative Map of Düsseldorf (10 administrative boroughs and their 50 quarters) and Location of Major Rivers.

2.3 Research area: neighborhoods in Flingern, Düsseldorf

To translate the city-scale planning and morphological context into a neighborhood-scale assessment of microclimate–building interactions, this study focuses on neighborhoods in Düsseldorf–Flingern. Flingern was selected because it represents a common urban residential typology of the "typical German neighborhood", where late-19th/early-20th-century perimeter-block development coexists with post-war infill and ongoing functional mixing (Hofmeister, 2003).

The study area covers 22 representative urban blocks spanning approximately 34.26 ha, accommodating over 10,000 residents (Figure 2.2).

The area is characterized by a heterogeneous residential building stock arranged along street fronts to form continuous perimeter blocks (*Blockrandbebauung*). These blocks feature enclosed or semi-enclosed courtyards and narrow street canyons, creating strong radiation and aerodynamic contrasts across short distances (Figure 2.2). In particular, the compact block layout and significant height gradients, typically featuring taller

buildings along major streets and lower-rise structures toward block interiors, produce spatially distinct shading patterns, longwave radiative exchange, and wind exposure. At the same time, the neighborhoods have mixed function patterns, where residential uses coexist with small workshops, offices and public facilities. This morphological and functional complexity provides an ideal setting for interpreting the relationship between neighborhood-scale microclimate variability and building energy responses.

This morphology creates strong edge–interior contrasts in shading and radiative exchange. On the one hand, these microclimatic variations govern the outdoor radiative environment and human thermal comfort, which is commonly evaluated using the mean radiant temperature (T_{mrt}). On the other hand, they modulate building surface solar exposure, exterior heat fluxes, and space-conditioning energy demand. Furthermore, enclosed courtyards can restrict natural ventilation and impede nighttime longwave radiation loss, thereby exacerbating heat retention and increasing the risk of indoor overheating during extreme heatwaves.

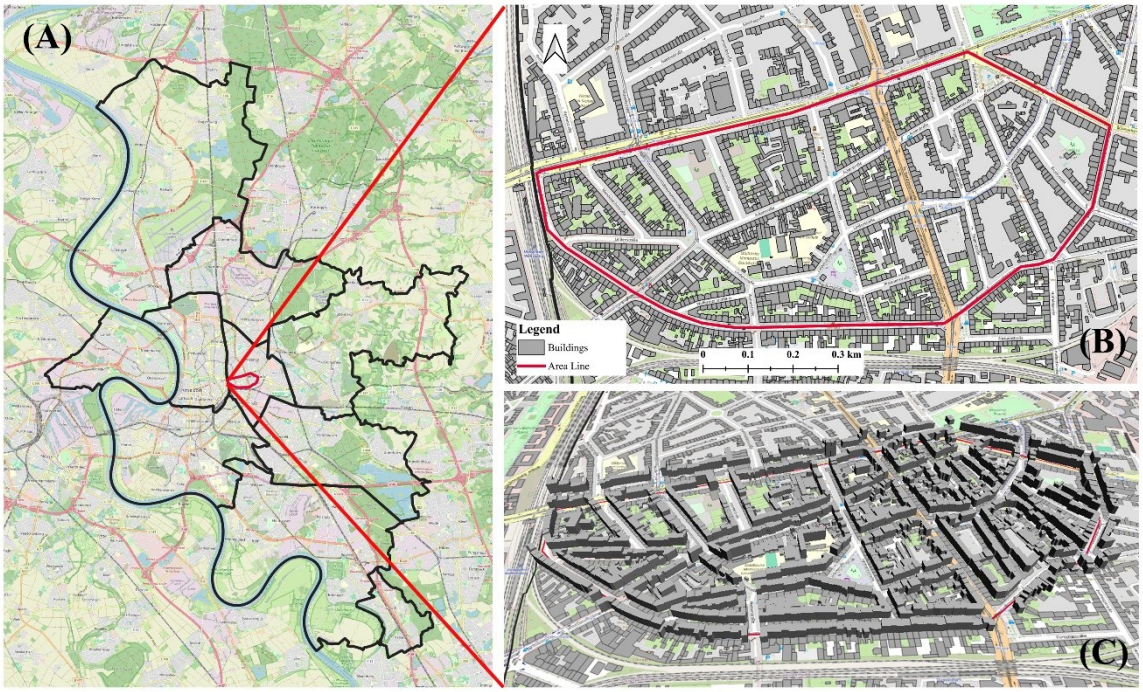


Figure 2.2 Study area overview: city-scale location and neighborhood-scale morphology.

Notes: (A) Location of the case-study area within Düsseldorf and its administrative boundaries; the red polygon indicates the selected neighborhoods in the Flingern district. (B) Detailed map of the study area boundary and surrounding urban fabric. (C) 3D visualization of the building heights and block typology. Basemap: OpenStreetMap.

3. Methods

3.1 Conceptual framework and workflow

This dissertation investigates the relationship between neighborhood-scale outdoor microclimate conditions and building energy responses, with urban form acting as one of the key controlling factors. A shared urban database is used as an intermediary layer to harmonize common inputs and to generate consistent, model-ready datasets for UCMs and UBEMs within the same study area. Figure 3.1 shows the overall workflow consists of four steps: (1) compile and standardize common urban and meteorological data across different models into a shared database (e.g., geometry, archetype-linked building parameters, surface descriptors, and weather forcing); (2) generate model-specific inputs from the shared database for both UCM and UBEM within the same study area; and (3) run UCM and UBEM simulations using these harmonized inputs under the different scenarios; and (4) link model outputs to quantify indoor–outdoor relationships and interpret the role of urban form through post-processing and statistical analyses.

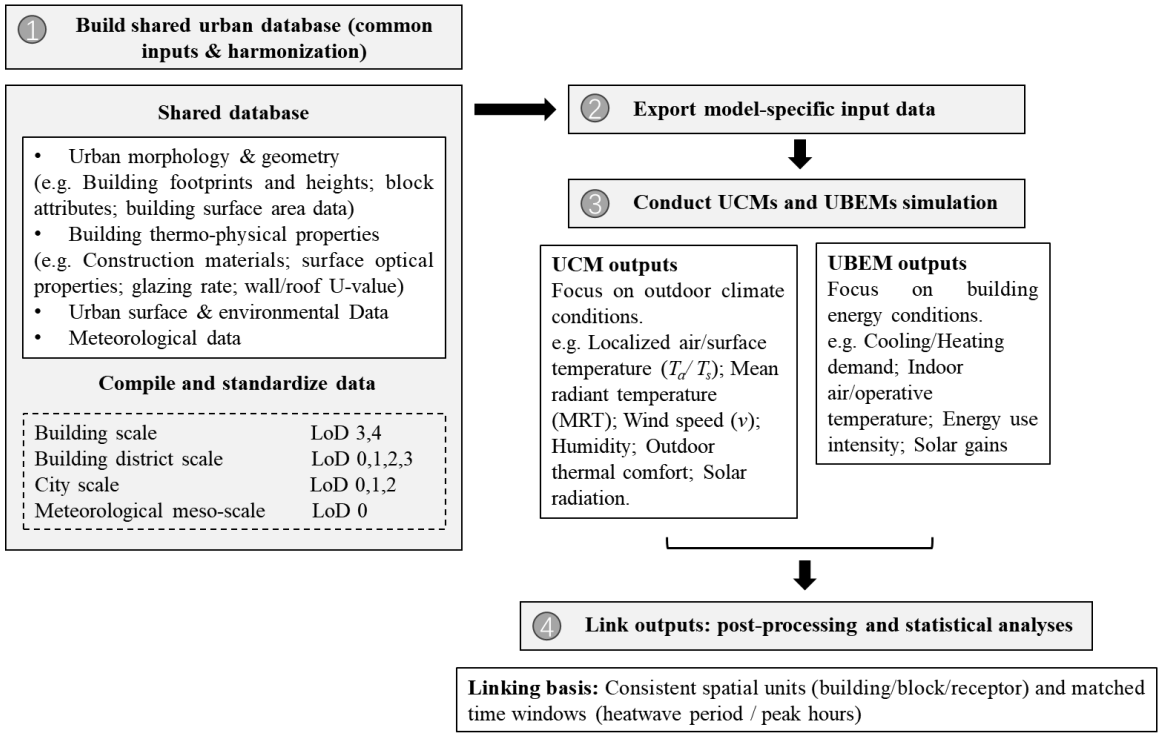


Figure 3.1 Database-driven integrated framework for urban climate and energy.

Note: *Database-centered, one-way integration; iterative two-way model coupling will be implemented for future work.*

3.2 Data sources and shared urban database

A shared urban database was developed to provide consistent geometric and semantic inputs for both UCM and UBEM applications. The database integrates: (1) 3D building geometry (e.g., CityGML LoD1/LoD2 footprints and height attributes), (2) building

typology information required for energy modelling (e.g., construction period, use type, system and archetype mapping based on the TABULA (Typology Approach for Building Stock Energy Assessment) framework) (Tabula WebTool, 2023), (3) land-surface descriptions relevant for surrounding environment (e.g., impervious/vegetated fractions and surface material categories, where applicable), and (4) meteorological data.

3.2.1 Building typology framework: TABULA archetypes

To address the common challenge of missing building-specific thermophysical data across urban building stocks, this dissertation incorporates the TABULA framework into the shared urban database (Loga and Diefenbach, 2016). Developed under the European Intelligent Energy Europe program, TABULA establishes a standardized, harmonized taxonomy for categorizing residential building stocks across 20 European countries based on national construction traditions and legislative energy standards (Tabula WebTool, 2023).

In the German context, this study establishs a two-dimensional classification matrix defined by two core parameters according to Germany Tabula:

(1) Construction Period Classes (Building age): Ranging from historical structures built before 1918 (Class 1) to contemporary buildings constructed post-2016 (Class 8), capturing the sequential evolution of national thermal insulation ordinances (Wärmeschutzverordnung and EnEV) (Yu et al., 2025b).

(2) Building Size Classes (Subtypes): Categorized into Single-Family Houses (SFH), Terraced Houses (TH), Multi-Family Houses (MFH), and Apartment Blocks (AB) (Tabula WebTool, 2023).

For each specific archetype combination (e.g., pre-1918 Multi-Family House [1 MFH] or 1949–1957 Terraced House [3 TH]), TABULA supplies comprehensive layer-by-layer material attributes and thermophysical parameters (Yu et al., 2025b). For each archetype, TABULA provides envelope properties, including the thermal transmittance of walls, roofs and ground slabs, window g-values, glazing transmittance and frame fractions, as well as energy-system parameters such as operational efficiencies, distribution losses and primary energy carriers (Tabula WebTool, 2023).

Crucially, this study defines two distinct physical states for each archetype: the Original (Non-refurbished) State, representing baseline construction conditions at the time of build, and the Refurbished (Standard Refurbishment) State, which models standardized energy efficiency upgrades (e.g., external thermal insulation compound systems, top-floor ceiling insulation, and multi-pane low-E glazing) aligned with national retrofit guidelines (Tabula WebTool, 2023).

3.2.2 Spatial integration, unique identifiers, and multi-scale alignment

All geospatial and semantic datasets in the shared database were transformed into a consistent coordinate reference system (UTM Zone 32N / ETRS89) and underwent topological quality control to ensure closed polygons, boundary consistency, and valid height attributes.

To enable seamless inter-model linkage, a core feature of the database design is the assignment of a unique, persistent building identifier (building ID) to every entity. This building ID is retained across all exported input files and simulation runs, serving as the relational key that binds GIS spatial footprints, TABULA-derived thermophysical attributes, UBEM energy simulation outputs, and UCM surface flux parameters at the individual building level.

In addition, the database follows a clear multi-scale/LoD alignment principle, where the level of geometric and semantic detail is tailored to the target model while preserving traceability to the common source dataset.

Note: *Detailed database design for Düsseldorf case study is provided in Chapter 5.*

3.3 UBEM: CitySim

Chapter 4 provides a review of UBEMs common workflow and compared advantages and limitations of widely used UBEM tools. Based on this, this dissertation adopts CitySim as the UBEM platform for neighborhood-scale simulations of building thermal performance and energy demand.

CitySim was selected primarily for its ability to simulate large building stocks efficiently while explicitly representing inter-building shading and radiative interactions, which are particularly important in compact perimeter-block morphologies (Blockrandbebauung) such as those in Düsseldorf–Flingern (Robinson et al., 2009). In dense urban fabrics, mutual shading and shortwave/longwave exchanges between façades can substantially alter solar gains and heat losses and consequently influence both indoor thermal conditions and heating/cooling demand. CitySim resolves these effects to the greatest extent possible at the neighborhood-scale without requiring computationally intensive building-by-building detailed modelling.

Another advantage is that the simplified inputs required for CitySim to operate, relying mainly on simple weather data and architectural prototypes categorized uniformly (Mutani et al., 2018). This balance between input requirements and model functionality makes CitySim well suited for this dissertation, where the objective is to investigate indoor–outdoor relationships across many buildings under different environmental conditions, with urban form spatial variability is used as a factor.

In this study, workflow of CitySim is shown in Figure 3.2 and includes four parts. (1) Input preparation from the shared urban database (Section 3.2): building geometry (e.g., footprint, height, and orientation), archetype-based parameters (e.g., envelope thermal properties and operational assumptions), and climate data are prepared for CitySim-ready inputs. (2) Pre-processing: the raw datasets are quality-checked and translated into CitySim input files by assigning archetype parameters to individual buildings (and zoning where required) and generating the corresponding model configuration files. (3) CitySim simulation core: CitySim then performs time-step calculations that account for inter-building shading and radiative exchanges together with each building's thermal balance and HVAC control, thereby producing building-level thermal loads and indoor conditions. (4) Output extraction and post-processing: key indicators, such as heating/cooling demand and, where relevant, indoor air/operative temperature of each building, are exported and aggregated to support scenario comparison and provide possible link with UCM-derived microclimate indicators.

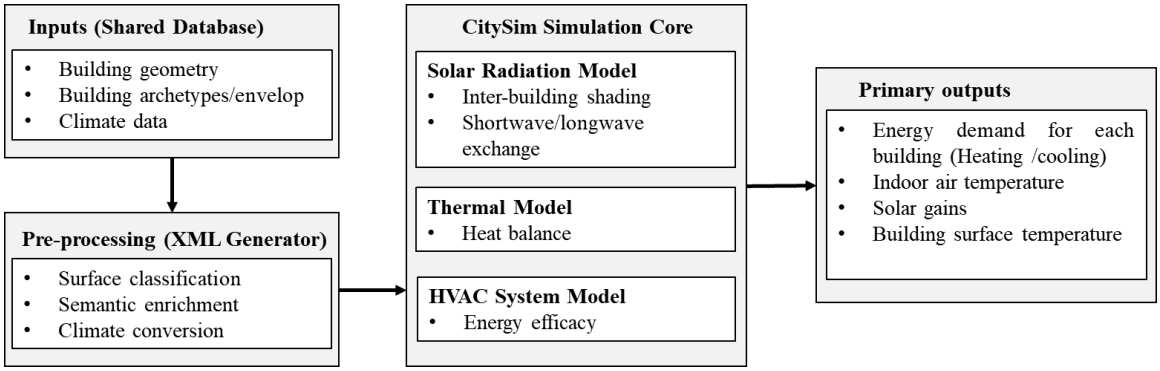


Figure 3.2 CitySim workflow.

Note: *Detailed CitySim application for Düsseldorf case study is both provided in Chapter 5 and Chapter 6. In Chapter 5, CitySim utilizes shared urban databases to simulate building energy performance of residential buildings under current and projected climate conditions. In Chapter 6, a one-way, offline integration of ENVI-met and CitySim has been used. ENVI-met provides CitySim high resolution and localized outdoor microclimate series that are used to refine the boundary conditions for CitySim simulations, enabling the assessment of indoor operative temperature responses under heat-stress situations.*

3.4 UCM: ENVI-met

Chapter 4 detailly introduces widely used UCMs that operate across various spatial scales with different levels of input detail. ENVI-met is a high-resolution, three-dimensional microclimate model widely used to represent the interactions between urban geometry, surface energy balance, radiation exchange, and near-surface airflow in complex urban canyons (Blazejczyk et al., 2012). This dissertation employs ENVI-met

as the UCM to simulate neighborhood-scale outdoor thermal conditions under heat-stress scenarios (Bruse, 2024).

ENVI-met was selected because the spatial scale and research objectives of this dissertation require a model capable of resolving pedestrian-level microclimatic variability at meter-scale resolution (Najafian et al., 2026). Although large-eddy simulation (LES) models provide more detailed representations of turbulent flow, they generally require substantially higher computational resources and are primarily applied to airflow studies rather than comprehensive urban microclimate assessments (Piomelli, 1999). ENVI-met clearly represents radiation exchange, vegetation, soil–plant–atmosphere interactions, and pedestrian-level thermal comfort, making it particularly suitable for evaluating the effects of building retrofit and urban greening at the neighbourhood scale considered in this dissertation.

In the dissertation workflow (Figure 3.1), ENVI-met and CitySim are run over the same study area using harmonized inputs exported from the shared urban database (Section 3.2), including building geometry and relevant surface descriptors required for microclimate simulations. ENVI-met simulations are configured to represent the selected heatwave period, on July 19, 2022, when Europe experienced one of its most severe heatwaves that year, with Germany being heavily impacted (Copernicus Climate Change Service/ECMWF, 2022). Outputs of ENVI-met are extracted at pedestrian-relevant height (1.5 m) and locations to characterize spatial contrasts driven by urban form (e.g., street canyons, block edges and interiors, and green land environments). The key outputs used for subsequent linkage and analyses include near-surface T_a, relative humidity (RH), wind speed (v), and mean radiant temperature (T_{mrt}).

T_{mrt} is a human-biometeorological measure of the total radiant environment experienced by a person. It is defined as the uniform temperature of a hypothetical enclosure in which the net radiant heat exchange between the human body and its surroundings would equal that occurring in the actual environment (Guo et al., 2020). T_{mrt} therefore differs from both air temperature and individual surface temperatures. It integrates the combined effects of direct, diffuse, and reflected shortwave radiation, together with longwave radiation emitted by the sky, buildings, vegetation, and ground surfaces (Schöneberger et al., 2025). In urban environments, T_{mrt} is strongly influenced by building geometry, street orientation, sky-view factor, shading, vegetation, and surface radiative properties (Lindberg et al., 2008). Consequently, daytime spatial variations in T_{mrt} can be substantially greater than variations in air temperature, particularly during clear-sky heatwave conditions.

Outdoor thermal stress is evaluated using UTCI. UTCI is a physiologically based thermal index that expresses the equivalent air temperature of a reference environment producing the same dynamic physiological response as the actual outdoor conditions

(Blazejczyk et al., 2012). It combines the effects of T_a, T_{mrt}, v, and humidity on the human heat balance and therefore provides a more comprehensive assessment of outdoor thermal stress than air temperature alone (Jendritzky et al., 2012). UTCI is particularly suitable for this dissertation because the investigated retrofit and greening scenarios primarily modify shading, surface radiation, wind exposure, and humidity, all of which influence human thermal exposure but may not be adequately represented by changes in T_a alone.

The UTCI calculations are based on ENVI-met outputs of T_a, T_{mrt}, RH, and v at 1.5 m. The resulting UTCI values are used to compare the magnitude and spatial distribution of outdoor heat stress across the alternative urban scenarios. Particular attention is given to Tmrt because it provides the direct link between changes in urban morphology, vegetation, surface radiation, and pedestrian thermal exposure. **Note.** *Detailed model configuration (domain, grid, forcing, material parameterization, vegetation settings, scenario implementation, and the implementation of the one-way ENVI-met–CitySim linkage) is provided in Chapter 6.*

3.5 Linking strategy and analyses

3.5.1 Linking strategy (database-centered, one-way/offline)

The methodological components introduced in Sections 3.2–3.4 are integrated through a database-centered，offline workflow between UCM and UBEM simulations. Rather than directly coupling CitySim and ENVI-met, both ENVI-met and CitySim are driven by harmonized geometry and archetype-based parameters derived from the shared urban database (Section 3.2), ensuring consistency in the representation of urban form and building-stock characteristics. Linkage is conducted during post-processing by aligning simulation outputs through (1) the shared spatial scenarios design and (2) persistent building identifiers where building-level correspondence is required.

For the heatwave-focused indoor comfort assessment presented in Chapter 6, the general database-centered workflow is extended through a one-way ENVI-met–CitySim linkage. ENVI-met provides localized outdoor boundary conditions for CitySim indoor simulations during the daytime window when microclimate heterogeneity is most pronounced.

Depending on the research question, linked datasets are analyzed at different spatial supports (building, block, or receptor micro-environment class). This flexible linkage strategy enables consistent comparison of indoor energy performance, outdoor thermal comfort, and their interactions across scenarios. All linked results are reported with both statistical evidence and physical effect magnitudes.

3.5.2 Analytic framework: scenario comparison, driver attribution, and economic indicators

The analytical framework presented here synthesizes the methodologies adopted in the journal papers reproduced in Chapters 5 and 6. Together, these analyses form following three complementary methodological components.

(A) Scenario-based comparison (applies to both UCM and UBEM)

Scenario impacts are quantified by comparing key indicators between designed scenarios to quantify the effect of retrofit and urban-intervention scenarios on outdoor heat stress and building energy responses.

Scenario differences are computed for key indicators: (1) UCM outputs (e.g., T_a, RH, v, T_{mrt}, and UTCI where derived) and (2) UBEM outputs (e.g., heating/cooling demand, energy use intensity, and where evaluated indoor temperatures).

Results are summarized at consistent spatial supports (grid mean, block mean, or receptors) and consistent time windows (daily profiles and peak hour).

(B) Statistical analysis for outdoor heat-stress drivers (primarily from Chapter 6)

To interpret why UTCI differs across scenarios and locations, statistical analyses are applied to linked UCM outputs. Three complementary components are applied to linked UCM outputs:

(1) Peak-hour hypothesis testing: detecting scenario effects at the heat-stress peak

This test evaluates whether influence factors produce a systematic change in UTCI at the peak heat-stress hour (14:00 CET). For each predefined scenario pair, UTCI values at 14:00 CET were compared using paired-sample t-tests (Field, 2013). The paired design exploits the one-to-one correspondence of spatial samples (either grid cells or receptor points), so that each location provides a matched observation across the two scenarios. Prior to inference, the Shapiro–Wilk test (Shapiro and Wilk, 1965) was applied to the distribution of paired differences to assess the normality assumption of the t-test. Levene's test (Levene, 1960) was additionally used as a diagnostic check for variance heterogeneity between scenario samples.
For each scenario pair, we report the t-statistic and p-value together with the effect magnitude (e.g., mean ΔUTCI at 14:00 CET and its dispersion across samples). Where multiple scenario comparisons were conducted, p-values were adjusted using the Benjamini–Hochberg (BH) procedure to control the false discovery rate (Benjamini and Hochberg, 1995).

(2) Multivariate attribution modelling: ranking drivers under multicollinearity

This analysis identifies which microclimatic variables most strongly explain spatial variability in UTCI, acknowledging that predictors such as T_a and T_{mrt} are often correlated.

Ridge regression is used specifically to mitigate multicollinearity while retaining all predictors, enabling stable coefficient estimates for explanatory ranking rather than variable elimination (McDonald, 2009). In this study, it has been used to standardize predictors, including pedestrian-level T_a, T_{mrt}, RH, and v at 1.5 m above ground. For post-processing and reporting, ENVI-met outputs are summarized using goodness-of-fit (e.g., R^2) and standardized coefficients/weights to compare the relative contribution of each driver. The regularization parameter is selected via cross-validation. Driver rankings are interpreted as scenario-specific sensitivities and are reported alongside descriptive statistics to ensure physical plausibility.

(3) Spatial analysis: translating statistics into urban-form mechanisms

Statistical attribution alone may ignore local micro-environment mechanisms (e.g., shading, canyon ventilation). Spatial analysis provides physically interpretable evidence for how urban form creates the modeled differences. A set of representative receptor locations (e.g., block edge vs. interior; shaded vs. sun-exposed) is selected to exam peak-hour UTCI and its component drivers.

(C) Energy and economic evaluation (primarily from Chapter 5)

For the UBEM retrofit assessment, the dissertation follows an indicator-driven evaluation. The purpose is to quantify how archetype-level retrofit strategies affect space-conditioning energy demand, associated CO_2 implications, and cost-effectiveness at the neighborhood- scale. Analyses include energy performance indicators, emissions implications and economic indicators.

Energy performance indicators report hourly heating and cooling demand under 2020, 2050, and 2100 the representative concentration pathway 8.5 (RCP8.5) scenarios, accounting for inter-building shading and radiative exchanges in dense urban fabrics. Because active mechanical cooling is uncommon in the German context, cooling demand is interpreted as potential cooling need rather than realized electricity consumption. Electricity for appliances loads was kept constant across scenarios and excluded from energy-savings accounting.

Emissions accounting considers CO_2 impacts, which were quantified from the difference in simulated heating demand between original and refurbished cases (consistent emission factors and fuel assumptions are applied across archetypes). Results are reported both as intensity metrics (e.g., kg $CO_2/m^2 \cdot a$) and aggregated neighborhood totals to support retrofit prioritization.

Economic evaluation and reporting use simple payback time and net present value (NPV) under standardized assumptions (e.g., retrofit investment per m^2, subsidy rate, discount rate, evaluation period). Carbon savings were quantified using a reference carbon price (e.g., DEHSt benchmark) and incorporated together with energy-cost savings in the NPV calculation. In addition, the analysis reports the environmental cost of delayed retrofitting (avoidable cumulative CO_2 emissions over a defined delay window), highlighting the value of early action even when NPV remains negative under current economic conditions.

4. Exploring the integration of urban climate models and urban building energy models through shared databases: a review

This work has been published under:

Yu, Q., Ketzler, G., Mills, G., et al. (2025). *Exploring the integration of urban climate models and urban building energy models through shared databases: a review.* Theoretical and Applied Climatology, 156, 266. https://doi.org/10.1007/s00704-025-05501-3

Highlights

Explores integration potential of urban climate and building energy models across multiple urban scales, from individual buildings to city-wide districts, enhancing planning accuracy and climate resilience

Emphasizes the need for shared databases and a common language to enable effective integration and knowledge transfer between Urban Building Energy Models (UBEMs) and Urban Climate Models (UCMs).

Identifies key challenges in data harmonization and model interoperability across urban scales, proposing solutions to enhance the practical applicability of integrated urban modelling for policymakers and urban planners.

Abstract

Urban energy demand and climate dynamics are inherently interconnected. However, existing modelling approaches often fail to integrate data effectively across multiple spatial scales. Urban building energy models (UBEMs) and urban climate models (UCMs) provide valuable insights into urban energy consumption and microclimate variations, respectively. However, their integration remains a challenge due to differences in spatial resolution, data structures, and computational requirements. While previous studies have explored models coupling, most focus on microclimatic interactions, lacking a standardized framework for data integration across different urban scales.

This review examines the current state of UBEM tools and UCMs, with a particular emphasis on the correspondence of model data integration at multiple spatial scales. We identify key challenges in harmonizing geospatial data, meteorological inputs, and simulation parameters, particularly the misalignment of Levels of Detail (LoD) between models operating at different spatial scales. To address this, we propose a multi-scale data framework that enables integration by aligning UBEMs and UCMs data structures through shared urban databases. This approach contributes to more accurate energy predictions, enhances urban climate resilience planning, and improves the applicability of integrated models for policymakers and urban planners.

Keywords

Urban building energy model (UBEM); Building archetypes; GIS; CityGML; Building energy use

4.1 Introduction

The Intergovernmental Panel on Climate Change (IPCC) identifies anthropogenic greenhouse gas (GHG) emissions as the primary driver of current global climate change (Lee et al., 2023). Urban areas are central to this issue, as they consume approximately two-thirds of the world's primary energy and are responsible for a significant portion of global carbon emissions (Ullah et al., 2024). Among urban activities, the building sector stands out as a major energy consumer and contributor to carbon emissions (Hu et al., 2022; Nik et al., 2021). As cities become the key point for sustainability efforts, urban design must consider the intricate relationship between building energy consumption and climate to achieve meaningful carbon reductions (Carter et al., 2015).

Cities also modify climates at urban scales, creating a distinctive urban boundary layer (UBL) that grows in depth downwind of the urban 'edge' (Ali et al., 2021). Below UBL is the urban canopy layer (UCL), where most human activity and energy exchange occur. Factors such as building arrangements, materials, and vegetation influence microclimate conditions in the UCL (Blocken, 2015; Chao et al., 2010; Crooks et al., 2015). These concentrated heat emissions and modified land surfaces cause the Urban Heat Island (UHI) effect and further intensify thermal discomfort and shift energy demand towards summer cooling (Masson et al., 2020; Zheng et al., 2023).

Buildings are central to these interactions, not only by consuming energy to maintain indoor comfort and simultaneously by releasing waste heat into the atmosphere but further by affecting the microclimate (Li et al., 2020; Sadineni et al., 2011; Santamouris et al., 2013). Waste heat, known as building anthropogenic heat flux, is a significant contributor to urban heat emissions, particularly at the neighborhood- scale (Vahmani et al., 2022). As such, urban climate can be partly recognized as an aggregate outcome of inside and outside climate of buildings (Futcher et al., 2013). Figure 4.1 illustrates how buildings influence and contribute to urban climate dynamics. Specifically, buildings, through their geometry and envelope materials, play a pivotal role in modifying the microclimate. These structures contribute to the urban heat dynamics not only through direct anthropogenic heat emissions from various building energy systems but also through the physical properties of building materials. Materials that make up building envelopes have distinct characteristics that can absorb, reflect, or radiate energy, thus impacting the microclimate (Sadineni et al., 2011; Santamouris et al., 2013). Furthermore, the orientation of building facades and the slopes of roofs are critical design elements that can significantly alter local energy flows, thereby influencing both indoor comfort and the broader urban temperature profiles (Li et al., 2020). This complex interaction underscores the importance of considering urban form and function when assessing energy dynamics and microclimatic conditions in urban planning processes (Vahmani et al., 2022).

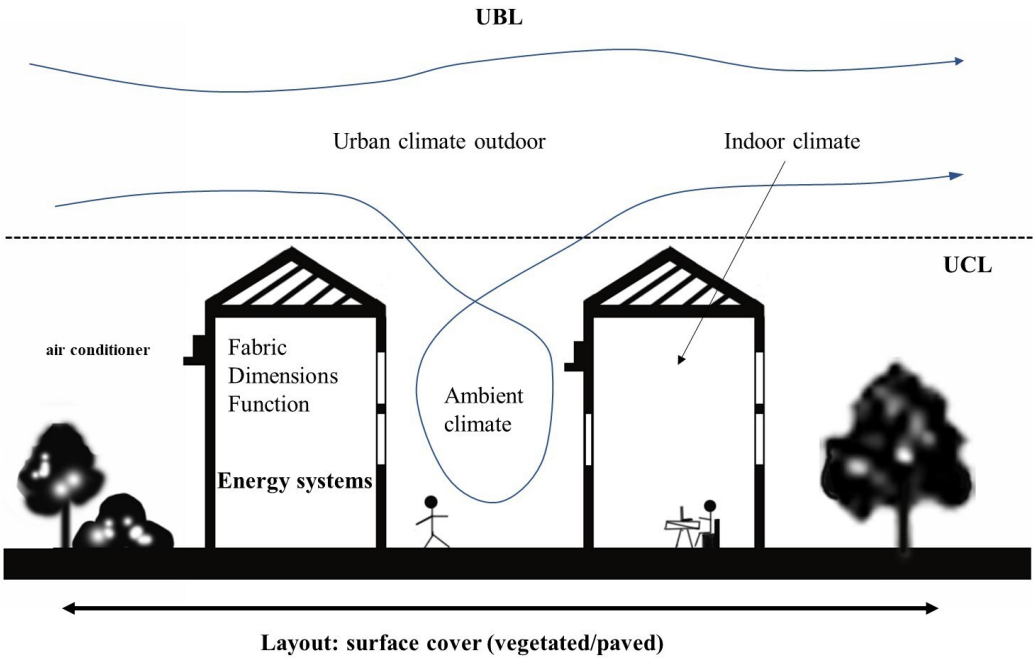


Figure 4.1 Buildings, their structure and influence on urban climate, highlighting the key roles of building geometry and material properties in altering local microclimates. (Futcher et al., 2013; Li et al., 2020; Sadineni et al., 2011; Santamouris et al., 2013; Vahmani et al., 2022).

Given the significant role that buildings play in shaping the urban climate, accurately estimating building energy demand is essential. This is typically done using either top-down or bottom-up approaches (Swan and Ugursal, 2009; Kavgic et al., 2010). Top-down approaches offer large-scale analysis by examining building energy demand across entire regions, which relates the energy sector to economic or climatic conditions (Wang et al., 2022). However, they often lack detailed insights into current and future technological options (Yang et al., 2022). In contrast, bottom-up approaches offer higher spatiotemporal detail and can identify potential efficiency improvements in the urban construction sector, which includes Building Energy Modelling and Urban Building Energy Modelling (Böhringer and Rutherford, 2008; Johari et al., 2023).

Traditional Building Energy Models (BEMs) are usually applied in energy demand simulation of a single building, emphasizing the optimization of indoor climate comfort in relation to energy demand by considering the building's dimensions, materials, and energy systems (Johari et al., 2022). While these models provide valuable insights, they often exhibit limitations in urban contexts where the complex interactions between buildings, such as overshadowing, building orientation, and facade retrofits (Luo and Hong, 2022). It is important to note, however, that some software packages like EnergyPlus, DesignBuilder, and TAS Engineering do incorporate these interactions by constructing a 3D model of the analysis area and representing nearby buildings as component blocks, which allows them to account for shading effects and reflections

(Chen et al., 2022; Dena et al., 2024; Hasan et al., 2020). This capability helps in capturing more accurate energy dynamics in urban settings, although it can still be resource intensive.

UBEMs expand this scope to multiple buildings, incorporating urban scale interactions, such as shading, heat transfer, and spatial energy distribution (Ferrando et al., 2020; Oke et al., 2017). Meanwhile, UBEMs incorporate urban layout factors and simplify large-scale analysis by categorizing buildings into archetypes based on shared characteristics, which allows for analysis with less computational resources (Ferrando and Causone, 2020; Javanroodi et al., 2023).

Urban climate models (UCMs) primarily focus on simulating outdoor climate conditions, which influence human well-being, thermal comfort and discomfort (Pigliautile et al., 2020). Like UBEMs, they rely on common input parameters, including meteorological data, land use, building geometry, and surface material properties, making them valuable for climate-responsive urban planning at various scales (Mills, 1997).

Although they share data requirements, both UCMs and UBEMs have traditionally operated in isolation. Building energy focuses primarily on indoor energy performance, while urban climate studies emphasize outdoor environmental conditions (D'Oca et al., 2018). Differences in spatial resolution, data structures, and computational requirements of common data make integration difficult and limits the ability to fully understand the dynamic interactions between buildings and urban climates, particularly when scaling from microclimate effects to city-wide impacts. For example, in the context of climate change, global warming coupled with local warming (UHI) will initiate a positive feedback loop in cities, as cooling demand increases energy consumption and enhances the UHI (Ang et al., 2023; Nidam et al., 2023). Rising temperatures and other climate related challenges require integrated strategies, not only reduce energy demand but also mitigate climate impacts such as UHI (Lee et al., 2024). A promising pathway is the integration of UBEMs with UCMs, allowing planners and policymakers to design cities that are both energy-efficient and climate-resilient (Reinhart, 2023; Santamouris, 2023).

However, in practice, urban climate analyses have often simplified the role of buildings, while in building energy literature, urban climate is typically treated as just one of many external factors (Krelling et al., 2024; Wang et al., 2024; Yang et al., 2024). While previous studies have explored the integration of UBEMs and UCMs, most have focused on microclimatic interactions (Boccalatte et al., 2020; Liu et al., 2023; Sherif et al., 2025; Worthy et al., 2025; Yang et al., 2023). Few have addressed how to integrate data across multiple urban scales in a standardized way. Without a common geospatial framework, inconsistencies in data resolution, spatial alignment, and model interoperability will continue to hinder model integration. Meanwhile, data privacy, protection, and security in integrated modelling is also essential for model integration. Effective integration

requires coordinated efforts across multiple disciplines to ensure data consistency, computational efficiency, and practical applicability.

In response to these gaps, this review examines the current state of UBEMs and UCMs, exploring how these tools can be coupled to provide a more comprehensive approach for urban energy and climate management to cover different spatial scales. A key focus is on developing a unified framework through a shared urban database, incorporating meteorological conditions, geographic information, building geometries, and material properties. Through using these shared resources, this review seeks to address three key questions:

(1) What are the most commonly used UBEMs and UCMs and how do their data structures and spatial resolutions differ?
(2) How can UBEMs be effectively integrated across multiple spatial scales, and what are the key challenges in geospatial data harmonization?
(3) And how can a standardized integration framework enhance integration interoperability and support sustainable urban design and policymaking?

In the following part, section 4.2 introduces methodology for searching relevant studies. This section details the methodology employed to identify and select the relevant studies that form the basis of this review, ensuring a rigorous and systematic approach. Section 4.3 provides a comprehensive overview of UBEM approaches, outlining their workflows, data requirements, and applications across various urban scales. Section 4.4 shifts focus on urban climatology, examining the methodologies used to analyze urban climate and the role of UCMs. In Section 4.5, we explore the integration of UBEMs with UCMs, highlighting challenges related to spatial resolution mismatches, data harmonization, computational scalability and privacy protection in data access, while proposing strategies to enhance model interoperability. The paper concludes with future research directions and implications of these integrations for sustainable urban design.

4.2 Methodology

This review uses a systematic and query-based methodology to identify and evaluate the most relevant publications in the field of UBEMs and UCMs. The objective is to ensure a comprehensive and repeatable review process that synthesizes the current state of knowledge and identifies gaps for future research.

The literature search was conducted primarily through Google Scholar, Web of Science (WoS) and Science Direct databases. This manual procedure was necessary because publications mentioning possible interfaces between the fields of building energy and urban climatology mostly do not have the intention to do so and, thus, would not use similar keywords. The search incorporated a combination of keywords relevant to urban building energy and climate modelling to ensure the capture of both empirical studies and comprehensive review articles. Figure 4.2 outlines the search criteria, and the structured approach used for model selection and integration. This figure visually represents the methodological flow, starting from the initial screening of descriptive and review articles through different related keywords to a more focused evaluation of the most commonly used UBEMs and UCMs. Article searching focuses on high-frequency citations and literature from 2015 to 2025 to capture the latest developments. The selected models were then analyzed to summarize their characteristics, applications, potential for integration, and limitations, aiming to identify how these models can be harmonized and what gaps exist in current methodologies. Overall, 137 papers matched the inclusion criteria were chosen for this study.

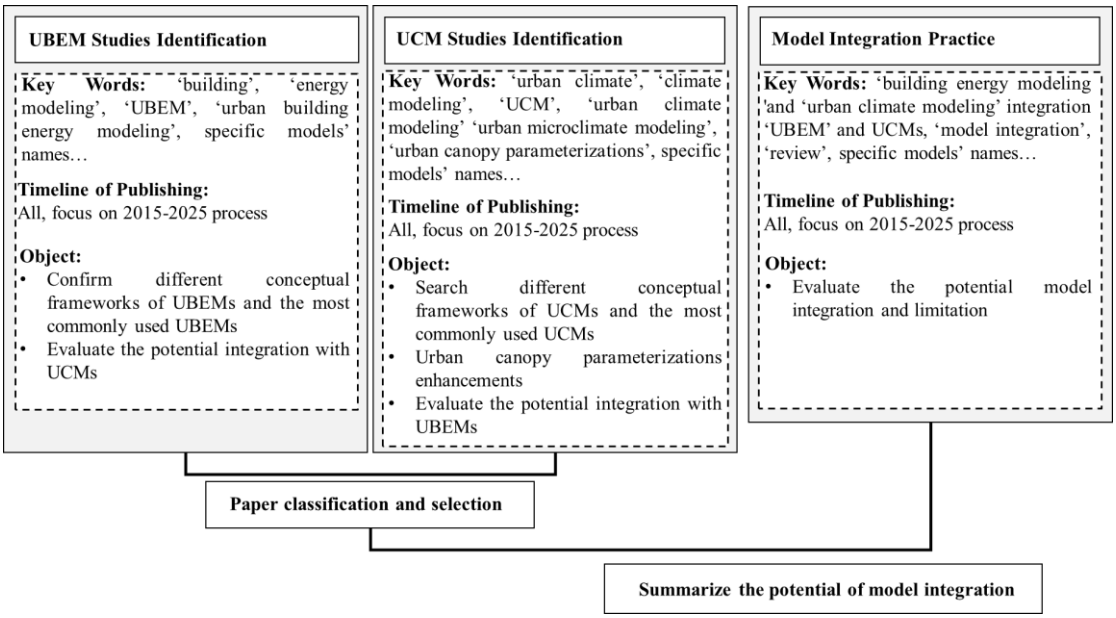


Figure 4.2 The research methodology used in this paper.

4.3 Urban building energy modelling approaches

4.3.1 UBEM tools and workflow

UBEM tools are designed to support energy simulation at different urban scales, from individual buildings to entire neighborhoods and cities. Some well-known UBEM tools include CitySim, City Building Energy Saver (CityBES), City Energy Analyst (CEA), Tool for Energy Analysis and Simulation for Efficient Retrofit (TEASER), Urban Modelling Interface (UMI), and UrbanOPT (El Kontar et al., 2020; Fonseca et al., 2016; Hong et al., 2016; Robinson et al., 2009; Remmen et al., 2018; Reinhart et al., 2013). Each tool follows a structured workflow to model energy performance. Figure 4.3 illustrates the main workflow of different UBEM tools, including three main stages: model characterization (data input), model generation (energy simulation), and model result analysis (simplification, validation, and visualization). The final stage involves a series of analyses and verifications to ensure the accuracy and reliability of the simulation results.

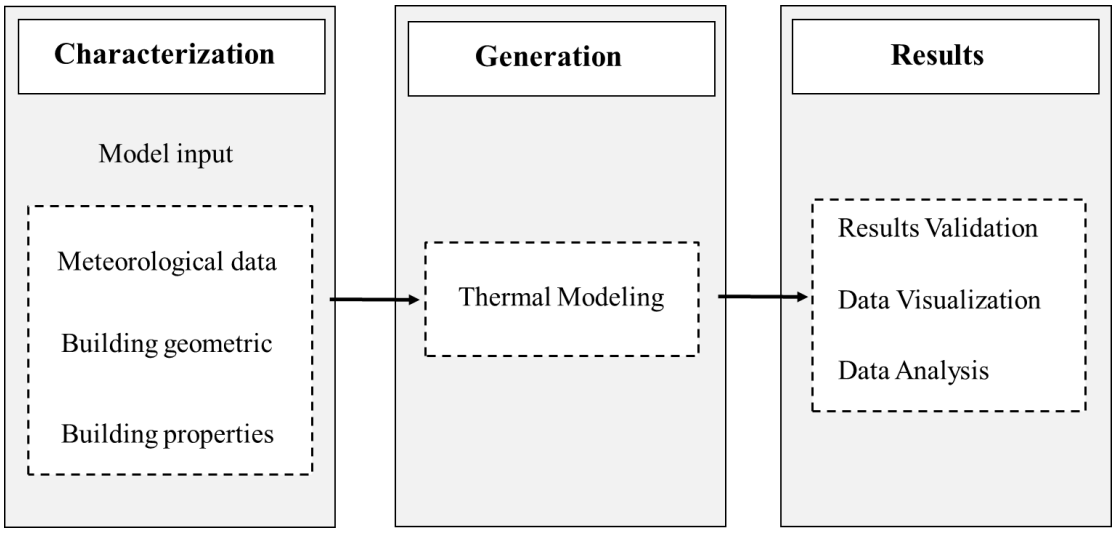


Figure 4.3 Generalized methodology of the UBEMs workflow based on the existing literature (Hong et al., 2020).

Note: Different input parameters are used for model characterization, and thermal modelling is conducted through simulation engines, and results then delivered for different uses. The final step requires a series of analysis and verification of the model results.

UBEMs rely on several input data sources, including meteorological data, building geometry, and fundamental building properties. Meteorological datasets, such as the Typical Meteorological Year (TMY) format, provide climate information like ambient temperature, RH, *v*, and solar radiation (Liu et al., 2021). These datasets are relevant for calculating heat and mass flows in and around buildings (Bouyer et al., 2011; Lauzet et al., 2019). Tools like Meteonorm, the EnergyPlus weather data format (EPW), and

Urban Weather Generator (UWG) are also commonly used to generate these meteorological inputs for UBEMs (see Table 4.1) (Bueno et al., 2013; Remund et al., 2010; Wang et al., 2021).

Building stock data, both geometric (building height, shape, window-to-wall ratio) and non-geometric (material properties, thermal characteristics), are stored in formats like GIS-based or CityGML (Table 4.1) (Malhotra et al., 2022). Together, these datasets facilitate the definition of various building archetypes (Le Hong et al., 2023). The Level of Detail (LoD) concept (simple 2.5D surfaces), ranging from LoD1 (basic geometry) to LoD4 (detailed 3D models) (see Figure 4.4), plays a key role in UBEMs, allowing for varying degrees of accuracy depending on the scale of the urban analysis (Löwner et al., 2013).

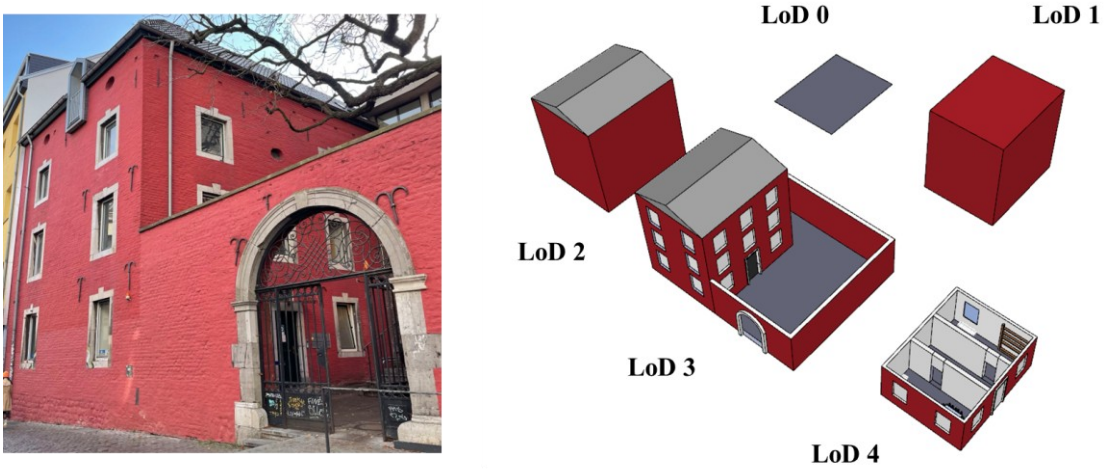


Figure 4.4 Five Levels-of-Detail (LoD) provided by CityGML in building modelling illustrated by an example building in the city of Aachen, Germany. Own representation after Löwner et al. (2013).

With meteorological data and building prototypes in place, the subsequent step involves integrating them into a thermal model, executing simulations via appropriate engines, and presenting the results to users (Reinhart and Davila 2016). These simulations calculate the energy demand for heating, cooling, lighting, and other building functions, while also accounting for interactions between buildings and the surrounding environment (Table 4.1). Physics-based simulation engines, such as EnergyPlus (mainly for CityBES, UMI and UrbanOPT), TRNSYS, and IDA-ICE, capture the full dynamic behavior of buildings, offering high-resolution results (Beckman et al., 1994; Björsell et al., 1999; Crawley et al., 2000). Among these, EnergyPlus stands out for its rapid simulation speed and precise energy consumption estimations over extensive timescales in complex urban building systems, which uniquely accommodates variable time intervals per thermal zone for HVAC systems (Chen et al., 2022). Additionally, while most simulation engines can calculate hourly energy use, only EnergyPlus and TRNSYS

offer sub-hourly energy calculations (Al Ka'bi, 2020). Alternatively, some UBEMs, such as CitySim, CEA, and TEASER, employ reduced-order models to expedite urban building thermal calculations. These models demand simpler inputs and standardized parameter values, offering computational efficiency at the expense of some modelling accuracy (Thebault et al., 2021).

Table 4.1 Weather file sources, building geometry datasets and thermal modelling for common UBEM tools.

UBEMs	Input meteorological data file	Building geometry dataset (LoD)	Thermal modelling
CityBES	EPW	CityGML (LoD1-3)	EnergyPlus
CEA	EPW/TMY	GIS-based (LoD1-3)	Reduced-order RC Model
CitySim	TMY	GIS-based (LoD1-2)	Reduced-order RC Model (CitySim solver)
TEASER	EPW	CityGML (LoD1-2)	Reduced-order RC Model
UMI	EPW/UWG	GIS-based (LoD1-3)	EnergyPlus
UrbanOPT	EPW	GIS-based (GeoJSON) (LoD 1-2)	EnergyPlus/OpenStudio

The final stage involves analyzing the simulation results (Table 4.2). Outputs can range from detailed energy consumption data to high-level evaluations of energy-saving measures. Visualization tools such as 3D models or heat maps help in assessing potential retrofits, efficiency improvements, and sustainability strategies.

The outputs can be subdivided into four main categories and summary of pros and cons: (i) building-related, (ii) potential analysis, (iii) large-scale general evaluations, and (iv) typology. Building-related outputs are the largest category, especially energy use of heating and cooling, building system and intensity. CitySim and UMI give extra consideration to indoor lighting. CityBES, CEA and UMI consider domestic hot water energy use and directly perform the analysis to calculate the solar potential. Especially, UrbanOPT is a Software Development Kit (SDK), which allows for significant customization and integration with other tools, that enhances its utility in complex urban energy studies (Charan et al., 2021).

CEA and CityBES stand out for their advanced model outputs, which enable comprehensive evaluations of building and infrastructure retrofits. These tools help

identify optimal energy generation strategies across various urban scenarios and scales. Although TEASER's output capabilities are somewhat more limited, it focusses on analyzing energy network efficiency and management across multiple urban scales. In contrast, UrbanOPT is specifically tailored for designing and optimizing grid-interactive efficient buildings (GEBs) at the district scale. It integrates distributed energy resources (DERs) and electric distribution systems to enhance its comprehensive urban energy modelling framework (De Rosa et al., 2021). Notably, all the tools provide outputs in the form of spreadsheet files (usually in CSV-format) and provide a graphic or 3D visualization of results except TEASER, which only provides a graph typology. Especially, CEA has a unique 4D interface to represent time-dependent energy flows between buildings and infrastructure.

Validation of UBEM results is essential for supporting decision-making in multi-building contexts. While in some simulation's errors are inevitable, their impact on decision-making is generally within acceptable ranges (Nagpal and Reinhart, 2018). However, it is important to clarify that the reliability of an UBEM depends not only on the software used but also significantly on the expertise of the modeler in accurately representing essential physical processes, carefully calibrating input parameters to local conditions, and validating the results against observational data. This comprehensive approach ensures that even when numerical models show accuracy within accepted ranges, their predictive value remains closely tied to the real-world applicability of their calibration and assumptions. Therefore, a model can be considered robust for multi-building decision-making when its inputs, assumptions, and calibrations are carefully defined and aligned with empirical data.

Table 4.2 Summary of UBEM models' outputs.

Tool	Outputs						
	Building related	Data format	Potential analysis	Large scale general evaluations	Typology	Pros	Cons
CitySim	Energy demand (heating, cooling and electricity) Energy use intensity Building system Thermal Comfort	CSV	Solar-potential	Mobility (MATsim-T)	3D-visualization Graph	The input parameters are simple, and the model runs fast	Inability to perform complex calculations, especially impacts with the natural environment; no daylight simulation
CityBES	Energy demand (heating, cooling and electricity) Energy use intensity Building system Thermal Comfort	CSV	Solar-potential	GHG emissions Equipment capacity Cost-benefit scenarios	3D-visualization Graph	User-friendly, web-based, supports multiple application scenarios	Requires detailed input data; complex setup; no daylight simulation
CEA	Energy demand (heating, cooling and electricity) Energy use intensity Building system Energy use for domestic hot water	CSV	Solar-potential Economic potential	GHG emissions Cost-benefit scenarios Low-Carbon Scenarios	4D interface 3D-visualization Graph	User-friendly, allows no programming capacities users. Supports extensive scenario analysis and economic potential evaluation	Limited compatibility with other tools; no daylight simulation
TEASER	Energy demand (heating, cooling and electricity) Energy use intensity	XML			Graph	Rapidly generate architectural prototype models; provide multiple data source interfaces	Requires certain programming skills; no visual output
UMI	Energy demand (heating, cooling and electricity) Energy use intensity Building system	XML	Solar-potential Transportation energy use potential	Environmental comfort	3D-visualization Graph	Support directly Rhinoceros 3D integration; supports extensive scenario analysis, especially environmental comfort analysis	Commercial software, requires high-detail urban data; high computational cost
UrbanOPT	Energy demand (heating, cooling and electricity) Energy use intensity Building system	CSV	Solar-potential Electric vehicle charging impacts	GHG emissions Distribution Integration Solution Cost Options	Graph	A flexible SDK, allowing customization and integration with various tools	Tools rely on integration and face compatibility issues

4.3.2 UBEM tools by scale

Different UBEM tools are designed to operate at specific scales, ranging from city-wide applications to neighborhood and building-level analyses. Table 4.3 summarizes frequently used UBEM tools, which are grouped by their scale of application.

CitySim conducts building energy simulations by modelling the scenario as a complex urban environment where energy flows interact with one another. It utilizes simplified urban morphology parameters to enable fast simulations at the scale of an urban district (comprising several hundreds of buildings) (Vermeulen et al., 2013). CityBES is an open, web-based platform for urban-scale building energy modelling and performance analysis. It utilizes 3D visualization and standardized datasets like CityGML to assist city managers in evaluating energy conservation measures, optimizing building retrofits, and achieving energy efficiency goals at scales ranging from districts to entire cities (Hong et al., 2018). CEA is an open-source software tool designed for urban energy modelling and analysis. It provides a platform for evaluating and optimizing energy systems at different scales, from neighborhoods to entire cities (Fonseca et al., 2016). TEASER is an open framework for urban energy modelling of building stocks at the scale from single building to city (Remund et al., 2010). UMI is an urban modelling platform to evaluate the environmental performance of neighborhoods and cities with respect to operational and embodied energy use, neighborhood walkability, access to daylighting, urban food production and district-level energy supply analysis (Vahid-Ghavidel et al., 2024).

Table 4.3 Summary of UBEM tool scales and main applications.

Tool	Scale	Application
CitySim	Neighborhood, District, City	Large-scale fast energy performance analysis
CEA	Neighborhood, District, City	Large-scale urban energy assessments and scenario planning
CityBES	District, City	Large-scale retrofitting and energy conservation
UMI	Neighborhood	Neighborhood-scale urban design evaluations
TEASER	Single Building, Neighborhood, District, City	Different level retrofitting and energy modelling

While UBEMs provide valuable insights into energy consumption at different levels, it is important to consider how these energy flows interact with broader urban climates. In the following, we explore the methods used to simulate urban climates, focusing on the interaction between buildings and their environment at different spatial scales.

4.4 Urban climate models

Urban climate modelling operates across various spatial scales, each requiring different levels of input detail and influencing the accuracy of predictions. These scales range from the microscale, which deals with fine turbulent eddies and detailed building-level interactions, to the mesoscale, which covers entire city regions or even larger areas (Chao et al., 2010; Mills, 2006). The choice of scale affects both the complexity of the model and the precision of its outputs.

To effectively study urban climates, detailed descriptions of urban areas, including meteorological inputs and urban morphology, are required (Barlow, 2014; Mills, 2014). These components are critical for determining how buildings and urban surfaces interact with their surrounding environments, affecting local climates (Hua et al., 2022; Santamouris and Kolokotsa, 2016). A key aspect of modelling is the LoD, which refers to the precision of the geometric data used in the models. Table 4.4 summarizes the various spatial scales and their corresponding models and input data, while Figure 4.5 illustrates the horizontal spatial scales and associated models.

Meteorological mesoscale (MM) models are designed to simulate weather and climate processes at regional scales (10 to 1000 km) (Oke, 2006). Traditionally, input data are usually represented at LoD0, which provides broad land cover information suited for fast simulations over large areas. This LoD, although beneficial for larger-scale studies,

lacks the resolution necessary to accurately model the complex energy and mass exchanges within urban settings (Chen et al., 2021). Mesoscale models (MM) were not originally designed for use in cities but the development of urban modelling schemes (Otte et al., 2004) allows urban canopy processes to be integrated with larger-scale meteorological and climate models. These schemes use detailed urban structural data (LoD1) to describe buildings, streets, and vegetation, which are used to improve simulations of urban effects in the UBL and provide simulations of these effects within the canopy layer (Tarasova et al., 2023).

One of the best-known and widely used MM is the Weather Research and Forecasting (WRF) model, which originally included urban landscapes as flat and impermeable surfaces. However, it now includes the Single-layer Urban Canopy Model (Kusaka et al., 2001) and Building Effect Parameterization (BEP) (Martilli et al., 2002) schemes which account for energy and momentum exchanges with the urban canopy. Further, Salamanca et al. (2010) and Salamanca and Martilli (2010) advanced these concepts by coupling the BEP with a simple BEM (BEP-BEM), enhancing the MM model capability to simulate detailed energy dynamics in cities. All urban modelling schemes require numerical descriptions of the urban landscape (UCPs) that are available in gridded form at the scale of the simulation; for typical urban MM applications this scale corresponds to a resolution of 500-1000m. These UCPs capture information on the radiative (albedo and emissivity), thermal (heat capacity and conductivity) and morphological properties (building heights and street width) of the urban landscape. Acquiring these data for cities has been a major obstacle to the application of MMs to city applications (Ching et al., 2018). Typically, these UCPs have been generated for individual cities using building morphology information that was locally available but significant advances in data acquisition and processing have allowed the development of global urban databases to support MM applications (e.g. Demuzere et al., 2022, Kamath et al., 2024 and Liao et al., 2024).

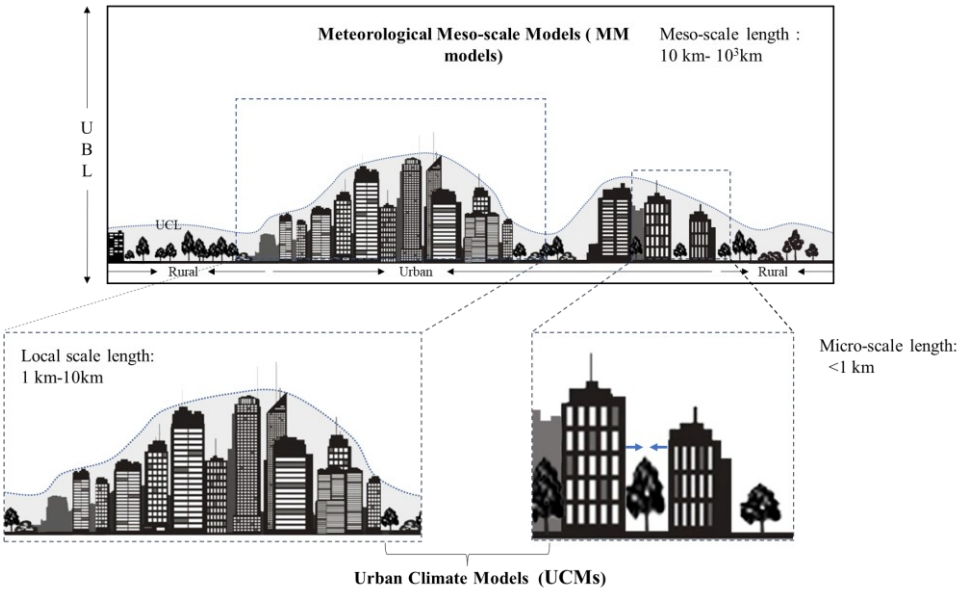


Figure 4.5 Different spatial scales and corresponding models based on Oke et al.

Note: The MM models are usually applied into atmospheric mesoscales; the UCMs are designed for urban research to simulate complex energy and mass exchange processes in urban environments.

Table 4.4 Different spatial scales and model input data.

Scales	Models	Input	Required LoD
Meteorological meso-scale	MM models with urban schemes (10km-103km)	Meteorological data Land cover data Meteorological data	LoD 0
City	UCMs (0-10 km)	Meteorological data Land cover, and building morphology	LoD 0,1,2
Building district	UCMs (<1 km)	Meteorological data Land cover, and building morphology Building information	LoD 0,1,2,3
Building	UCMs (<1 km)	Meteorological data 3D Building information	LoD 3,4

In addition to the urban models that are integrated with larger scale weather and climate models, there are other, stand-alone, UCMs that simulate processes at a fine spatial scale, typically less than one kilometer (from building to street to neighborhood- scales). These are used to evaluate the urban effect on airflow, shading, air and surface temperatures variations and outdoor thermal comfort (Blocken et al., 2011) and require high-resolution geometric data (LoD2 and LoD3) (Huang et al., 2022; Kim and Brown, 2023). These models can capture the interactions between buildings, vegetative features and the ground and are used to explore common urban configurations (e.g. urban canyons) and urban effects (e.g. the urban heat island) (e.g. Zhao et al., 2023). Table 4.5 categorizes these by scale into neighborhood and building/street scales and the typical inputs and outputs. These models are used for planning and designing applications.

Table 4.5 Representative UCMs, their typical outputs and LoD needs.

Scale	UCMs (Examples)	Outputs	LoD (UCP)
Neighbourhod Scale (0-10 km)	e.g.SUEWS	Air temperature & Humidity Surface temperature Wind speed Solar radiation Urban energy balance UHI modelling Outdoor thermal comfort	LoD 1,2
Building/street Scale (<1 km)	e.g. ENVI-Met	Atmospheric properties Surface fluxes for ground, roofs, and walls High-resolution airflow modelling including turbulence Detailed surface temperature distribution	LoD 1,2,3

The Urban Multi-Scale Environmental Predictor describes a suite of UCMs that are used to simulate urban effects. One of its core UCMs is the Surface Energy and Water Balance Scheme (SUEWS), which requires data on meteorology and urban surface cover (LoD1 and LoD2) and has been used to simulate urban energy fluxes and the urban heat island (e.g. Meehl and Tebaldi, 2004). It is a gridded model that is often typically applied to neighborhood and city scales and requires UCPs based on 2D urban land use and landcover data. By comparison, ENVI-met is a commonly used model that is applied at the urban microscale and can simulate the surface-air exchanges on walls and roofs and the 3D wind field (Bruse and Fleer, 1998). It considers building geometry, vegetation, and human activities, allowing for detailed analysis of temperature distributions, wind patterns, and other microclimatic variables to analyze the effects of various design interventions on the thermal comfort and overall urban climate, helping to promote sustainable and climate-resilient urban development (Liu et al., 2021).

UCMs are important tools for understanding energy exchange dynamics within densely urbanized areas (Hashemi et al., 2024) and require much of the same data needed by UBEMs. Clearly there is value in linking urban data at different LoD levels to the UCPs that these models require.

4.5 Integrating UBEMs and UCMs

The integration of UBEMs with UCMs can play an important role in improving energy efficiency and climate resilience in urban environments (Sezer et al., 2023). While UBEMs focus on building-level energy performance, UCMs simulate microclimatic and mesoscale climate conditions. By coupling these models, researchers and policymakers can better assess the interactions between buildings and the surrounding climate, contributing more data-driven urban energy planning and climate adaptation strategies (Alexander et al., 2016; Mondal et al., 2024; Xu et al., 2024). However, their integration presents several challenges, including differences in data structure, spatial resolution,

computational requirements, and model validation. Addressing these issues is critical for enabling a standardized multi-scale framework that allows these models to work together effectively.

4.5.1 Exploring applications of UBEMs in climate-responsive urban practices

UBEMs are increasingly vital in two key areas: the design of new urban layouts that are climate-adapted and energy-efficient, and the renovation of existing structures to enhance energy performance (Ang et al., 2020).

Designing new urban layouts within a climatological context involves creating cities that are not only adapted to local climate conditions but also reduce energy demand and greenhouse gas emissions—key drivers of climate change (Mauree et al., 2019). For example, Davila et al. (2016) developed a citywide UBEM workflow that integrated GIS datasets to construct building archetypes and employed EnergyPlus for thermal modelling in Boston. Similarly, in the UK, Rosser et al., (2019) automated urban scene generation to estimate residential heating demand, utilizing CityGML and CitySim+ for large-scale energy modelling that supports urban planning. Charan et al. (2021) and Fallahi et al. (2022) used UrbanOPT to design for Zero Energy and Zero Carbon on a multi-building scale. It is worth noting that UrbanOPT has unique advantages in evaluating the application of PV systems at the community level.

On the other hand, refurbishment initiatives aim to improve the energy efficiency of aging and poorly insulated buildings. The 'renovation wave' strategy under the EU Green Deal is a notable example of this effort in Europe (Wolf et al., 2021). In Dublin, Buckley et al., (2021) used the Tabula/Episcope framework to create a GIS database of building archetypes and simulated neighborhood-scale building interactions using UMI. In historical districts, where renovations are particularly complex, Caro and Sendra (2018) developed an alternative UBEM approach to assess the thermal behavior of heritage buildings in Seville, using GIS to differentiate between residential and historical structures. Similarly, Teso et al. (2022) employed CityBES in Venice to evaluate energy conservation measures, considering the unique lighting and plug-load distribution in densely built heritage sites.

Despite their strengths, current UBEM applications operate independently of UCMs, relying on simplified meteorological inputs that do not capture localized climate variations (Sezer et al., 2023). This lack of climate sensitivity limits their ability to assess climate-adaptive strategies.

4.5.2 Utilizing shared databases for effective integration of UBEMs and UCMs

A key challenge in UBEMs' and UCMs' integration is scale alignment. It requires harmonized geospatial databases that align modelling inputs and outputs across different spatial scales (Erell, 2008; Mills and Erell, 2024). In addition to aligning spatial scales,

standardizing the input and output data formats across integrated models is important for seamless data exchange. Different models often use disparate data structures and file formats, ranging from building information models to climate data, which makes direct data exchange difficult. To achieve effective integration, this review highlights the importance of establishing common data schemas or implementing metadata conversion pipelines that ensure all models speak a "common language."

In practice, this can involve converting or mapping data into widely accepted formats. For instance, detailed building geometry and attributes can be shared via standards like CityGML or other GIS-based formats (e.g. GeoJSON or shapefiles), which many UBEM tools already support. Likewise, meteorological inputs can be standardized using formats such as EPW files or NetCDF (Network Common Data Form) for climate data, so that UCM outputs (e.g., high-resolution T_a and v) are directly usable by UBEMs after appropriate spatial and temporal downscaling. In addition, adopting Industry Foundation Classes (IFC) or Green Building XML (gbXML) for building information and GeoJSON or shapefiles for urban context data is another strategy to harmonize inputs across platforms (Dong et al., 2007).

In this framework, a shared urban database would use consistent metadata definitions, units, and coordinate systems for all exchanged variables. This means, for example, that building identifiers, geographic coordinates, timestamps, and variable names are standardized, minimizing misinterpretations between models. Overall, investing effort into data format alignment, via standardized schemas or integration middleware, makes the foundation for true interoperability between UBEMs and UCMs allowing models to interface with one another more readily and reliably.

At the urban microscale, BEMs may be particularly useful in conjunction with urban microclimate models to capture detailed microclimatic interactions around buildings, such as airflow, shading, and heat exchange. For larger meso-scale scenarios, such as city-level analyses, UBEMs may be integrated with broader scale meteorological models to account for regional climate influences, such as prevailing wind patterns and solar radiation (Liu et al., 2021). At the core of this integration is the connection between building-scale models and meteorological scales. Each scale (micro-, local-, and meso-) relies on urban environmental and energy simulation models that are interconnected through shared databases (Dorer, 2013). Figure 4.6 illustrates the interconnected database structure shared between climate models and UBEMs to provide a standardized approach of data exchange and data format, because they rely on common datasets such as local meteorological data, detailed building properties, and characteristics of intervening spaces, such as paved areas, greenery, and trees.

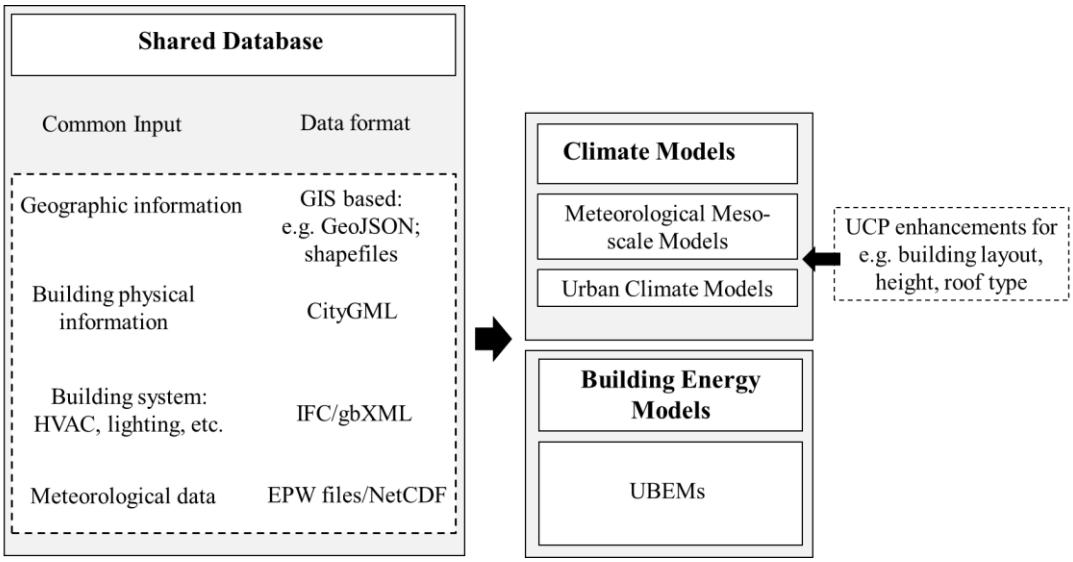


Figure 4.6 Shared Database Framework that supports different climate models and UBEMs (Ali et al., 2021; Oke et al., 2017).

Note: Especially, the UCP method enhances the representation of urban environments in both the MM model and the urban climate model, improving their capability to simulate complex urban settings (Salamanca and Martilli, 2010; Salamanca et al., 2010).

4.5.3 Challenges in multi-scale model integration

Despite the potential of shared databases, several key challenges remain in UBEMs and UCMs integration, particularly in spatial scale differences, model interoperability, as well as data-sharing constraints stemming from privacy and security concerns (Krelling et al., 2023; Wang et al., 2023).

One challenge in building energy simulations is the reliance on standard meteorological datasets, such as Typical Meteorological Year (TMY) files, which are generated from long-term weather observations often made at sites where the urban effect is small or unknown. Tools like the Urban Weather Generator (UWG) (Bueno et al., 2013) can be used to adjust TMY data to account for the urban effect on temperature based on UCPs. This adjustment requires neighbourhood-scale UCP data including building LoD1 information. However, for some simulations more detailed weather data (on airflow, especially may be needed. Mauree et al. (2017) used a canopy interface model (CIM) to generate the boundary conditions for CitySim; a CIM derives this information by adjusting the output of larger scale weather models to account for complex surfaces. Similarly, Mohammed et al. (2024) used WRF simulations coupled with an urban canopy model to generate meteorological data but for a particular period, which was then used in CitySim for building energy analysis. Another example is Mosteiro-Romero et al. (2020), who integrated ENVI-met and CEA for energy performance analysis in Zurich, using ENVI-met's microclimate data to generate boundary conditions for urban cooling demand. The improvements focus on the need for dynamic climate-sensitive

meteorological inputs, rather than static TMY datasets, to improve the accuracy of energy demand predictions at multiple spatial scales.

Another challenge is the mismatch in model resolution and LoD between UBEMs and UCMs (Masson et al., 2020). UCMs typically rely on simpler urban morphological input data (e.g., LoD0-LoD2) for broader, city-scale analyses (Revesz et al., 2020). In contrast, UBEMs need more detailed information (e.g., LoD3-LoD4) to simulate the energy performance of individual buildings. Table 4.6 exhibits these LoD mismatches across different integration levels, illustrating the spatial resolution challenges in model coupling. At the same scale, the required LoD for UCMs is lower than for UBEMs. As a result, most existing integrations rely on one-way coupling, using a UCM to enhance the boundary conditions of the UBEM. Aligning data at appropriate LoDs remains an open issue. For example, translating a city-scale climate model's outputs to inputs meaningful for each building, or aggregating building-level energy outputs so they can inform city-scale climate effects.

Table 4.6 Applicated LoDs for UBEMs and UCMs.

Scales	UBEMs LoD	UCMs LoD	Data Harmonization Challenge
Regional scale	LoD1-2	LoD0-1	UBEMs lack detailed regional climate data, and UCMs simplify energy processes.
Local scale (city level)	LoD1-3	LoD0-1	UCMs lack building-scale energy use details, UBEMs require refined climate variables.
Micro-scale (neighborhood and district level)	LoD1-3	LoD0-2	Inconsistent resolution between UBEMs' detailed building archetypes and UCMs' broader urban zones.
Building scale	LoD1-4	LoD1-4	Model coupling must account for complex heat exchanges and microclimatic feedback.

Beyond these technical issues, data privacy, protection, and security concerns pose a further challenge to model integration. Effective coupling often demands combining datasets from various sources and scales, such as smart meter readings, building occupancy profiles, or GIS building attributes, which may include sensitive information about individuals or private properties (Janghyun et al., 2022). Sharing such fine-grained urban energy data is frequently impeded by privacy regulations and data ownership issues. For example, Europe's General Data Protection Regulation (GDPR) classifies detailed building energy usage (e.g. smart meter data) as personal data, imposing strict requirements on its use and exchange (Voigt and von dem Bussche, 2017). As a result, even if UBEM and UCM platforms are technically interoperable, legal and ethical constraints may limit what data can actually be shared through an integrated framework. This means data interoperability efforts must account not only for format and scale differences, but also for who is permitted to access or contribute data.

4.5.4 Computational trade-offs and scalability

While integrating high-resolution UBEMs with UCMs enhances simulation accuracy, it introduces significant computational burdens, particularly when simulations expand to city-wide or regional applications. Models that require higher level LoD and/or UCP input significantly increase computational complexity and time costs, especially in large-scale urban environment simulations.

In urban climate research, it is often necessary to consider multiple different scenarios or conduct parametric studies. Using complex architectural prototypes can make scene adjustments more difficult, while simple prototypes are easier to implement in multi-scene analysis (Mills et al., 2021). However, this means that detailed information about the building will be lost such as internal heat sources (e.g., occupants, appliances, lighting). It is also impossible to model vertical details like windows and roof slopes in simple models. These contribute to the local microclimate but are often neglected in simplified models (Ambrosini et al., 2014). To balance model complexity and computational feasibility, recent researchers have explored adaptive-resolution approaches. For example, Jin et al. (2021) coupled a BEM with the CCLM climate model to simulate heat fluxes during winter and summer in Berlin. This coupled approach improved the representation of near-surface energy fluxes and T_a at the city scale, dynamically computing the anthropogenic heating of buildings and their heat exchange with the outdoor environment.

In future studies, more hybrid-resolution models are needed. For example, detailed UBEM models are applied to high-impact urban zones, while lower-resolution models cover regional-scale interactions. Cloud-based computing frameworks will also be a good choice for large-scale model simulations, improving computational efficiency.

4.5.5 Advantages and limitations

This review presents a multi-scale perspective on the integration of UBEMs UCMs through shared databases, highlighting how this approach can improve the precision of energy demand forecasting and climate-resilient urban planning. Unlike previous reviews, which have examined UBEMs and UCMs in isolation or focused only on localized micro-scale interactions, this study emphasizes harmonized data exchange and interoperability across spatial scales as the foundation for linking these models dynamically.

A key advantage of the proposed framework lies in its ability to unify different input datasets, including meteorological conditions, urban geometry, and building material properties into a consistent data environment accessible by both UCMs and UBEMs. This integration enables feedback loops where climate simulations can inform building energy use patterns, and conversely, anthropogenic heat emissions from UBEMs can influence local urban climate models. The incorporation of UCPs further enhances UCM

outputs by providing finer representations of building morphology and urban energy fluxes, allowing UBEMs to operate with more realistic boundary conditions.

Despite its contributions, this study acknowledges several limitations that must be addressed in future research. One key challenge is data harmonization, as integrating UCMs and UBEMs requires high-resolution urban morphology, energy consumption, and meteorological datasets, which are often inconsistent or incomplete. Standardized data formats, such as CityGML for urban geometry, EPW for meteorological inputs, and NetCDF for climate data, have improved interoperability, yet gaps remain in their implementation across different models. Furthermore, the mismatch in LoD between models operating at different urban scales remains a key limitation, requiring multi-scale geospatial data frameworks to ensure consistency in energy and climate modelling inputs. Additionally, computational trade-offs must be considered, as high-resolution multi-scale simulations demand significant computing power, often necessitating reduced-order models or downscaling techniques to maintain efficiency.

A critical but often overlooked challenge is data privacy, protection, and security in integrated modelling. UBEMs frequently rely on occupancy patterns, smart meter data, and HVAC control strategies, while UCMs require detailed urban morphology and climate datasets. The aggregation and sharing of such data pose risks related to privacy regulations, proprietary restrictions, and cybersecurity threats. Ensuring compliance with regulations like the General Data Protection Regulation (GDPR) and leveraging privacy-preserving technologies such as differential privacy or federated learning could enable secure and ethical data sharing, fostering wider adoption of integrated UBEM–UCM approaches.

4.6 Conclusion

This review has synthesized the current state of UBEM and UCM integration through shared databases, proposing a unified framework to support overall urban energy and climate management. Adopting such a framework would improve accuracy in assessing urban heat mitigation strategies, energy retrofits, and long-term sustainability goals. Realizing this integrated vision requires ongoing efforts to standardize data formats, resolve model interoperability barriers, and address privacy and computational constraints. The development of open-access, multi-scale urban datasets, similar to efforts like UT-GLOBUS, GloUCP and WUDAPT (Bechtel et al., 2019; Kamath et al., 2024; Liao et al., 2024), will be essential for advancing model integration and improving predictive accuracy. Furthermore, continued advancements in artificial intelligence and machine learning offer promising pathways for data assimilation and parameter optimization, further enhancing the predictive capacity of integrated models.

In summary, this review underscores that integrating UBEMs and UCMs through shared data environments is not only feasible but also essential to achieving energy-efficient

and climate-adaptive urban development. It lays a foundation for more comprehensive, data-driven approaches to urban sustainability, connecting building-level insights with city-scale dynamics to guide smarter, more resilient cities.

Declaration of Competing Interest

The authors declare that they have no known competing financial interests or personal relationships that could have appeared to influence the work reported in this paper.

Acknowledgements

The authors would like to acknowledge funding from China Scholarship Council. The project was partly co-funded under the Excellence Strategy of the Federal Government and the Länder (Project SFBLE003 TRUKLIB).

5. Developing an urban geographic archetype dataset to support energy retrofit strategy on residential buildings in Düsseldorf, Germany

This work has been published under:

Yu, Q., Mills, G., Ketzler, G., & Leuchner, M. (2025). Developing an urban geographic archetype dataset to support energy retrofit strategy on residential buildings in Düsseldorf, Germany. *Energy Reports*, *14*, 282-293.

https://doi.org/10.1016/j.egyr.2025.06.004

Highlights

Development of georeferenced building datasets are replicable and adaptable for Urban Building Energy Models (UBEMs).

The integration with UBEMs to provide actionable insights into building energy efficiency and carbon reduction potential.

Evaluation of energy consumption and refurbishment impacts on residential buildings under current and future climate scenarios.

Identification of high-energy-demand building based on cost-effectiveness and emission reduction.

Support for tailored energy saving retrofits and policymaking to achieve sustainable urban energy goals aligned with the EU’s decarbonization targets.

Abstract

Cities play an important role in climate change mitigation, with building energy use often accounting for the largest share of urban CO_2 emissions. This study introduces an urban geographic archetype dataset integrated with the Urban Building Energy Model (UBEM) tool, CitySim, to assess the long-term impact of refurbishment strategies in residential areas. While the case study focuses on Düsseldorf, Germany, the methodology uses different building archetypes provided by the European TABULA project and climate data under RCP8.5 scenario for the years 2020, 2050, and 2100 to offer broader insights applicable to other European cities. Unlike many existing UBEM applications that neglect boundary conditions, our framework accounts for buildings surrounding the study area, improving simulation accuracy. Our results identify high-energy-demand building types, especially historic and older multi-family residential buildings built before 1957, which occupy over 60% of the housing stock, accounted for 70% of the total heating energy demand. Tailored renovation strategies in these buildings can significantly reduce annual CO_2 emissions by 42% to 46% and decrease heating energy demand by approximately 70% by 2050. Such strategy also can bring significant cost savings, with annual energy costs decreasing from 16.6-18.2 €/m² to 9.6-9.9 €/m². This work contributes to urban sustainability planning by prioritizing retrofit strategies based on building archetypes, climate projections, and spatial context, thus aligning with EU decarbonization targets.

Keywords

Urban building energy model (UBEM); Building archetypes; GIS; CityGML; Building energy use

5.1 Introduction

Cities are recognized as important actors in climate change mitigation strategies due to their significant contribution to global energy consumption and greenhouse gas emissions. Building energy use, in particular, accounts for a substantial portion of urban emissions, presenting both challenges and opportunities for energy efficiency improvements (Mondal et al., 2024). In the EU, commercial and residential buildings account almost equally for energy consumption and the main use of energy by households in 2021 was for heating (64.4%) (Eurostat, 2021a; Eurostat, 2021b). Addressing this, the European Commission has intensified efforts to enhance building energy performance through legislative measures, including the implementation of Minimum Energy Performance Standards (MEPS) as part of the Energy Performance of Buildings Directive (EPBD). These standards are crucial as they set compulsory energy efficiency targets for both new constructions and existing buildings undergoing significant renovations, aiming to significantly reduce their environmental impact. MEPS ensure that buildings take minimum energy efficiency requirements, thus reducing overall energy consumption and promoting environmental sustainability (European Commission, 2021).

However, one key challenge in city-scale energy planning is how to effectively prioritize building retrofits under constrained resources (Buckley et al., 2021; Heracleouset al., 2022). Older urban districts, where buildings vary significantly in age, form, and usage, require location-specific assessments that can guide cost-effective interventions (Jareemit et al., 2025).

As the 7th largest city in Germany with around 619,300 inhabitants (City of Düsseldorf, 2023a), Düsseldorf features large, dense housing areas built outside the city center, characterized by variable energy performance levels associated with age of construction and building standards, which exemplifies this challenge (Landeshauptstadt Düsseldorf, 2011). Older residential buildings constructed before 1978 still made up 70.3% of the total housing stock in 2021 (Datenblatt zum Wohnungsmarkt, 2022). Given their prevalence and significant energy demand, retrofitting these older buildings is key to achieving energy savings with limited resources. Effective decision-making, however, requires not only identifying these high-priority buildings but also thoroughly evaluating the costs and carbon savings associated with various retrofit strategies.

To support such decision-making, energy modelling approaches are commonly used. These fall into two main categories: top-down (Swan and Ugursal, 2009) and bottom-up approaches (Kavgic et al., 2010). The top-down method aggregates energy data at a macro level to estimate overall consumption, while the bottom-up approach provides detailed insights by analyzing individual or grouped buildings based on specific characteristics like thermal properties and energy systems (Böhringer and Rutherford,

2008, Ferrando et al., 2020). This study utilizes the latter by applying an Urban Building Energy Model (UBEM).

UBEMs extend traditional Building Energy Models (BEMs) to the urban scale and consider multiple buildings and the interactions between them as well as the impact of urban infrastructure and microclimate (Ang et al., 2020). UBEMs simplify building stock descriptions by categorizing structures into archetypes while accounting for spatial factors such as proximity, layout, and green spaces. This makes them particularly useful for analyzing energy performance at the neighborhood or city scale (Reinhart and Davila, 2016; Giuzio et al., 2025). Beyond simulating energy use, UBEMs enable policymakers to prioritize interventions by identifying high-energy-use building clusters, estimating the costs of retrofit measures, and calculating carbon savings under future climate scenarios (Excell et al., 2024, Kong et al., 2023).

However, a common limitation in UBEM studies is the assumption of spatially closed systems. Many simulations only consider buildings within the boundaries of the study area while omitting adjacent structures that can affect energy performance through solar obstruction, wind buffering, or mutual thermal exchange (e.g., Cerezo et al., 2017; Li et al., 2020; Ullah et al., 2024). This oversight can lead to incomplete or inaccurate energy performance assessments of buildings at the edges of the study area.

To address these gaps, this study develops a replicable UBEM framework based on a georeferenced archetype dataset and applies it to a densely built residential neighborhood in Düsseldorf. The dataset integrates GIS-based urban morphology with TABULA building typologies (Tabula WebTool, 2023). It contains precise locations and structural characteristics of buildings, such as dimensions, construction materials, and energy usage information, mapped onto an accurate model of urban morphology. Through the use of this dataset in one of UBEMs, CitySim, and combining future climate projections, the study provides a scalable method for identifying high-priority retrofit targets and quantitatively analyzes how specific energy-efficient renovations impact the overall energy performance of buildings within the neighborhood. This is a model study concerning energy use but with the real data part of geodata from a real neighborhood. Besides, unlike other UBEM approaches, our model clearly incorporates adjacent buildings outside the simulation core to account for boundary effects. While grounded in a specific case study, the framework is designed to be transferable to other European cities covered by the TABULA database.

This research is guided by the following key questions: i) How can a replicable framework integrating UBEM simulations and georeferenced datasets be designed to support urban energy planning and renovation strategies across European cities?, ii) Which types of residential building contribute most to energy consumption and CO_2 emissions, and how can they be effectively prioritized for retrofitting?, and iii) What are

the potential impacts of targeted renovation strategies on energy demand, carbon emissions, and cost-effectiveness at different time horizons (e.g., 2020, 2050, and 2100)?

In the following, we detail the procedure used to create the UBEM inputs and run energy simulations using CitySim. These steps involve generating georeferenced datasets, integrating climate and building archetype data, and conducting simulations to evaluate the energy consumption of the neighborhood under various scenarios.

5.2 Methodology

The UBEM workflow used in this study consists of three parts: (1) Input data preparation (includes a georeferenced building dataset and climate data), (2) the CitySim Pro simulation and (3) result analysis (Fig 5.1). The output is an assessment of neighborhood energy effects that can be used to evaluate the impact of building refurbishing and climate change. Yu et al. (2025) reviewed the use of different existing UBEM tools and data formats, and compared the advantages, disadvantages, and applicability of each UBEM in different city analyses.

CitySim as an UBEM was selected due to its efficiency in processing fewer inputs while still providing comprehensive energy assessments. It only needs climate data and urban building data (Mutani et al., 2018). The input climate data was generated by Meteonorm 8, a tool that produces synthetic weather series based on historical climate records (Remund et al., 2020). The input urban building data are derived by combining publicly available Geographic Information System (GIS) data (neighborhood layout) with building data acquired from the Episcope Tabula project (Loga and Diefenbach, 2016), which created residential building typologies for 20 European countries. This case study is based on the Germany Tabula type. In terms of operation, CitySim utilizes these inputs to simulate energy flows and interactions within urban environments. The reliability of model results has been verified by several previous studies (Walter and Kämpf, 2015; Haneef et al. 2021).

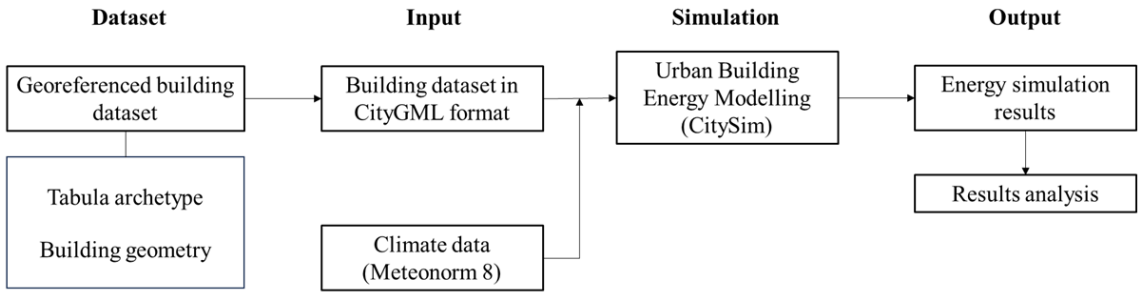


Figure 5.1 Workflow used in this study.

Note: The geospatial building dataset is GIS integrated georeferenced building information and Tabula archetypes to create a database in CityGML format. These data are used with climate data to run CitySim.

5.2.1 Georeferenced building datasets and study area

The first step of the workflow is the creation of a georeferenced building dataset using publicly available sources that integrate detailed building characteristics with spatial urban morphology. The primary data source for building characteristics was the Tabula WebTool, which provides detailed information on residential building types across Europe. This includes data on construction periods, insulation levels, and other energy-related features for energy modelling (Tabula WebTool, 2023). The comprehensiveness of the Tabula database allows for the application of this workflow in various national contexts within the Tabula program, making it adaptable for future studies across different European cities. Meanwhile, we acquired a comprehensive GIS dataset from the North Rhine-Westphalia Information and Technical Department (2022). This dataset includes details about the urban morphology of Düsseldorf, such as building footprints, heights, layouts, as well as population data from the Düsseldorf Census (Düsseldorf Census, 2020). The integration of the GIS data with the building typologies from the Tabula WebTool enabled us to form a robust foundation for our energy simulation models. The georeferenced building dataset thus created not only allowed an accurate representation of the physical and thermal properties of the built environment but also facilitates the mapping of the neighborhood's structure, identifying building clusters, and capturing shading effects.

The case study area is Düsseldorf-Flingern, a neighborhood characterized predominantly by residential buildings of different ages arranged as terraces along roads, creating perimeter block development. Flingern is a typical German neighborhood (Hofmeister, 2003), here a typical sub-set of 22 blocks is investigated. The residential buildings in each block are interspersed with others used as small workshops, offices, and schools. A notable feature of the block is the variation in building heights, with taller buildings at the edges of blocks (on major roads) and lower rise houses in the interior (Figure 5.2). The target residential buildings are categorized into eight major archetypes using Tabula, based on age and construction materials (Figure 5.3). These archetypes represent 52% of the generic residential building types in Germany (Loga et al., 2012). We can find that taller structures, such as Multi-Family Houses (MFH) and Apartment Buildings (AB) (average height ~20m), typically exceed 12 meters in height and are mainly located at the periphery of each block forming a terrace, with only a few buildings isolated within block interiors. In contrast, Terraced Housing (TH) and Single-Family Houses (SFH) are generally lower (average height ~9 m), typically under 12 meters, and are usually situated within the interior of each block. While the focus of this work is on the residential buildings inside the study area (861 buildings in total), the model setup includes an additional 461 buildings outside and inside the study area (yellow color buildings in Figure 5.2), and non-residential buildings within the case-study area to account for radiation exchanges, including shadowing and daylight effects.

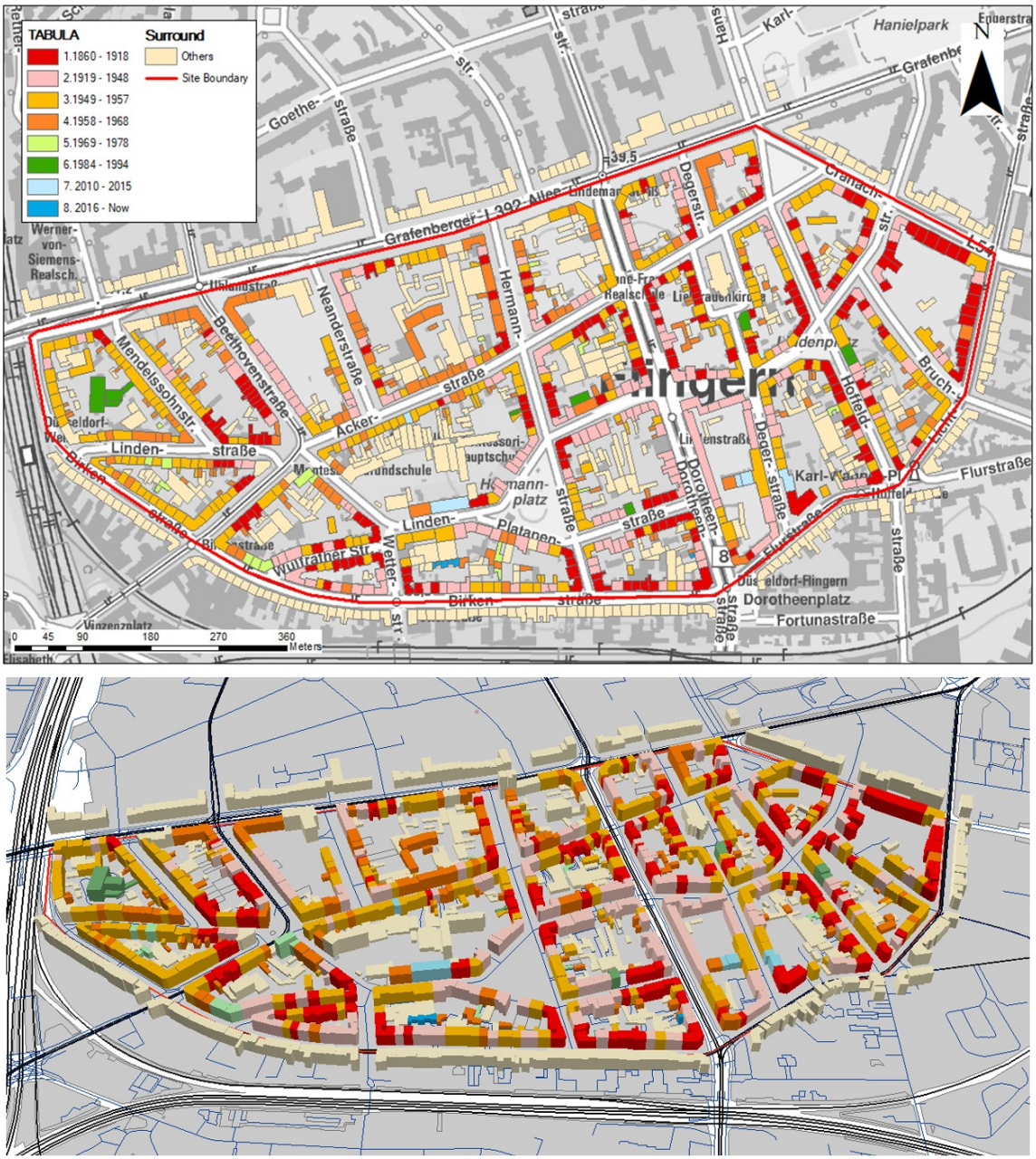


Figure 5.2 The distribution of buildings in the study area.

Note: top: target residential buildings and surrounding buildings, target residential buildings are categorized into 8 Tabula classes; bottom: a 3D sketch of the study area indicating the building height structure.

The classification of buildings in Flingern was based on fieldwork and Google Street View data. While observations using the Tabula example images were mostly accurate, some misclassification can occur. For example, some buildings may display a vintage aesthetic that may not match its construction period; to mitigate this, we cross-referenced our work using aerial photographs and interviewing occupants. The historical aerial photographs of Düsseldorf come from the development team of the surveying and cadastral office (City of Düsseldorf, 2023b). One example for such a challenging age

determination is the building at Ackerstraße 168a (Figure 5.4). Its architecture is indicative of the Wilhelminian era (1860-1918). Contrary to this initial assessment, our examination of historical aerial photographs revealed that the building existed in 1927, then was missing – likely through war impact - in the aerial photograph of 1958 and was re-constructed between 1958 and 1979. Subsequently, our interviews with residents at the site yielded information indicating that the precise construction date for this edifice was in 1963; this date is also used to define the material standard for modelling.

1 TH (1860-1918) 1 MFH (1860-1918) 2 MFH (1919-1948) 2 AB (1919-1948)






3 TH (1949-1957) 3 MFH (1949-1957) 3 AB (1949-1957) 4 TH (1958-1968)






4 MFH (1958-1968) 4 AB (1958-1968) 5 SFH (1969-1978) 5 TH (1969-1978)






5 AB (1969-1978) 6 TH (1984-1994) 6 MFH (1984-1994) 7 TH (2010-2015)



7 MFH (2010-2015) 8 TH (2016-now)



Figure 5.3 Examples of Single-Family House (SFH), Terraced House (TH), Multi Family Houses (MFH), and Apartment Blocks (AB) built in Düsseldorf in different periods (see Table 5.1 for details).



Figure 5.4 The building at Ackerstraße 168a.

Note: Left and right pictures from the development team of the surveying and cadastral office (City of Düsseldorf, 2023b); center picture is the on-site photo.

Details on the characteristics of walls, roofs and glazing features and building HVAC systems in the potential original state are given in Table 5.A.1 and Table 5.A.2 in supplementary information based on the Tabula WebTool (Remmen et al., 2018) (cf SI: Table 5.A.1 and Table 5.A.2). These building data are stored in a GIS database.

Population per block from Düsseldorf Census (2020) is shown in Table 5.1 Statistically, the study area accommodates 10427 residents with primary residences.

Table 5.1 The number and population distribution of different buildings in the study area are summarized (Düsseldorf Census, 2020).

Tabula	Year of construction	Subtype	Building Number	Total Floor Area (m^2)	Percentage	Population Census
1	1860-1918	TH	4	399.84	0.46%	2960
		MFH	188	120628.64	21.81%	
2	1919-1948	AB	24	36377.85	2.78%	3160
		MFH	157	112600.55	18.21%	
3	1949-1957	TH	35	5412.08	4.06%	4270
		AB	34	49219.8	3.95%	
		MFH	203	165220.22	23.58%	
4	1958-1968	TH	91	15230.24	10.57%	1960
		AB	24	31227.93	2.79%	
		MFH	62	48939.04	7.20%	
5	1969-1978	SFH	4	378.03	0.46%	210
		TH	7	858.19	0.81%	
		AB	7	7555.39	0.81%	
6	1984-1994	TH	4	552.96	0.46%	290
		MFH	7	10422.74	0.81%	
7	2010-2015	TH	2	1396.28	0.23%	170
		MFH	3	5989.51	0.35%	
8	2016-now	TH	6	914.84	0.70%	60

Note: Total Floor Area = sum of the area of each floor (for the Tabula classes), population per block is extrapolated to the Tabula classes proportional to the surface.

5.2.2 Construction of a CityGML database for UBEM

UBEMs rely on standardized input data to enable large-scale simulation and analysis of building energy performance. The second stage of our workflow involves converting the georeferenced building dataset into the CityGML format for use in energy simulations with CitySim (Gröger and Plümer, 2012). Among available data formats, CityGML and its Application Domain Extension (ADE) are the most commonly used standards in UBEM applications (Chen et al., 2019, Noardo et al., 2021). CityGML provides 3D geometric representations of buildings and urban environments, while the Energy ADE enhances this format by embedding energy-related attributes, such as construction year, thermal characteristics, and HVAC system details (Fallside and Walmsley, 2004).

In our study, the ADE schema includes detailed information such as TABULA-linked building typologies, construction year, wall and roof U-values, window material and g-values, HVAC system types, and primary heating fuel sources (cf. SI in Chapter 5.5: Table 5.A.1, 5.A.2, and 5.A.3). These attributes are essential for CitySim simulation, which use them to calculate heating and cooling demands. All data are in the semantic structure of each CityGML building object to ensure interoperability and maintain modelling accuracy.

CityGML supports multiple Levels of Detail (LOD), ranging from basic block representations (LOD1) to more detailed architectural models (LOD2 and higher) (Yu et al., 2025). In this study, we used both LOD1 and LOD2 to ensure sufficient geometric accuracy for our simulation needs. The GIS-based building dataset was converted into CityGML using a custom ArcMap plugin. During this process, each building was assigned a unique identifier (ID), and manual verification was conducted to ensure ID uniqueness and data integrity. This unique ID enables robust linkage between the GIS spatial dataset and the energy attributes required by CitySim, facilitating consistent and traceable model inputs across platforms.

5.2.3 Climate data and climate indicators for energy demand

The CitySim energy simulations require hourly climate data as input (Chen et al., 2020). Here, we used climate data generated by Meteonorm 8, which uses historical climate records to generate typical mean year (TMY) hourly values for T_a, solar irradiation, v, humidity, and other relevant meteorological parameters (Remund et al., 2020). We used the series for current Düsseldorf climate (2020) and for future climate scenarios (2050 and 2100). The data for 2020 were generated using the empirical Heliosat method, which simulates hourly observations from various sources, mostly based on synoptic meteorological stations located at airports. For future climate, we selected the high greenhouse gas emissions scenario (based on the Intergovernmental Panel on Climate Change), which results in a representative concentration pathway associated with an 8.5 Wm-2 radiative forcing (i.e., RCP8.5) at the end of the 21st century as a worst-case scenario (Veal, 2021).

These hourly data are used to construct indices of heating and cooling needs using Heating Degree Days (HDD) and Cooling Degree Days (CDD), respectively (Spinoni et al., 2018). These indices provide insight into how climate changes will affect the energy demand for space conditioning over time (Escandón et al., 2023, Park, et al., 2021, D'Amico et al., 2019). Here, daily HDD values are calculated by using 15 °C as a base temperature, while daily CDD values are calculated by 22 °C (DWD Climate Data Center, 2019). Degree days are calculated using (European Commission, 2020):

$$\text{If } T_m \leqslant 15°C \text{ Then } [HDD = \sum_i (15 - T^i_m)] \text{ Else } [HDD = 0] \quad (1)$$

$$\text{If } T_m \geqslant 22°C \text{ Then } [CDD = \sum_i (T^i_m - 22)] \text{ Else } [CDD = 0] \quad (2)$$

Where T_m is daily mean air temperature and T^i_m means air temperature of day i (day 1-365). These calculations were executed on a daily basis and summed up to a calendar month and subsequently to calendar years.

Düsseldorf (51°14’N, 6°48’E) experiences a temperate oceanic climate. Figure 5.5 illustrates the monthly HDD and CDD for the years 2020, 2050, and 2100, alongside the corresponding annual average temperatures for these years. In the 2020 data set, the

coldest month is January with an average of ~3.3°C and the warmest month is July with an average of ~20.3°C. In the RCP8.5 future climate scenario, January average temperatures in 2050 and 2100 are projected to be ~ 4.8 °C and 7.4 °C, respectively, while July average temperatures are projected to be 21.4°C and 25.2°C, respectively. Figure 5.6 also shows a decreasing trend in HDD from 2020 to 2100 with a nearly 35% decrease in HDD for winter months (January, February, December). On the contrary, there is a noticeable increase in CDD from 2020 to 2100, especially in summer months (June, July, August), indicating hotter summers and higher cooling demands; notably there is a projected 400% increase in the 'shoulder' months (May, September), indicative of a longer cooling season. The increase of overall CDD by 2100 in the RCP8.5 scenario is expected to exceed the decrease in HDD for the period April to October compared to 2020.

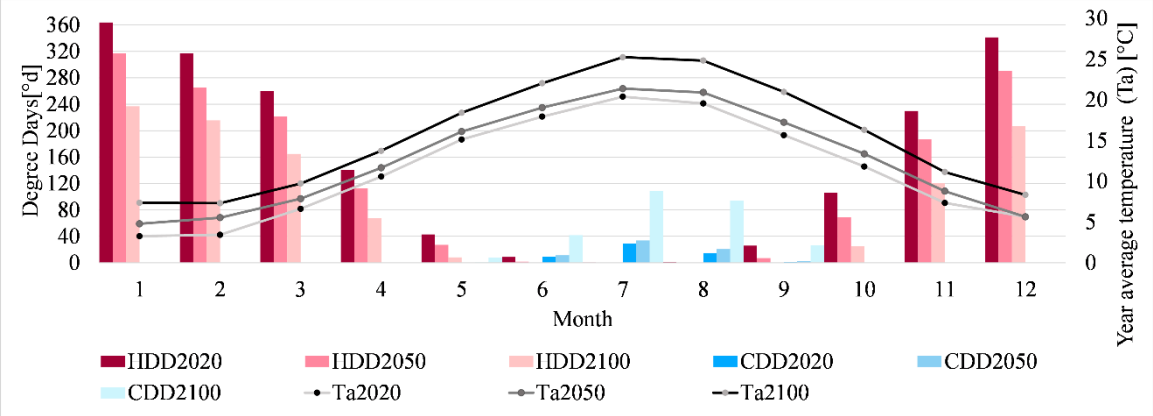


Figure 5.5 Monthly heating degree days (HDD) and cooling degree days (CDD) in 2020, 2050 and 2100 and corresponding monthly mean air temperature data.

5.2.4 CitySim experiments

The CitySim UBEM platform was used to simulate the thermal energy performance of residential buildings under current and projected climate conditions. Model inputs included CityGML-formatted building geometries with energy-related attributes and hourly weather data for three representative years: 2020, 2050, and 2100. These datasets were generated using Meteonorm 8.0 based on the RCP8.5 scenario, allowing the evaluation of retrofit performance under high-emission climate scenarios.

The model processes building geometry, surface characteristics, and microclimate interactions to compute hourly heating, cooling, and lighting energy needs (Chen et al., 2020). The CitySim simulations account for dynamic solar gain, longwave radiation exchange, internal heat gains, and the interaction of buildings with surrounding structures and vegetation (Evins and Carmeliet, 2014). Both heating and cooling

demands were simulated using CitySim. Active cooling systems were not included (because they're rare), but cooling demand was still computed based on thermal balance, representing potential cooling needs rather than actual energy use. Electricity use for appliances and lighting was held constant across all scenarios and excluded from the energy savings calculation.

Building refurbishment strategies were defined using options from the TABULA WebTool for Germany, including insulation upgrades, window replacement, and heating system improvements. Among that, older buildings built before 1970 primarily use gas or oil boilers, and newer buildings built after 1970 use district heating or condensing boilers (Remmen et al., 2018). Each archetype was simulated in both its original and refurbished state, enabling direct comparison under current and future climate scenarios.

To assess the financial viability of retrofitting, we calculated the simple payback period and net present value (NPV) for each archetype using standardized economic assumptions (Haneef et al., 2021; Heracleous et al., 2022). These include an average retrofit cost of €600 per square meter, a 30% government incentive on initial investment, a discount rate of 3% per annum, and a 30-year evaluation period (CPI, 2011; Galvin, 2023). CO_2 emission reductions were calculated from differences in simulated heating demand between original and retrofitted cases and were monetized using a carbon price of €55 per ton, based on the 2025 benchmark set by the German Emissions Trading Authority (DEHSt) (North Rhine-Westphalia Information and Technical Department, 2022; The German Federal Government, 2020). Energy cost is assumed to remain constant (i.e. no inflation), and energy savings are calculated as the difference in energy cost per m² before and after refurbishment. The resulting annual carbon savings in €/(m²·year) were added to the energy cost savings in the NPV calculation, as detailed in Section 3.3.

While the structure of this workflow is consistent with established UBEM methodologies, this study introduces several innovations. First, we include adjacent buildings beyond the target simulation area in the CitySim model to capture edge conditions such as shading, wind blocking, and heat exchange, effects that are often neglected in UBEM implementations. Second, the building dataset integrates a CityGML-ADE schema with field-verified TABULA typologies to improve the semantic and thermal accuracy of each building object. Third, our process includes a partially automated process for converting GIS data into CityGML format for simulation, which was manually validated for consistency and completeness. These refinements enhance spatial realism and typological precision, offering a replicable and transferable method for assessing retrofit potential in other European cities.

5.3 Results and discussion

5.3.1 Prioritization of retrofitting efforts

Figure 5.6 presents the annual average heating and cooling energy intensities (in kWh/m²) for target residential buildings in the study area. Both heating and cooling demands were simulated using CitySim; however, it is important to note that mechanical cooling systems were not explicitly modelled due to their low prevalence in the region (as detailed in Section 5.2.4). As a result, the reported cooling energy intensity reflects theoretical demand required to maintain thermal comfort in warm periods, rather than actual operational energy use.

Across all years and building states, heating energy intensity consistently exceeds cooling energy intensity, emphasizing that heating remains the primary target for energy efficiency improvements. Despite variations among building types and scenarios, this pattern holds true even in the most climate-stressed conditions projected for 2100, highlighting that energy efficiency efforts should continue to prioritize heating performance.

Heating energy intensity exhibits a consistent decrease from 2020 to 2100 in both original (Figure 5.6A) and refurbished (Figure 5.6B) states. This trend corresponds to the reduction in HDD as global temperatures rise under future climate scenarios. Refurbished buildings show significantly lower heating energy intensity compared to their original counterparts, demonstrating the effectiveness of retrofitting measures in reducing heating demands. For example, heating intensity in older Type 1 MFH buildings drops from over 60 kWh/m² in the original state to below 20 kWh/m² in the refurbished state in both 2020 and 2050. The reduction rate is approximately 70%.

In contrast, cooling energy intensity shows a steady upward trend from 2020 to 2100 across all building types, driven by the increase in CDD associated with warming climates. However, even by 2100, cooling intensity remains substantially lower than heating intensity. Refurbished buildings exhibit slightly lower cooling energy intensity than original states, but the differences are modest. For example, cooling intensity for older Type 1 MFH buildings decreases from just over 3 kWh/m² in the original state to slightly below 2 kWh/m² after refurbishment. This suggests again that refurbishment measures are primarily designed to improve heating efficiency, with limited direct impact on cooling demand.

Older buildings, particularly MFH and TH types built before 1978 (Types 1-5), exhibit the highest heating energy intensity in their original state. These buildings benefit the most from refurbishment, with substantial reductions in energy intensity post-retrofit.

In contrast, buildings constructed after 1980 demonstrate a significant drop in heating energy intensity, even in their original state. Representative examples, Types 7 and 8,

built after 2010, exhibit relatively low heating energy intensity in their original states due to modern construction standards, resulting in only minor reductions after refurbishment.

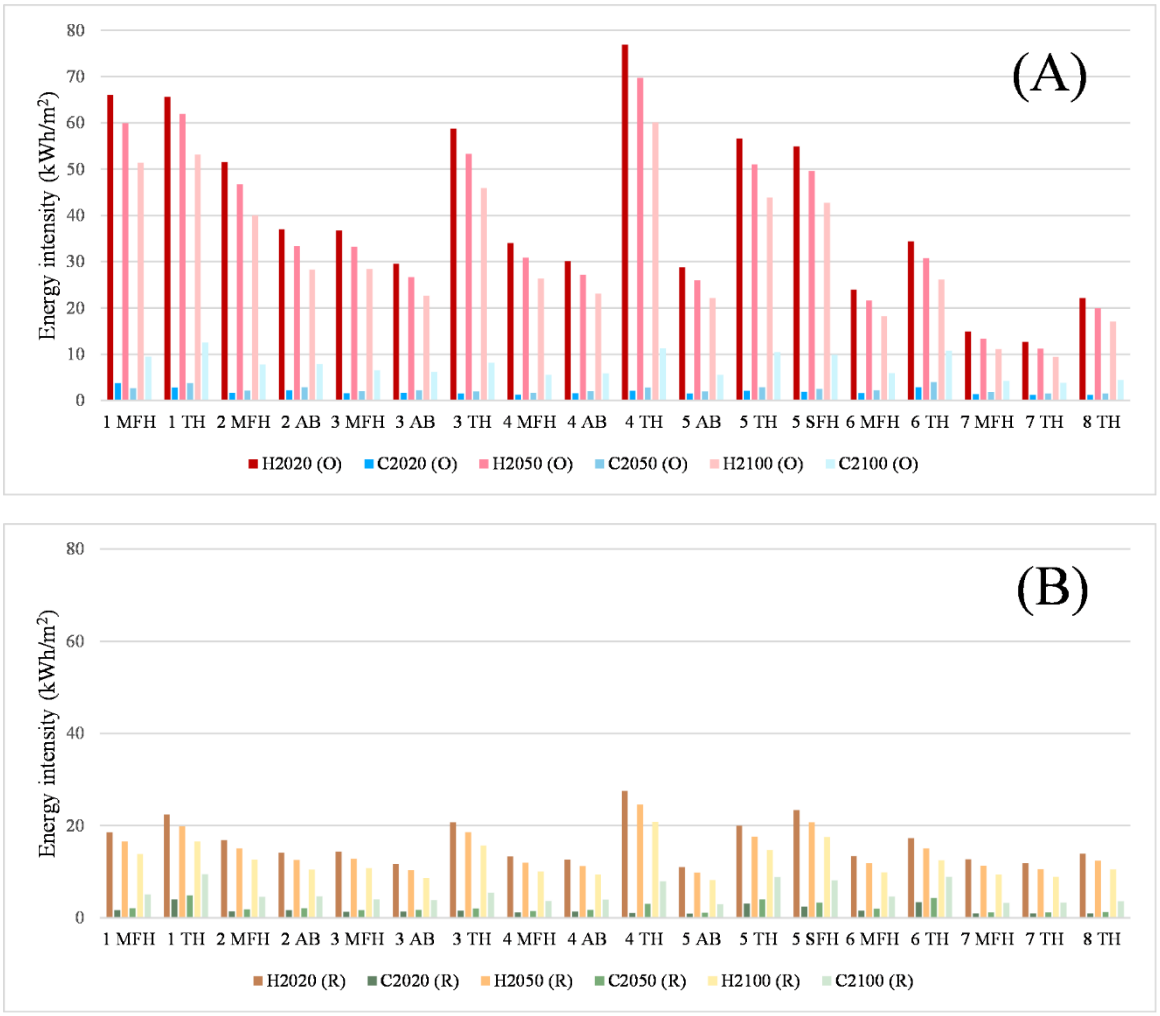


Figure 5.6 Annual average heating and cooling energy intensity (kWh/m²) for target residential buildings.

Note: Target residential buildings under original states (above A) and refurbished states (below B) in 2020, 2050 and 2100. H2020 (O) and H2050 (O) represent original heating energy intensity in 2020 and 2050, respectively; H2020 (R) and H2050 (R) represent refurbished heating energy intensity in 2020 and 2050, respectively.

Table 5.2 highlights the annual heating energy consumption in 2020 and 2050 for residential buildings in their original and refurbished condition, aligning with the EU's decarbonization goals. The exclusion of 2100 data reflects the consideration that building stocks and technologies are likely to undergo significant changes by then, making long-term projections less reliable. The data is sorted in descending order based on the number of residential buildings, highlighting the contribution of each type to the overall energy demand. This organization allows for a clear understanding of which

building types contribute the most to heating energy use and should be prioritized for retrofitting.

Table 5.2 highlights the capital contribution of 1, 2, and 3 MFH types to overall heating energy consumption in both 2020 and 2050, making them the primary targets for refurbishment. These building types not only have the largest populations and total floor areas but also exhibit significant reductions in energy demand after refurbishment. In 2020, these three MFH types account for more than 70% of the total heating energy consumption in both their original and refurbished states. For example, 1 MFH alone consumes 7,963,903 kWh in its original state in 2020 (H2020 (O) %), representing 29% of the total heating demand. In the original scenario of the future 2050 (H2050 (O) %), even if the total energy consumption decreases (7,230,481 kWh), the total heating share is still as high as 29%, which is almost the same as in 2020. After refurbishment, although this value decreases substantially to 2,235,248 kWh, it still accounts for ~23% of the total heating energy consumption. This substantial energy savings reinforces the need to prioritize these three MFH types for retrofitting efforts to achieve meaningful energy and carbon reductions.

Other building types constructed before 1978, such as 4 TH, 3 TH, 3 AB and 4 MFH, also consume significant heating energy relative to their size. For example, 4 TH comprises about 10% of the total population in this study area (Table 5.1), yet it only consumes ~4% of the total heating energy in 2020, or 1,135,435 kWh in its original state. However, the potential reduction through refurbishment is significant, reaching 64% post-retrofit. These older building types should be the next priority for retrofitting efforts once the refurbishment of 1, 2, and 3 MFH types is completed. Their smaller contribution to overall energy use makes them less critical initially but still valuable for further extending energy savings.

In contrast, modern building types such as 7 MFH, 7 TH, and 8 TH have lower energy consumption due to their adoption of modern building technologies and compliance with stricter energy efficiency standards. These newer buildings contribute minimally to total energy consumption and therefore do not require prioritization in retrofitting programs. Their emissions and energy costs are already low.

Table 5.2 Total annual heating demand (H in kWh) in original (O) and refurbished (R) buildings under different climate scenarios in 2020 and 2050.

Count	Pop (%)	Types	Total area (m^2)	H2020 (O) (kWh)	H2050 (O) (kWh)	H2020 (O) (%)	H2050 (O) (%)	H2020 (R) (kWh)	H2050 (R) (kWh)	H2020 (R) (%)	H2050 (R) (%)
203	23.6%	3 MFH	165220.2	6066886	5495225	22.1%	22.1%	2372562	2121428	24.8%	24.9%
188	21.8%	1 MFH	120628.6	7963903	7230481	29.0%	29.0%	2235249	1997610	23.4%	23.4%
157	18.2%	2 MFH	112600.6	5797802	5260698	21.1%	21.1%	1895067	1693512	19.8%	19.8%
90	10.5%	4 TH	14765.1	1135435	1029127	4.1%	4.1%	407074	363074	4.3%	4.3%
62	7.2%	4 MFH	48939.0	1663927	1509280	6.1%	6.1%	652847	583843	6.8%	6.8%
35	4.1%	3 TH	5412.1	317960	288464	1.2%	1.2%	112355	100448	1.2%	1.2%
34	3.9%	3 AB	49219.8	1453953	1312200	5.3%	5.3%	573903	509917	6.0%	6.0%
24	2.8%	2 AB	36377.9	1346708	1214293	4.9%	4.9%	514383	456906	5.4%	5.4%
24	2.8%	4 AB	33553.7	1009295	911653	3.7%	3.7%	423783	377479	4.4%	4.4%
7	0.8%	6 MFH	10422.7	249729	225131	0.9%	0.9%	139665	123822	1.5%	1.5%
7	0.8%	5 AB	7555.4	217293	196667	0.8%	0.8%	82883	73892	0.9%	0.9%
7	0.8%	5 TH	858.2	48591	43793	0.2%	0.2%	17181	15061	0.2%	0.2%
6	0.7%	8 TH	914.8	20255	18242	0.1%	0.1%	12707	11335	0.1%	0.1%
4	0.5%	1 TH	399.8	26226	24770	0.1%	0.1%	8968	7937	0.1%	0.1%
4	0.5%	5 SFH	378.0	20758	18750	0.1%	0.1%	8835	7837	0.1%	0.1%
4	0.5%	6 TH	553.0	19022	16992	0.1%	0.1%	9533	8311	0.1%	0.1%
3	0.3%	7 MFH	5989.5	89483	79780	0.3%	0.3%	75767	67442	0.8%	0.8%
2	0.2%	7 TH	1396.3	17677	15694	0.1%	0.1%	16602	14731	0.2%	0.2%

Note: The retrofits are based on Tabula Usual Refurbishment (North Rhine-Westphalia Information and Technical Department, 2022). The table also includes building numbers (Count), population percentage (Pop %), total floor area (m2), and total heating energy percentage per building type. They are sorted by building type count (from largest to smallest). For example, H2020 (O) % and H2020 (R) % represent the percentage of total energy consumption in 2020 for each type of building in its original or refurbished state.

5.3.2 Financial and carbon reduction benefits of retrofitting

To create an effective neighborhood transformation plan for carbon reduction (for example, 50% reduction) while maximizing energy cost savings, it is essential to focus on refurbishing buildings with both high energy consumption and high carbon emissions. Table 5.3 compares the CO_2 emissions (in kg/m² per year) and associated costs for different residential building types in their original (O) and refurbished (R) states, as outlined in the Tabula renovation plan (North Rhine-Westphalia Information and Technical Department, 2022). It also includes the CO_2 reduction rate (%) and energy costs (original and refurbishment) per square meter annually, helping to identify building types with the greatest potential for CO_2 reductions and cost-effectiveness when retrofitted.

Older building types of 1 MFH, 2 MFH, and 3 MFH show the highest total CO_2 emissions in their original state, with values exceeding 6,8Mt per year for 1 MFH and 9,8Mt per year for 3 MFH. Refurbishment can reduce CO2 emissions for these building

types significantly with CO_2 reduction rates ranging between 42% and 46%. Among them, 2 MFH achieves the highest CO_2 reduction rate at 46.25%, with annual emissions decreasing from 62.7 kg/m² to 33.7 kg/m². In contrast, newer buildings such as 7 MFH, 7 TH, and 8 TH have much lower original CO_2 emissions, ranging from 25 to 28.7 kg/m² per year. Their refurbishment results in smaller reductions in CO_2 emissions (28–33%) due to their already efficient construction standards.

In monetary terms, retrofitting these older buildings of 1 MFH, 2 MFH, and 3 MFH also results in significant energy cost savings. After refurbishment, energy costs can drop significantly from 16.6-18.2 €/m² to 9.6-9.9 €/m² annually, making these buildings highly cost-effective targets for retrofitting. Other older building types, such as 4 AB, 4 MFH, and 4 TH also offer good opportunities for CO_2 reductions (37–45%) and moderate cost savings. These buildings can be considered for refurbishment after addressing the high-priority MFH types. Newer buildings, such as 7 MFH and 8 TH, already have low existing energy costs (7.8-8.9 €/m² annually) and exhibit limited potential for savings. Their refurbishment energy costs are further reduced to 5.7-6.2 €/m² annually, but the savings are minimal. Thus, these newer buildings should not be a focus of retrofitting efforts, given their already efficient performance and limited return on investment.

Table 5.3 Annual CO_2 emissions (kg/m²·a) total annual CO_2 emission reduction (Mt/a), and the annual energy costs (€/ (m^2. a)) for residential building types in original (O) and refurbished (R) states.

Types	CO_2 (O) (kg/(m²·a))	CO_2 (R) (kg/(m²·a))	Total CO_2 (O) (Mt/a)	Total CO_2 (R) (Mt/a)	CO_2 Reduction Rate (%)	Energy Cost (O) (€/ (m^2·a))	Energy Cost (R) (€/ (m^2·a))
1 MFH	57.1	33.1	6.89	3.99	42.00%	16.6	9.7
1 TH	62.9	39.3	0.03	0.02	37.50%	18.4	11.7
2 MFH	62.7	33.7	7.06	3.79	46.30%	18.2	9.9
2 AB	56.5	30.5	2.06	1.11	46.00%	16.4	9
3 MFH	59.5	32.8	9.83	5.42	44.90%	17.3	9.6
3 AB	56	30.2	2.76	1.49	46.10%	16.3	8.9
3 TH	62.1	36.2	0.34	0.2	41.70%	18.2	10.8
4 MFH	52.6	29.5	2.57	1.44	43.90%	15.3	8.7
4 AB	53	28.9	1.78	0.97	45.50%	15.4	8.5
4 TH	49.3	30.8	0.73	0.45	37.50%	14.6	9.3
5 AB	49.3	27.9	0.37	0.21	43.40%	14.4	8.2
5 TH	54.7	34	0.05	0.03	37.80%	16.1	10.2
5 SFH	62.4	38.6	0.02	0.01	38.10%	18.3	11.5
6 MFH	50.5	30.9	0.53	0.32	38.80%	14.7	9.1
6 TH	46.8	33.5	0.03	0.02	28.40%	13.9	10.1
7 MFH	27.7	19.9	0.17	0.12	28.20%	8.3	6
7 TH	28.7	19.2	0.04	0.03	33.10%	8.9	6.2
8 TH	25	17.5	0.02	0.02	30.00%	7.8	5.7

[*]**The energy cost values are based on EnEV 2009/2014/2016 (North Rhine-Westphalia Information and Technical Department, 2022). Inflation and advancements in techniques and materials may have changed current costs.**

Note: The total floor area is used as the basis for calculating all square meter measurements.

To further support policy decision-making, we estimated the simple payback time and NPV (Haneef et al.,2021; Heracleous et al.,2022). Here, we only discuss TABULA 1-4 building types, that are in prioritization (Figure 5.7).

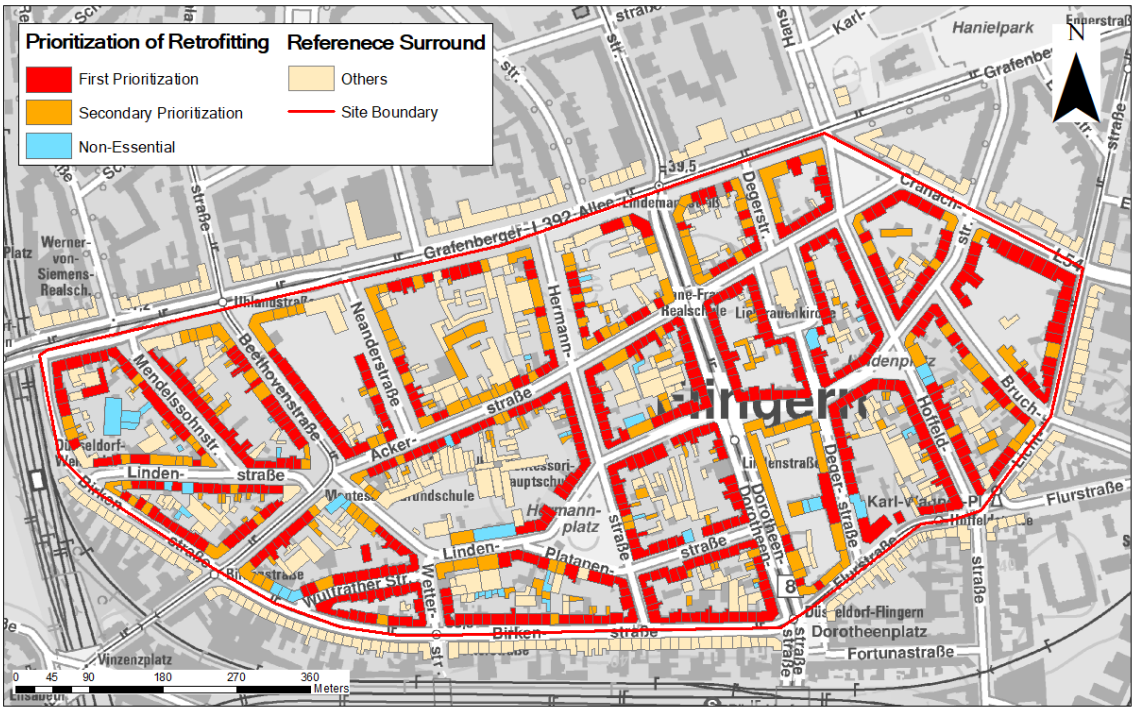


Figure 5.7 Prioritization map of potential residential retrofit.

Table 5.4 shows the annual energy savings (€/m²·a), annual CO_2 saving, (€/m²·a), simple payback time (years), NPV (€/m²), and cumulative CO_2 emissions incurred between 2020 and 2025 as a result of delayed retrofitting for each building type. As can be seen from Table 5.4, the present net value NPV of the refurbishment investment is negative regardless of building type, confirming that energy efficiency improvements alone are not sufficient to recover retrofit investments over a 30-year period. These findings align with recent literature, which highlights that deep energy renovations are not yet financially viable without enhanced subsidies or long-term carbon pricing (Galvin, 2024). However, the data also highlights the significant environmental cost of inaction. Delaying refurbishment leads to huge cumulative emissions, weakening the long-term effectiveness of any future mitigation strategies. For example, if refurbishment of type 1 MFH buildings is postponed by five years (from 2020 to 2025), it would result in approximately 14.5 Mt of additional CO_2 emissions. It missed an opportunity for early abatement that cannot be offset later by higher carbon prices alone. These numbers stress the importance of timing in climate policy: early retrofit action delivers not only higher cumulative CO_2 reduction but also preserves the economic value of each ton avoided.

In summary, while retrofit investment may not yet be financially cost-effective on energy savings alone, incorporating avoided emissions, timing of action, and policy incentives into the analysis strengthens the economic rationale. NPV and payback analyses should thus be viewed not in isolation, but as part of a broader cost-benefit framework that includes environmental and temporal dimensions.

Table 5.4 Annual energy savings (€/(m²·a)), annual CO_2 saving, (€/(m²·a)), simple payback time (years), NPV (€/m²), and cumulative CO_2 emissions incurred between 2020 and 2025 as a result of delayed retrofitting for each building type.

Building Type	Annual Energy Savings (€/(m²·a))	Annual CO_2 Saving (€/(m²·a))	Simple Payback Time (years)	NPV (€/m²)	2020-2025 additional CO_2 emissions (Mt)
1 MFH	6.9	1.3	51.1	-258.9	14.48
1 TH	6.7	1.3	52.5	-263.2	0.05
2 MFH	8.3	1.6	42.4	-226.1	16.33
2 AB	7.4	1.4	47.6	-246.9	4.73
3 MFH	7.7	1.5	45.8	-240.3	22.06
3 AB	7.4	1.4	47.6	-247.1	6.35
3 TH	7.4	1.4	47.6	-247.0	0.70
4 MFH	6.6	1.3	53.4	-265.7	5.65
4 AB	6.9	1.3	51.1	-258.8	4.04
4 TH	5.3	1.0	66.5	-296.2	1.37

***Notes: NPV assumes 30% subsidy and 3% discount rate over 30 years. Payback time is calculated as initial investment (post-subsidy) divided by total annual savings (energy +carbon). CO_2 savings based on 2025 carbon price of €55/ton. (CPI, 2011; Galvin, 2023; Haneef et al.,2021; Heracleous et al.,2022)**

5.3.3 The role of urban effects and climate in retrofitting

The results presented in this study are based on simulations using TMY data generated by Meteonorm 8. While this approach captures global climate effects such as changes in HDD and CDD, it does not account for specific urban effects like wind patterns or local heat islands, which can significantly influence building energy performance. For future scenarios, incorporating these factors using tools such as the Urban Weather Generator (UWG) would allow for a more comprehensive assessment by modifying TMY files (Bueno et al., 2013).

Future research could integrate UWG-generated climate data into the UBEM framework to address both specific urban and global climate effects. This would enhance the accuracy of simulations, particularly for densely built neighborhoods like those studied in Düsseldorf and provide more robust insights into the interaction between buildings and their surrounding environment.

5.4 Conclusion

In this study, we have developed and used an urban geographic archetype dataset in conjunction with one of UBEMs, CitySim, to assess the energy, environmental, and financial impacts of residential retrofitting in Düsseldorf. The key contributions and findings are summarized as follows:

Novel methodological integration: We introduced a UBEM framework that combines CitySim with a custom-built urban archetype dataset based on TABULA, spatial GIS data, and CityGML-ADE. The workflow includes edge-condition-aware simulation (i.e., inclusion of adjacent buildings for targe study area), improving realism and transferability across European cities.

Identification of high energy consuming building types: It provides actionable insights for prioritizing retrofits and highlights the need for stronger policy levers. Our findings identified that for the case study in the city of Düsseldorf, historic and older multi-family residential buildings, particularly those built before 1957, such as type 1 MFH, 2 MFH, and 3 MFH types, are in urgent need of renovation. These buildings, characterized by inefficient envelopes and outdated heating systems, are significant contributors to overall energy consumption and emissions within the city. Through targeted retrofit strategies, our simulations suggest that heating energy demand could be reduced by approximately 70%, and CO_2 emissions could be cut by 42% to 46% by the year 2050.

Integrated energy, carbon, and financial analysis: The study evaluates not only energy and emissions reductions but also simple payback time and NPV. Despite negative NPVs under current economic conditions, early refurbishment offers clear environmental value. By quantifying avoidable emissions between 2020 and 2025, the study demonstrates the climate impact of inaction. For instance, delaying retrofits of type 1 MFH buildings alone results in over 14.5Mt of additional CO_2 emissions.

Future improvements to the framework require addressing key limitations, foremost among them the lack of disaggregated, geographically resolved energy use data. This remains a major obstacle to progress in UBEM-based energy planning. Without spatially clear consumption records, it is difficult to calibrate models or fully capture urban energy heterogeneity. To address this, future work should focus on integrating municipal refurbishment records, enhancing climate inputs to reflect urban microclimates, and enriching databases such as TABULA to include post-retrofit performance. Incorporating household-level energy data would further improve model accuracy, supporting better policy and retrofitting strategies.

In summary, this work supports the design of location-specific, climate-aligned renovation strategies for Europe’s aging building stock and reinforces the urgency of early retrofit action for long-term emissions reductions.

Declaration of Competing Interest

The authors declare that they have no known competing financial interests or personal relationships that could have appeared to influence the work reported in this paper.

Acknowledgements

The authors would like to acknowledge funding from China Scholarship Council. The authors also would like to thank Maxim Shamovich, Lehrstuhl für Energieeffizientes Bauen E3D, RWTH Aachen University for his support with the CityGML format transformation. The project was partly co-funded under the Excellence Strategy of the Federal Government and the Länder (Project SFBLE003 TRUKLIB).

5.5 Supporting information

Table 5.5 Specific constructions of eight common Tabula residential building types and subtypes in the study area according to Tabula WebTool (Tabula WebTool, 2023).

Types	Tabula Subtypes	Wall (material, thickness)	U-Wall ($W/m^2 \cdot K$)	Roof (material, thickness)	U-Roof ($W/m^2 \cdot K$)	Windows (material, G-Value)
1	TH	Solid brick, 0.38m	1.7	Wood ceiling, 0.25m	0.65	Wooden/Plastic frame with Dual-Pane Glazing, 0.68
1	MFH	Solid brick, 0.26m	2.2	Concrete ceiling, 0.295m	1.08	Wooden/Plastic frame with Dual-Pane Glazing, 0.68
2	MFH	Solid brick, 0.38m	1.7	Concrete ceiling, 0.295m	1.08	Wooden/Plastic frame with Dual-Pane Glazing, 0.68
2	AB	Brickwork, 0.31m	1.4	Concrete ceiling, 0.295m	1.08	Wooden/Plastic frame with Dual-Pane Glazing, 0.68
3	TH	Masonry of hollow blocks, 0.32m	1.2	Wood ceiling, 0.25m	1.08	Wooden/Plastic frame with Dual-Pane Glazing, 0.68
3	MFH	Masonry of hollow blocks, 0.32m	1.2	Concrete ceiling, 0.295m	1.08	Wooden/Plastic frame with Dual-Pane Glazing, 0.68
3	AB	Masonry of hollow blocks, 0.32m	1.2	Concrete ceiling, 0.295m	1.08	Wooden/Plastic frame with Dual-Pane Glazing, 0.68
4	TH	Masonry of hollow blocks, 0.32m	1.2	Concrete ceiling, 0.32m	0.51	Wooden/Plastic frame with Dual-Pane Glazing, 0.68
4	MFH	Masonry of hollow blocks, 0.32m	1.2	Concrete ceiling, 0.32m	0.51	Wooden/Plastic frame with Dual-Pane Glazing, 0.68
4	AB	Masonry of hollow blocks, 0.32m	1.2	Concrete ceiling, 0.32m	0.51	Wooden/Plastic frame with Dual-Pane Glazing, 0.68
5	SFH	Masonry of hollow blocks 0.4m	1.2	Concrete ceiling, 0.33m	0.5	Wooden/Plastic frame with Dual-Pane Glazing, 0.68
5	TH	Masonry of hollow blocks, 0.4m	1	Concrete ceiling, 0.32m	0.51	Wooden/Plastic frame with Dual-Pane Glazing, 0.68
5	AB	Concrete, 0.3m	1	Concrete ceiling, 0.32m	0.51	Wooden/Plastic frame with Dual-Pane Glazing, 0.68
6	TH	Masonry of light honeycomb bricks, 0.425m	0.6	Solid brick, 0.16m	0.4	Wooden/Plastic frame with Dual-Pane Glazing, 0.68
6	MFH	Masonry of light honeycomb bricks, 0.425m	0.6	Concrete ceiling, 0.37m	0.4	Wooden/Plastic frame with Dual-Pane Glazing, 0.68
7	TH	Concrete, 0.33m	0.28	Solid brick, 0.25m	0.2	Double glazing, argon filled, and low-E, 0.5
7	MFH	Concrete, 0.365m	0.28	Fiberglass, 0.35m	0.2	Double glazing, argon filled, and low-E, 0.5
8	TH	Concrete, 0.43m	0.16	Solid brick, 0.33m	0.13	Double glazing, argon filled, and low-E, 0.5

Table 5.6 Specific HVAC systems of eight common and refurbished Tabula residential building types and subtypes in the study area according to Tabula WebTool (Tabula WebTool, 2023).

Types	Tabula Subtypes	System-original state	Centralized/Independent (original state)	System-refurbished state	Centralized/Independent (refurbished state)
1	TH	Traditional central heating system with boiler (gas /oil)	Central heating system	Condensing boiler Improved distribution Thermal solar system	Central heating system
1	MFH	Traditional central heating system with boiler (gas /oil) Electr.DHW	Central heating system	Condensing boiler Improved distribution Thermal solar system	Central heating system
2	MFH	Traditional central heating system with boiler (gas /oil) Electr.DHW	Central heating system	Condensing boiler Improved distribution Thermal solar system	Central heating system
2	AB	Traditional central heating system with boiler (gas /oil) Electr.DHW	Central heating system	Condensing boiler Improved distribution Thermal solar system	Central heating system Independent for each unit
3	TH	Traditional central heating system with boiler (gas /oil) Electr.DHW	Central heating system	Condensing boiler Improved distribution Thermal solar system	Central heating system
3	MFH	Traditional central heating system with boiler (gas /oil) Electr.DHW	Central heating system	Condensing boiler Improved distribution Thermal solar system	Central heating system Independent for each unit
3	AB	Traditional central heating system with boiler (gas /oil) Electr.DHW	Central heating system	Condensing boiler Improved distribution Thermal solar system	Central heating system Independent for each unit
4	TH	Traditional central heating system with boiler (gas /oil) Electr.DHW	Central heating system	Condensing boiler Improved distribution Thermal solar system	Central heating system
4	MFH	Traditional central heating system with boiler (gas /oil) Electr.DHW	Central heating system	Condensing boiler Improved distribution Thermal solar system	Central heating system Independent for each unit
4	AB	Traditional central heating system with boiler (gas /oil) Electr.DHW	Central heating system	Condensing boiler Improved distribution Thermal solar system	Central heating system Independent for each unit
5	SFH	Traditional central heating system with boiler (gas /oil) Electr.DHW	Central heating system	Condensing boiler Improved distribution Thermal solar system	Central heating system

Types	Tabula Subtypes	System-original state	Centralized/Independent (original state)	System-refurbished state	Centralized/Independent (refurbished state)
5	TH	Traditional central heating system with boiler (gas /oil) Electr.DHW	Central heating system	Condensing boiler Improved distribution Thermal solar system	Central heating system
5	AB	Traditional central heating system with boiler (gas /oil) Electr.DHW	Central heating system	Condensing boiler Improved distribution Thermal solar system	Central heating system Independent for each unit
6	TH	Traditional central heating system with boiler (gas /oil) Electr.DHW	Central heating system	Condensing boiler Improved distribution Thermal solar system	Central heating system
6	MFH	Traditional central heating system with boiler (gas /oil) Electr.DHW	Central heating system	Condensing boiler Improved distribution Thermal solar system	Central heating system Independent for each unit
7	TH	New gas central heating system Condensing boiler Thermal DHW solar system	Central heating system	New gas central heating system Condensing boiler Thermal DHW solar system Exhaust air ventilation system	Central heating system
7	MFH	New gas central heating system Condensing boiler Thermal DHW solar system Exhaust air ventilation system	Central heating system	New gas central heating system Condensing boiler Thermal DHW solar system Exhaust air ventilation system	Central heating system
8	TH	New gas central heating system Condensing boiler Thermal DHW solar system Exhaust air ventilation system	Central heating system	New gas central heating system Condensing boiler Thermal DHW solar system Exhaust air ventilation system	Central heating system

DHW: Domestic hot water

Table 5.7 Specific constructions of eight refurbished Tabula residential building types and subtypes in the study area according to Tabula WebTool (Tabula WebTool, 2023).

Types	Tabula Subtypes	Wall (material, thickness)	U-Wall (W/m²·K)	Roof (material, thickness)	U-Roof (W/m²·K)	Windows (material, G-Value)
1	TH	Solid brick 0.38m Insulation 0.08m Total thickness 0.46m	0.34	Wood ceiling, 0.25m Insulation 0.12m Total thickness 0.37m	0.2	Windows with double glazing, argon filled, low-E 0.5
1	MFH	Solid brick 0.26m Insulation 0.08m Total thickness 0.34m	0.36	Concrete ceiling, 0.295m Insulation 0.12m Total thickness 0.515m	0.23	Windows with double glazing, argon filled, low-E 0.5
2	MFH	Solid brick 0.38m Insulation 0.13m Total thickness 0.51m	0.25	Concrete ceiling, 0.295m Insulation 0.12m Total thickness 0.515m	0.23	Windows with double glazing, argon filled, low-E 0.5
2	AB	Brickwork, 0.31m Insulation 0.12m Total thickness 0.43m	0.24	Concrete ceiling, 0.295m Insulation 0.12m Total thickness 0.515m	0.23	Windows with double glazing, argon filled, low-E 0.5
3	TH	Masonry of hollow blocks, 0.32m Insulation 0.26m Total thickness 0.58m	0.23	Wood ceiling, 0.25m Insulation 0.12m Total thickness 0.37m	0.2	Windows with double glazing, argon filled, low-E 0.5
3	MFH	Masonry of hollow blocks, 0.32m Insulation 0.14m Total thickness 0.46m	0.23	Concrete ceiling, 0.295m Insulation 0.12m Total thickness 0.515m	0.23	Windows with double glazing, argon filled, low-E 0.5
3	AB	Masonry of hollow blocks, 0.32m Insulation 0.14m Total thickness 0.46m	0.23	Concrete ceiling, 0.295m Insulation 0.12m Total thickness 0.515m	0.23	Windows with double glazing, argon filled, low-E 0.5
4	TH	Masonry of hollow blocks, 0.32m Insulation 0.14m Total thickness 0.46m	0.23	Concrete ceiling, 0.32m Insulation 0.12m Total thickness 0.44m	0.19	Windows with double glazing, argon filled, low-E 0.5
4	MFH	Masonry of hollow blocks, 0.32m Insulation 0.14m Total thickness 0.46m	0.23	Concrete ceiling, 0.32m Insulation 0.12m Total thickness 0.44m	0.19	Windows with double glazing, argon filled, low-E 0.5
4	AB	Masonry of hollow blocks, 0.32m Insulation 0.14m Total thickness 0.46m	0.23	Concrete ceiling, 0.32m Insulation 0.12m Total thickness 0.44m	0.19	Windows with double glazing, argon filled, low-E 0.5
5	SFH	Masonry of hollow blocks 0.4m Insulation 0.14m Total thickness 0.54m	0.22	Concrete ceiling, 0.33m Insulation 0.12m Total thickness 0.45m	0.18	Windows with double glazing, argon filled, low-E 0.5
5	TH	Masonry of hollow blocks, 0.4m Insulation 0.26m Total thickness 0.66m	0.22	Concrete ceiling, 0.32m Insulation 0.18m Total thickness 0.34m	0.19	Windows with double glazing, argon filled, low-E 0.5
5	AB	Concrete, 0.3m Insulation 0.14m Total thickness 0.44m	0.23	Concrete ceiling, 0.32m Insulation 0.18m Total thickness 0.34m	0.19	Windows with double glazing, argon filled, low-E 0.5
6	TH	Masonry of light honeycomb bricks, 0.425m Insulation 0.26m Total Thickness 0.685m	0.2	Solid brick, 0.16m Insulation 0.18m Total thickness 0.34m	0.16	Windows with double glazing, argon filled, low-E 0.5
6	MFH	Masonry of light honeycomb bricks, 0.425m	0.2	Concrete ceiling, 0.37m Insulation 0.12m Total thickness 0.49m	0.16	Windows with double glazing, argon filled, low-E 0.5

Types	Tabula Subtypes	Wall (material, thickness)	U-Wall ($W/m^2 \cdot K$)	Roof (material, thickness)	U-Roof ($W/m^2 \cdot K$)	Windows (material, G-Value)
		Insulation 0.26m Total Thickness 0.685m				
7	TH	Concrete, 0.33m Insulation 0.1m Total Thickness 0.43m	0.2	Solid brick, 0.25m Insulation 0.04m Total thickness 0.29m	0.16	Windows with triple glazing, Argon or Krypton filled, low-E, insulated frame, improved version 0.3
7	MFH	Concrete, 0.365m Insulation 0.135m Total Thickness 0.5m	0.14	Fiberglass, 0.35m Insulation 0.17m Total thickness 0.52m	0.1	Windows with triple glazing, Argon or Krypton filled, low-E, insulated frame, improved version 0.3
8	TH	Concrete, 0.43m Insulation 0.11m Total Thickness 0.54m	0.15	Solid brick, 0.33m Insulation 0.1m Total thickness 0.43m	0.13	Windows with triple glazing, Argon or Krypton filled, low-E, insulated frame, improved version 0.3

6. Summer thermal consequences of EU retrofit strategies: an integrated microclimate and indoor comfort study in Düsseldorf

This work has been published under:

Yu, Q., Mills, G., Ketzler, G., & Leuchner, M. (2026). Summer thermal consequences of EU retrofit Strategies: An integrated microclimate and indoor comfort study in Düsseldorf. *Energy and Buildings*, 117163. https://doi.org/10.1016/j.enbuild.2026.117163

Highlights

Realistic building archetypes alter simulated outdoor heat stress by up to 1.5 °C compared with model defaults.

T_{mrt} explains over 91% of UTCI variance at peak hour, confirming radiation and shading as the dominant drivers.

Urban greenery cools peak UTCI by up to 6.0 °C, clearly outperforming insulation-only retrofits.

A crossover effect shows that winter-optimized retrofits increase daytime indoor overheating by up to 3.8 °C.

A one-way ENVI-met–CitySim linkage reveals a mitigation–adaptation trade-off in EU residential retrofits.

Abstract

Building retrofits in temperate European climates primarily target winter heat losses, yet their dynamic implications for outdoor microclimate and indoor thermal safety under heatwaves remain poorly understood. This study investigates how winter-oriented retrofits modify both outdoor microclimate and indoor thermal conditions during July 2022 Central European heatwaves, using a one-way, offline integration of ENVI-met and CitySim. A dense residential neighborhood in Düsseldorf, Germany, was simulated under multiple retrofit and greening scenarios, incorporating realistic building data derived from the EU TABULA archetype database to ensure reliable façade–microclimate interactions.

Methodologically, results show that using realistic archetypes alters simulated outdoor heat stress by up to 1.5 °C compared to generic defaults. In terms of mitigation, façade retrofits alone slightly reduce outdoor Universal Thermal Climate Index (UTCI) by up to 0.8 °C, while green infrastructure provides the strongest cooling, lowering local UTCI by up to 6 °C through shading and evapotranspiration. Typically, indoor simulations revealed a crossover effect, where retrofitted buildings remained cooler at night but became up to 3.8 °C warmer during daytime peaks, increasing short-term overheating risks in the absence of active cooling.

These findings highlight a mitigation–adaptation trade-off in EU retrofit strategies: measures optimized for winter energy savings can exacerbate summer heat stress if not combined with greenery and summer-oriented design measures. The proposed framework offers a scalable workflow to support climate-resilient, human-centric retrofit planning in other TABULA-covered cities.

Keywords

ENVI-met; CitySim; Building archetypes; Building retrofit; UTCI; Urban microclimate

6.1 Introduction

Rapid urbanization and the densification of cities have intensified the modification of natural land surfaces, replacing them with impervious materials such as asphalt and concrete (Martinez et al.,2021). These changes, coupled with increased anthropogenic heat emissions from transportation and buildings, have contributed to the intensification of the urban heat island (UHI) effect (Stewart et al., 2021). UHI exacerbates urban energy demand for cooling (Santamouris, 2020), deteriorates air quality (Coates et al., 2016) and increases heat-related health issues during periods of extreme heat (Aghamohammadi et al., 2022). At the local scale, UHI also intensifies the impacts of more frequent and severe heatwave events (Hashemi et al., 2024). Recent studies report substantial excess mortality during heatwaves in different regions, and during summer 2022 Europe experienced particularly severe impacts, including several thousand heat-related deaths in Germany alone (Ballester et al., 2022). These figures highlight the need for urban environments that limit both outdoor thermal exposure and indoor overheating during persistent heatwaves.

Most existing urban heat mitigation strategies focus on the use of green infrastructure (trees, parks, green roofs/façades) and reflective or high-albedo materials to improve outdoor thermal comfort (Kraemer and Kabisch, 2022; Wang et al., 2022; Hui et al., 2024; Jiang et al., 2025). Meanwhile, a growing body of work has examined advanced energy-efficiency and retrofit technologies, including alternative envelope configurations and façade photovoltaic systems, primarily targeting reductions in heating demand and operational carbon emissions (Xiong et al., 2023; Yang et al., 2025). Building- and room-scale studies have also developed sophisticated monitoring and control approaches, including mobile thermal-comfort monitoring robots, demand-side energy management for HVAC, and reinforcement-learning-based optimal ventilation strategies to balance energy use, indoor air quality and thermal comfort (Cheng et al., 2023; Ma et al., 2019; Shang et al., 2025). However, far less attention has been paid to the unintended summer consequences of winter-driven building retrofit measures.

In much of Western and Central Europe, where temperate oceanic climates dominate (Cfb in the Köppen classification) (Peel et al., 2007), the historical climate focus has been on cold stress in winter rather than summer overheating. Düsseldorf, with comparatively mild but warming summers and still cold winters, provides a representative Central European testbed for examining these trade-offs. At the same time, a substantial share of the residential building stock predates the first German thermal insulation ordinance in 1978, indicating considerable potential for energy retrofits (Verordnung über einen energiesparenden Wärmeschutz bei Gebäuden, 1977). Consequently, most retrofit strategies have emphasized improving insulation and reducing heat loss (Mata et al.,2018). One such popular housing retrofit project is the EU TABULA project (Typology Approach for Building Stock Energy Assessment)

(Loga et al., 2016), which developed comprehensive national building typologies and retrofit strategies across 20 European countries, focusing primarily on improving winter energy performance.

The European Green Deal's Renovation Wave and the recast Energy Performance of Buildings Directive (EPBD) aim to at least double renovation rates by 2030 and steer the building stock towards very low or zero operational emissions by 2050 (The European Parliament and the Council of the European Union, 2010). Current strategies for winter energy-saving home retrofits mainly quantify benefits in terms of energy savings, emissions reduction and affordability, while explicit treatment of summer thermal comfort and heat–health resilience remains limited (Mata et al., 2018). Concurrently, studies from the perspective of governance and equity have highlighted that carbon reduction policies may exacerbate inequality if structural constraints are disregarded (Preziuso and Odonkor, 2025). Together, these developments underline the need to assess not only the mitigation benefits of standard retrofit packages, but also their implications for thermal comfort and heat-health resilience.

In light of intensifying and more frequent heatwaves in Europe, it is crucial to investigate whether building retrofits designed for winter performance might compromise summer thermal safety, both indoors and outdoors. This study addresses that gap by using a real-world case in Düsseldorf, Germany to evaluate the microclimatic and thermal effects of EU-standard retrofit strategies under extreme summer heatwave conditions.

In earlier work, Yu et al. (2025b) developed an urban geographic archetype dataset and applied it to Düsseldorf's residential buildings using the Urban Building Energy Model (UBEM), CitySim (Mutani et al., 2018). That work demonstrated that standardized retrofitting strategies could reduce annual CO2 emissions by 42–46% and lower heating energy demand by around 70% by 2050. However, those simulations were winter-oriented and did not explore potential trade-offs during summer. Moreover, CitySim's simplified climate inputs and lack of vegetation modelling limited its ability to represent the complex interactions between building surfaces and the urban microclimate (Vermeulen et al., 2013).

To bridge this gap, we linked ENVI-met (Bruse, 2004) and CitySim in the same neighborhood through a one-way, offline integration scheme. ENVI-met enables simulation of surface–atmosphere interactions, capturing how vegetation, urban morphology, and façade properties influence outdoor comfort as quantified by the Universal Thermal Climate Index (UTCI) (Blazejczyk et al., 2012). CitySim is used to simulate indoor operative temperatures in buildings, using the same construction properties. In a novel step, we replaced CitySim's default weather profiles with high-resolution, scenario-specific microclimate data extracted from ENVI-met outputs. This

cross-model linkage allowed us to evaluate how building retrofit decisions shape both indoor and outdoor thermal performance under extreme summer conditions.

Yu et al. (2025b) reviewed recent integrative microclimate-building studies, finding that most of integration are sequential from microclimate to building energy approaches, such as ENVI-met–CEA and ENVI- met–TRNSYS workflows, used to examine the combined effects of urban form, greenery and building operation on energy demand and outdoor comfort (Kämpf et al., 2020; Perini et al., 2017). More recent works published between 2023 and 2025 have extended such integrations to different climates and design questions (Silva et al., 2025; Crank et al., 2023). However, even when these studies include site-specific validation, they typically rely on simplified or generic urban morphologies and thermophysical properties and often treat "retrofits" as idealized parameter variations. To fill this gap, a further innovation of this study is the use of detailed, archetype-based building information for both simulation environments. We investigated how realistic, archetype-based building data influences modeled UTCI and thermal comfort outcomes. This study does not attempt a new, site-specific validation of ENVI-met or CitySim against local measurements in Düsseldorf. Instead, we build on existing validation studies of both models and focus on how building envelope realism affects the simulated magnitude and spatial distribution of outdoor heat stress, and the associated indoor responses under extreme conditions.

To fill the existing research gap in linking retrofit-driven envelope modifications with outdoor–indoor thermal responses, this study addresses the following questions:

(1) To what extent does the use of realistic building data influence the magnitude and spatial distribution of simulated outdoor thermal comfort outcomes compared to generic default settings under extreme heat conditions? (2) Can energy retrofit measures focused on winter performance unintentionally worsen outdoor comfort and increase daytime indoor overheating risk by a threshold amount (e.g., >3.0 ◦C) during summer heatwaves? (3) How effectively can the integration of green infrastructure with building retrofits reduce peak UTCI and alleviate indoor overheating during summer heatwaves?

The core achievements of this study are threefold. First, we developed a transparent, data-driven ENVI-met–CitySim framework with a one-way, offline integration that consistently applies EU TABULA archetype data across both microclimate and building energy simulations. Second, we provide a quantitative, dual-domain assessment of a critical policy trade-off, revealing a crossover effect where winter- optimized retrofits significantly increase the risk of daytime indoor overheating by up to 3.8 ◦C during heatwaves, while only moderately improving outdoor comfort. Third, we confirm the essential role of nature-based solutions, demonstrating that integrating green infrastructure is the single most effective strategy for localized heat mitigation, capable of reducing UTCI by up to 6.0 ◦C in shaded areas.

Beyond the specific case of Düsseldorf, the proposed integrated modelling framework provides a scalable and transferable evaluation tool for integrating retrofit policy design to other European cities covered by the TABULA database, human-centric comfort, and low- carbon objectives in future climate-resilient building programs.

6.2 Methodology

6.2.1 Study area

The study area is located in Düsseldorf, Germany, the seventh-largest city in the country, with a population of over 600,000 residents (City of Düsseldorf, 2023a). Düsseldorf experiences a temperate climate with distinct seasonal variability, with the mean annual temperature over the standard 1991–2020 climate normal period of approximately 11.2 °C. During the summer, the city experiences a moderate number of summer days, where maximum temperatures reach or exceed 25 °C, usually ranging from 15 to 26 days per year. Hot days, where temperatures reach or exceed 30 °C, are relatively rare. Winters are often cold, with frost days (minimum temperatures below 0 °C) frequently occurring, sometimes reaching up to 90 days annually (Open Data Düsseldorf, 2022). Historically, the city has been more concerned with winter cold stress than extreme summer heat. Figure 6.1 shows the geographic location of Düsseldorf in Germany and the location of the meteorological station at Düsseldorf Airport.

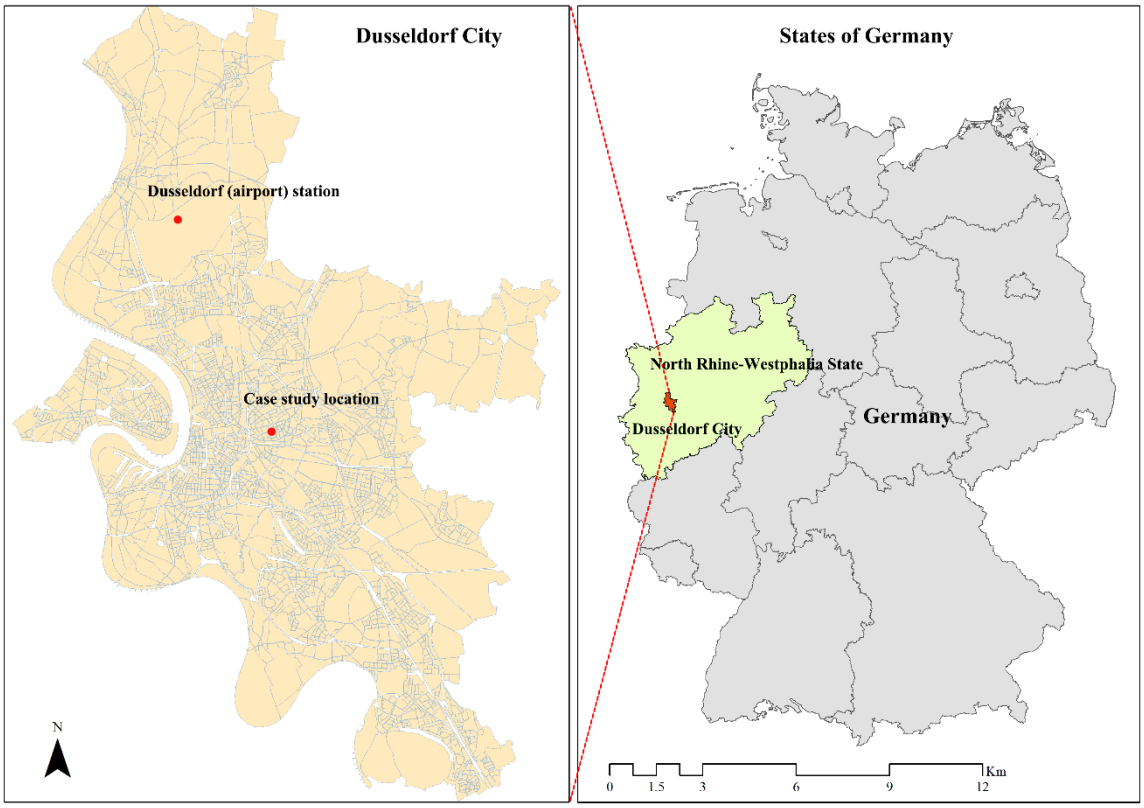


Figure 6.1 The location of the research area and meteorological station in Düsseldorf (left). Location of the city and North Rhine-Westphalia in Germany (right).

The case study area is situated in Düsseldorf's Flingern district, consisting of three blocks and one street park (Figure 6.2). The buildings are predominantly residential, with some mixed-use buildings serving as small workshops, offices, and schools. The layout follows a typical German block design, where buildings along the major roads

are taller, while elsewhere there are low-rise terraced houses (Hofmeister, 2003). In this study area, the average height of periphery buildings of each block is 21 m, while for the interior building of the blocks it is 5 m. Figure 6.2 shows building heights in 10-meter intervals as two classes. The street park, cutting through the center of the research area, offers environmental and social amenities. The total study area is approximately 34.26 ha, including 44% paved roads and walkways, 37% buildings and 19% green ground cover (lawns, gardens).



Figure 6.2 Different land covers are divided into seven classes, namely, asphalt red pavement, asphalt pavement, single stones pavement, concrete pavement, building, grass and soil.

Note: The locations of trees are also shown in the map (Landeshauptstadt Düsseldorf, Umweltamt, 2022). The red line indicates the area of interest for model simulations.

6.2.2 Outdoor microclimate simulation with ENVI-met

To examine the effect of retrofitting strategies on outdoor thermal comfort, we used ENVI-met (v5.5.1), which is a three-dimensional, non-hydrostatic microclimate model designed to simulate surface–plant–air interactions in urban environments at high spatial and temporal resolutions (Bruse,2004). It is widely used for assessing the effects of urban design strategies, such as vegetation, materials, and building geometry on local thermal comfort and microclimate conditions (Song et al., 2024; Silva et al., 2025).

Simulations were conducted for July 19, 2022, beginning at 05:00 CET and continuing for 17 h (until 22:00 CET). This date was chosen because Europe experienced one of its most severe heatwaves that year, with Germany being heavily impacted (Copernicus, 2022). Meteorological data from Düsseldorf Airport Station supported the selection of

July 19, 2022, as the simulation day (Ibebuchi and Abu, 2023). This date was at the peak of the heatwave, characterized by high-pressure atmospheric conditions and stable, cloud-free skies over the region, resulting in intense surface heating (Figure 6.3). Figure 6.3 displays the surface synoptic weather chart issued by the German Weather Service (DWD) at 00:00 UTC, confirming the dominance of an anticyclonic system over Central Europe during the selected period (Deutscher Wetterdienst, 2022).

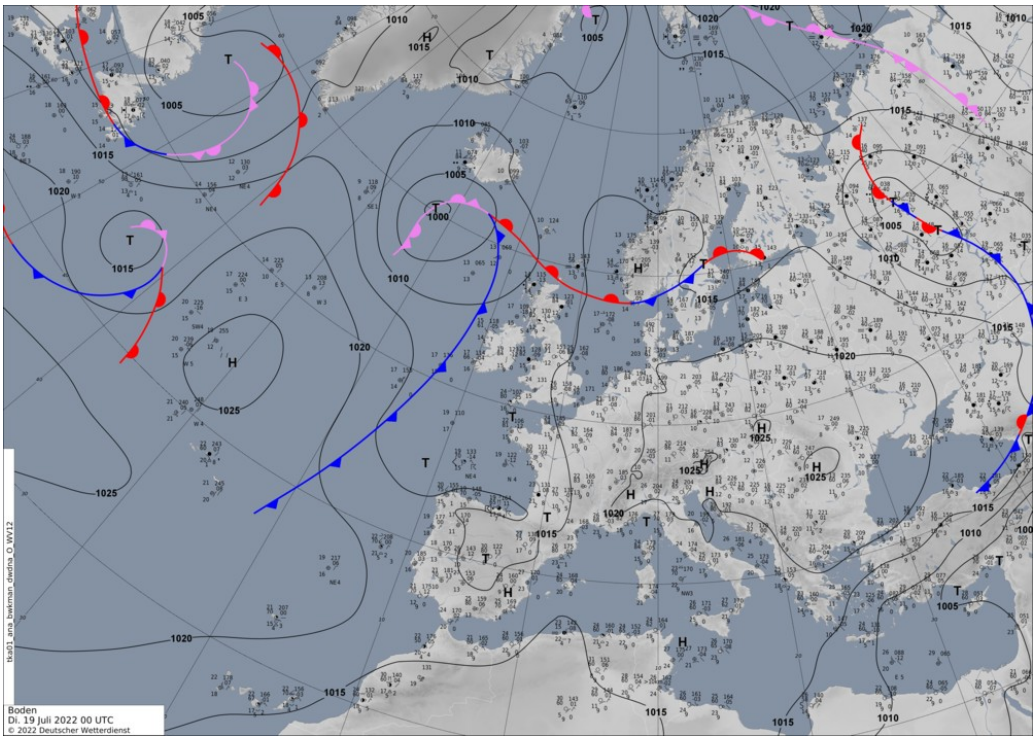


Figure 6.3 Surface Synoptic Weather Map during the July 2022 Heatwave in Europe (00 UTC, July 19).

Note: Source: Deutscher Wetterdienst (DWD), via Wetterzentrale (https://www.wetterzentrale.de) (Deutscher Wetterdienst, 2022).

The simulation used full forcing from observed meteorological data recorded at Düsseldorf Airport Station, including solar radiation (downward direct and diffuse shortwave radiation), T_a, RH, v and direction.

The spatial resolution of the ENVI-met model was set at 3 m. This value is commonly adopted in ENVI-met applications at the neighborhood- scale as a compromise between resolving street-canyon and tree-crown geometry and keeping simulation times computationally manageable (Bruse, 2004). A 63-meter buffer zone was applied to cover the whole study area of interest (within the red line in Fig 6.2). To further capture edge interactions, the full simulation area extended at least 100 m beyond the target study area in all directions.

UTCI was calculated using the Biomet post-processing module of ENVI-met, which applies a thermophysiological model to assess outdoor thermal comfort. The input

parameters included T_{mrt}, T_a, RH and v, enabling the evaluation of pedestrian thermal stress across different outdoor locations. We used the default value of pedestrians in the model: a 35-year-old man, 1.75 m tall, with a weight of 75 kg, walking (1.34 m/s).

Building geometry and construction details for ENVI-met and also CitySim were taken from an urban archetype dataset previously developed for Düsseldorf (Yu et al., 2025b). This dataset provides layer-wise constructions and U-values for the main TABULA residential archetypes and their retrofitted counterparts (see Tables A1 and A3 in Yu et al. (2025b)). This insulation reduces heat transfer and improves both energy efficiency and thermal comfort. While these measures are designed to reduce winter heat loss, they can alter summer outdoor thermal conditions by reducing inward heat flux and elevating surface façade temperatures, which in turn affects T_{mrt} and pedestrian-level thermal comfort. The main thermophysical and radiative properties (λ, ρ, cp, α albedo A, and emissivity ε) of the envelope and surface materials are summarized in Table 6.1.

Table 6.1 Thermophysical (λ, ρ, c_p) and radiative (α or albedo A, ε) properties of the main envelope and surface materials.

Building Materials						
Type	Material	λ (W/(m·K))	ρ (kg·m^{-3})	c_p (J/(kg·K))	α	ε
Masonry	Solid brick	0.44	1500	650	0.7	0.93
Masonry	Hollow brick / block	0.3	930	840	0.7	0.94
Masonry	Light honeycomb brick	0.2	620	840	0.7	0.94
Masonry	Structural concrete	1.6	2220	850	0.7	0.9
Insulation	Generic external insulation board	0.07	400	1500	0.5	0.9
Plaster	ENVI-Met default plaster	0.6	1500	850	0.6	0.93
Roof	Tile	0.84	1900	800	0.7	0.93
Roof	PVC	0.19	1200	1470	0.3	0.9
Surface Materials						
Type	Material	A	ε			
Pavement	Asphalt	0.12	0.9			
Pavement	Asphalt red	0.4	0.9			
Pavement	Concrete	0.3	0.9			
Pavement	Single stones	0.35	0.9			
Soil	Loamy soil	0.2	0.9			
Vegetation	Grass	0.2	0.97			

*Thermal Conductivity: λ (W/(m·K)); Density: ρ (kg·m^{-3}); Specific Heat: c_p(J/(kg·K)); Absorption: α; Albedo:A; Emissivity: ε
For surface materials, the user interface only exposes radiative properties (albedo and emissivity); bulk thermophysical properties are taken from ENVI-met's internal defaults. All volumetric properties of asphalt, concrete and soil surfaces therefore follow the ENVI-met standard database.

Urban green elements were integrated based on publicly available data from Düsseldorf's tree database (Hofmeister, 2003). The area includes 262 individual trees, primarily Plane, Lime, and Hornbeam species. Tree heights range from 5–20 m, with crowns of 6–8 m diameter. Both street and garden trees were modeled explicitly in ENVI-met. Within ENVI-met, these trees were represented using the standard deciduous broadleaf parameterizations. This includes default summer Leaf Area Density (LAD) profiles (typically peaking in the mid-canopy) and phenological settings corresponding to full-leaf conditions in July, ensuring that evapotranspiration and shading effects were simulated based on established model defaults.

6.2.3 Scenario design

Four simulation scenarios were designed for this study at 14:00 CET when UTCI values reach their peak, corresponding to the highest heat stress experienced by urban pedestrians. These include combinations of existing vs. retrofitted buildings and with vs. without vegetation. Specifically, Scenario A represents the baseline condition of existing buildings with current urban vegetation, while Scenario B simulates existing buildings with vegetation removed. Scenario C incorporates retrofitted building envelopes with retained vegetation, and Scenario D combines retrofitted buildings with no vegetation. Each scenario was designed to isolate and examine the effects of key urban design elements.

T_a (°C), T_{mrt} (°C), RH (%), and v (m/s) were selected as key microclimatic variables because they directly influence human thermal comfort as represented by UTCI (°C). By analyzing these factors, we can better understand how different urban configurations and interventions affect the thermal environment.

We deliberately restricted the scenario set to combinations of standard TABULA-based envelope retrofits and the presence or absence of urban greenery in order to focus on widely implemented, policy-relevant measures and to control the overall computational load. More exploratory configurations, such as reflective surfaces or adaptive natural ventilation strategies, are prioritized for future work rather than being included in the present analysis.

6.2.4 Outdoor–Indoor simulation using a one-way ENVI-met–CitySim integration

To assess whether building retrofits optimized for winter efficiency may compromise indoor thermal safety during summer heatwaves, we conducted a simulation using CitySim to simulate effective indoor temperatures under realistic outdoor microclimate conditions.

CitySim cannot directly simulate vegetation surrounding shading elements such as trees. To overcome this limitation and account for green infrastructure effects, we used high-

resolution ENVI-met simulation results from two scenarios: Scenario A (existing, non-retrofitted buildings with green space) and Scenario C (retrofitted buildings with green space).

From both ENVI-met simulations, we extracted average hourly outdoor climate variables, including T_a, RH, v and wind direction, for July 19th, 2022, a peak day during the 2022 Central European heatwave. These values were used for the period 05:00–22:00 CET, when ENVI-met was actively simulated. For the remaining hours of the day (00:00–04:00 and 23:00 CET), the original observations from Düsseldorf Airport Station were retained. The resulting mixed profiles were then reformatted to serve as customized weather input profiles for CitySim, replacing standard meteorological files. Radiation inputs (beam and diffuse) were preserved from the original dataset to ensure consistency and to avoid double-counting shading effects, as CitySim already accounts for solar obstruction due to building geometry but does not model vegetation-induced shading. Our analysis of UTCI and indoor temperatures focuses on the common simulation window between both models (06:00–22:00 CET), when ENVI-met-derived microclimate fields are available; earlier and later hours mainly provide thermal preconditioning and are not interpreted in detail.

Indoor simulations were then performed on a representative building typology in two conditions: a non-retrofitted existing building using Scenario A climate data and a retrofitted building using Scenario C climate data. Each building was assigned standard occupant schedules and no active cooling, aligning with common practice in Central European residential buildings. This ensures that the model would simulate the actual passive indoor temperature without artificial truncation. CitySim does not model windows as independent operable elements. Instead, window-related effects are represented indirectly through facade-level parameters such as glazing ratio and solar heat gain coefficient (g-value), which control solar gains but not dynamic ventilation behavior (Miller et al.,2018; Robinson and Haldi, 2009). We therefore interpret the resulting indoor temperatures as a conservative “closed window, no-cooling” worst-case estimate of overheating risk.

6.2.5 Analysis methodology

Before analyzing the outdoor thermal comfort outcomes across the four design scenarios, we first examined whether the level of detail in building data has an influence on simulated UTCI results. Specifically, we compared a realistic setting based on detailed building archetypes derived from the EU TABULA dataset with ENVI-met’s default building setting, where all buildings are treated as having the same genetic material and structure.

The comparison was conducted for Scenarios A and B, which differ only in urban greenery but share identical building layouts. In both cases, we compared UTCI values

at 14:00 CET and at a height of 1.5 m. This height corresponds to average human breathing level and is widely accepted for thermal comfort assessments (Yu et al., 2025a). The goal was not to determine which configuration is more accurate, since no observational validation data are available but to examine whether using realistic building data results in materially different microclimatic outcomes.

Then, to evaluate the effects of different urban design strategies on outdoor thermal comfort, we conducted a statistical analysis of the simulated microclimate data. We extracted UTCI and four key microclimatic variables (T_a, T_{mrt}, RH, and v) at 1.5 m height from 6,032 raster cells within the defined study area (within the red boundary in Figure 6.2). These raster data were used to compute area-averaged UTCI values at 2-hour intervals from 06:00 to 22:00 CET under four predefined scenarios (A, B, C, and D). Meanwhile, paired t-tests were used to compare UTCI values between key scenario pairs at 14:00 CET (Field, 2013). Specifically, (i) A vs. B for the effect of urban green, (ii) C vs. D for the effect of urban green after retrofit, (iii) B vs. D for the effect of renovation alone. Prior to hypothesis testing, the Shapiro-Wilk test was used to verify the normality of the data, and Levene's test was used to assess the homogeneity of variances (Levene, 1960; Shapiro and Wilk, 1965). Benjamini-Hochberg (BH) corrections were applied where necessary to adjust for multiple comparisons and control the false discovery rate (Benjamini and Hochberg, 1995).

Next, to quantify the relative impact of each environmental variable on UTCI, we performed ridge regression analysis using four standardized predictor variables (T_a, T_{mrt}, RH, and v) for each scenario (McDonald, 2009). Ridge Regression was selected because it mitigates the strong multicollinearity especially between T_a and T_{mrt} that is typical under heatwave conditions while retaining all predictors in the model. This method introduces a regularization parameter (α), which stabilizes coefficient estimates, prevents overfitting, and improves model robustness by applying shrinkage to less-influential variables. All input variables were standardized prior to regression to ensure coefficient comparability. The optimal α values were determined automatically via cross-validation for each scenario (Arum et al., 2025). For each model, we report: R^2 values; standardized regression coefficients; variance inflation factors (VIFs); and variable weights. The purpose of this analysis is explanatory rather than predictive: ridge regression is used here as a robust regularized regression tool to rank the influence of T_a, T_{mrt}, RH and v, rather than to compare alternative multivariate techniques (e.g. partial least squares).

To further examine the spatial variability of microclimatic influences on thermal comfort, we selected three representative site pairs (six observation points in total) for detailed analysis. Pair 1 is located within a street park, with one observation point situated in the park grass area (Point 1) and the other in the shade of the main road trees (Point 2). Pair 2 is positioned in a neighborhood, with one observation point strategically placed in an

open area exposed to direct sunlight (Point 3) and another beside a tall building offering shade (Point 4). Pair 3 spans across a road, with one point on the north side (sun exposed) (Point 5) and another on the south side (shadowed) (Point 6). Figure 6.4 illustrates the spatial arrangement of these observation sites.



Figure 6.4 The location of six observation points. The land cover map is consistent with **Figure 6.2.**

6.3 Results and discussion

6.3.1 Necessity of realistic building dataset

The spatial UTCI differences between simulations using the TABULA-based realistic building settings (Scenarios A and B) and the ENVI-met default building settings are presented in Figure 6.5. The figure illustrates both positive and negative UTCI deviations resulting from the use of realistic building data. Scenario B, which lacks urban green, exhibits a larger UTCI difference compared to Scenario A. The maximum UTCI difference reaches 1.46 °C. The difference is particularly evident in densely built areas with high surface exposure, where realistic material and envelope variations alter the simulated heat storage and radiation balance. These findings demonstrate that the level of building detail plays a critical role in outdoor thermal simulation and can materially affect thermal comfort assessments. The magnitude of modeled differences (e.g., 1.5 °C UTCI sensitivity to archetype realism) is comparable to or larger than

reported inter-model variability in ENVI-met-based studies, supporting the robustness of the relative findings.

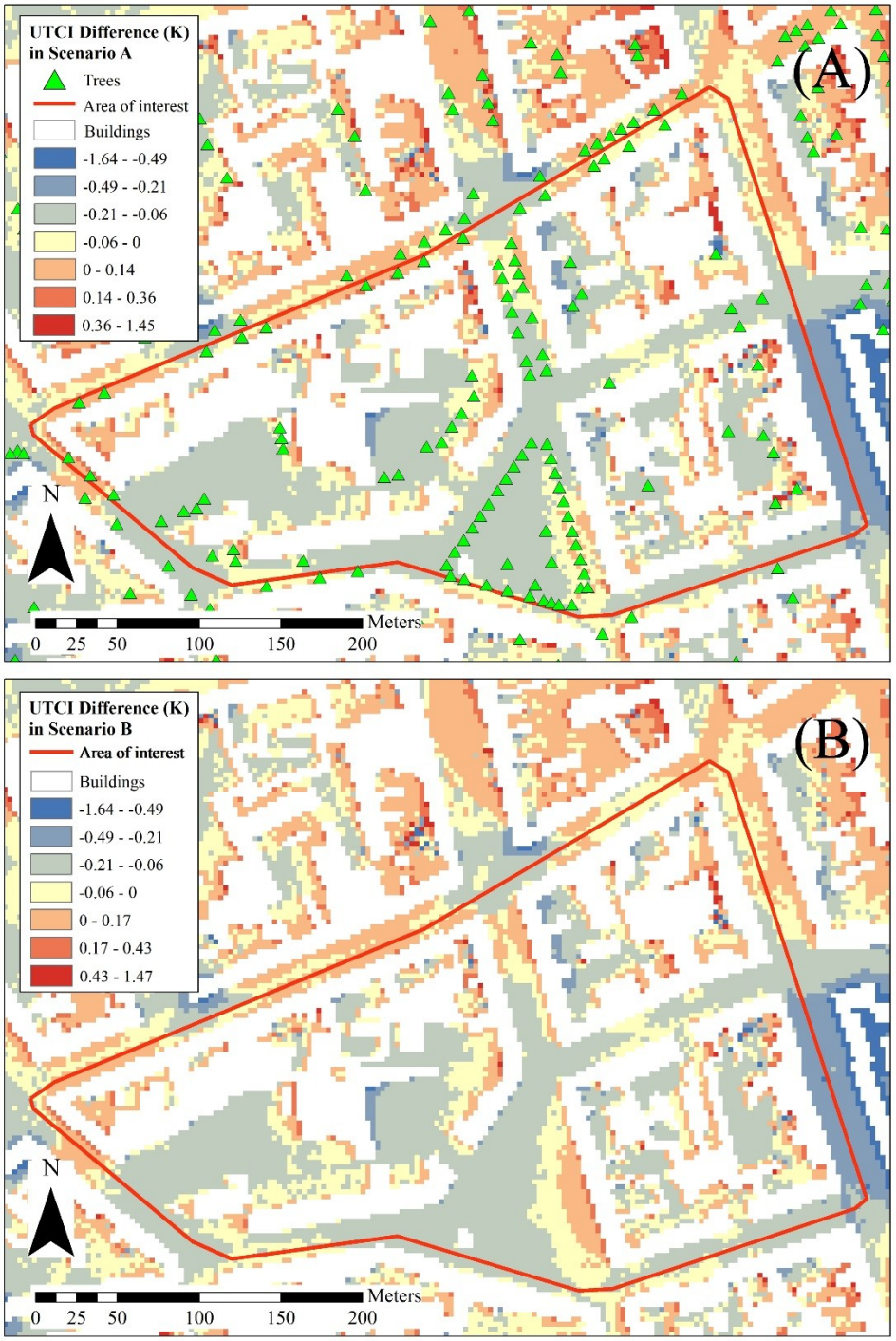


Figure 6.5 UTCI difference map at 14:00 CET, 1.5m height.

Note: (A) difference between Scenarios A with Tabula building setting and with ENVI-met default building setting (Tabula setting - default setting), (B) difference between Scenarios B with Tabula building setting and with ENVI-met default building setting. Solar azimuth was 189.49° and solar elevation 59.2°.

6.3.2 Indoor thermal performance under heatwave conditions

Figure 6.6 presents the hourly average indoor temperatures of all buildings in research area both their original and retrofitted states on July 19, 2022, the peak of the heatwave. The external meteorological temperature from the Düsseldorf Airport Station is shown as dashed line. This allows us to assess potential unintended indoor consequences of winter-focused retrofits during summer extremes. In line with the modelling setup described in Section 6.2.4, the interpretation below focuses on the daytime period between approximately 06:00 and 22:00 CET, when the indoor simulations are driven by ENVI-met-derived local microclimate. Hours outside this window mainly provide thermal preconditioning.

The results reveal a clear "crossover pattern." During the late evening and early morning (roughly 22:00–07:00 CET), the retrofitted buildings (blue line) are slightly cooler than the existing stock (orange line). However, as solar radiation intensifies, this advantage quickly reverses. From late morning to evening (about 08:00–21:00 CET), retrofitted buildings exhibit consistently higher indoor temperatures. Starting around 08:00 CET, indoor temperatures in both typologies rise; however, the retrofitted building exhibits a significantly sharper temperature increase, finally reaching a much higher peak. The maximum difference exceeded 3.8 °C around 15:00 CET, pushing the absolute peak indoor temperature to approximately 36.8 °C.

This extreme overheating confirms the severity of the "closed window" worst-case scenario described in Section 2.4. Such temperatures far exceed typical adaptive comfort limits (e.g., 26 °C to 28 °C) and pose a serious health risk to occupants, demonstrating the danger of relying on envelope retrofits without integrating night ventilation or active cooling strategies.

This behavior aligns with fundamental building physics. Retrofitted buildings typically have thicker insulation and reduced air permeability, which significantly slows heat transfer through the envelope. Combined with improved airtightness, which limits unintentional air exchange, retrofitted buildings begin the day with slightly higher internal temperatures. In the absence of active cooling and limited ventilation (as assumed here, in line with typical Central European housing), once solar radiation enters directly through glazing, governed by the defined glazing ratio and g-value, the retained heat cannot be dissipated effectively, causing the retrofitted buildings to warm more rapidly than the existing ones.

These findings underscore the dual-edged nature of winter-oriented retrofit strategies under extreme summer conditions. While they improve energy efficiency and night-time comfort, they can significantly worsen indoor thermal safety during hot afternoons, particularly in heatwave scenarios and in the absence of adaptive cooling technologies. From a resilience perspective, these results suggest that, under prolonged heatwave

conditions and without effective passive or active cooling, retrofitted buildings may struggle to maintain indoor conditions compatible with passive survivability. Specifically, the simulated peak indoor temperatures of approximately 36.8 °C significantly exceed these survivability thresholds, posing severe heat-health risks—particularly for vulnerable populations such as the elderly—who may lack the physiological or technical means to adapt to such extreme internal environments without active cooling.

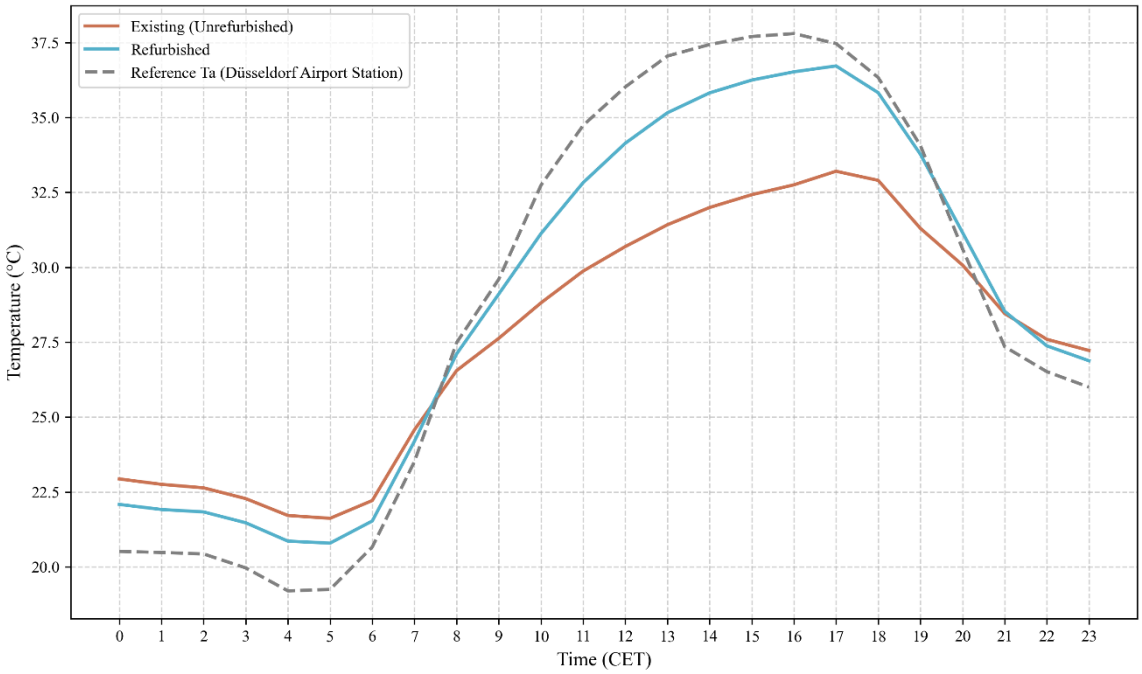


Figure 6.6 Hourly average indoor temperatures for all buildings in their existing and retrofit states on July 19, 2022.

Note: The dashed line represents the reference external meteorological temperature, sourced from the Düsseldorf Airport Station. The solid lines represent the simulated indoor conditions in the dense study neighborhood.

6.3.3 Overview of thermal comfort across scenarios

Table 6.2 summarizes the simulated spatial averages of key climate variables across the entire study area at 14:00 CET across the four scenarios. The UTCI exceeded 41 °C in all scenarios, indicating very strong heat stress during the peak of the heatwave. According to the UTCI stress assessment scale (Blazejczyk et al., 2012), values between 38 °C and 46 °C fall within the 'very strong heat stress' category, posing significant health risks to pedestrians. Scenario B recorded the highest UTCI (43.70 °C), while Scenario C showed the lowest (41.45 °C). T_{mrt} ranged from 55.43 °C in Scenario C to 63.21 °C in Scenario B, confirming the dominance of radiative heat in shaping thermal conditions. T_a remained consistently high across scenarios (>37 °C), averaging between 37.85 °C and 38.25 °C. RH stayed extremely low (21.39–21.95%), which is a result of

this hot, dry summer afternoon. The domain-average simulated pedestrian-level v at 1.5 m height was 0.49 m/s in all four scenarios at 14:00 CET (Table 6.2). This similarity arises because the tested design changes (building insulation and the presence or absence of trees) had a limited impact on the bulk airflow momentum passing through the domain boundaries. However, local sheltering and turbulence, and channeling effects around buildings and trees were fully resolved at the grid-cell level. These localized variations are reflected in the spatial heterogeneity of the UTCI distribution (discussed in Section 6.3.6) rather than in the aggregated domain-average value.

Table 6.2 ENVI-met simulated average values of climatic parameters across four scenarios at 14:00 CET in the study area.

	Scenario A	Scenario B	Scenario C	Scenario D
UTCI (°C)	42.03	43.70	41.45	43.11
T_{mrt} (°C)	56.93	63.21	55.43	61.64
T_a (°C)	38.11	38.25	37.85	37.85
RH (%)	21.64	21.39	21.95	21.69
v (m/s)	0.49	0.49	0.49	0.49

Note: Scenario A: Existing+Green; B: Existing+No Green; C: Retrofitted+Green; D: Retrofitted+No Green

Figure 6.7 illustrates the average UTCI values of the whole interest study area (within the red boundary in Fig 6.2) under four different scenarios, measured from 06:00 CET to 22:00 CET. Across all scenarios, UTCI values reach their maximum at 14:00 CET, coinciding with the period of highest heat stress. At this peak hour, Scenario B exhibits the highest average UTCI (43.70 °C), followed by Scenario D (43.11 °C), Scenario A (42.03 °C), and Scenario C (41.45 °C). The maximum UTCI values range from 46.75 °C to 47.87 °C, with the lowest values (35.02 °C to 36.79 °C), as indicated by the vertical error bars. By 06:00 CET, the start of the simulation period, average UTCI values range from 19.82 °C to 20.89 °C across the scenarios. All scenarios converge to similar UTCI levels (approximately 23.6 °C) by 22:00 CET.

Notably, Scenario C shows the lowest UTCI values across all hours, indicating the effectiveness of combining building retrofit with urban green infrastructure. The UTCI values of Scenarios B, D, and A fall between the two, in descending order.

Figure 6.8 illustrates the distribution of UTCI at 1.5 m height for Scenario A and Scenario B at 14:00 CET, the time of day when UTCI peaked. Scenario A and B were selected as representative cases to assess the influence of existing building conditions in combination with and without urban green on localized outdoor thermal comfort.

The results highlight the important roles of tree coverage and building heights in shaping the local microclimate. In Scenario A (Figure 6.8 left), UTCI values range from a cooler 34.91 °C in vegetated or shaded areas to a peak of 50.14 °C in sun exposed open spaces.

Compared to Scenario B (Figure 6.8 right), which lacks vegetation, the overall presence of green in Scenario A reduces the average UTCI by 1.67 °C at peak hour. These microclimatic dynamics show the importance of urban morphology and landscape design in mitigating heat stress.

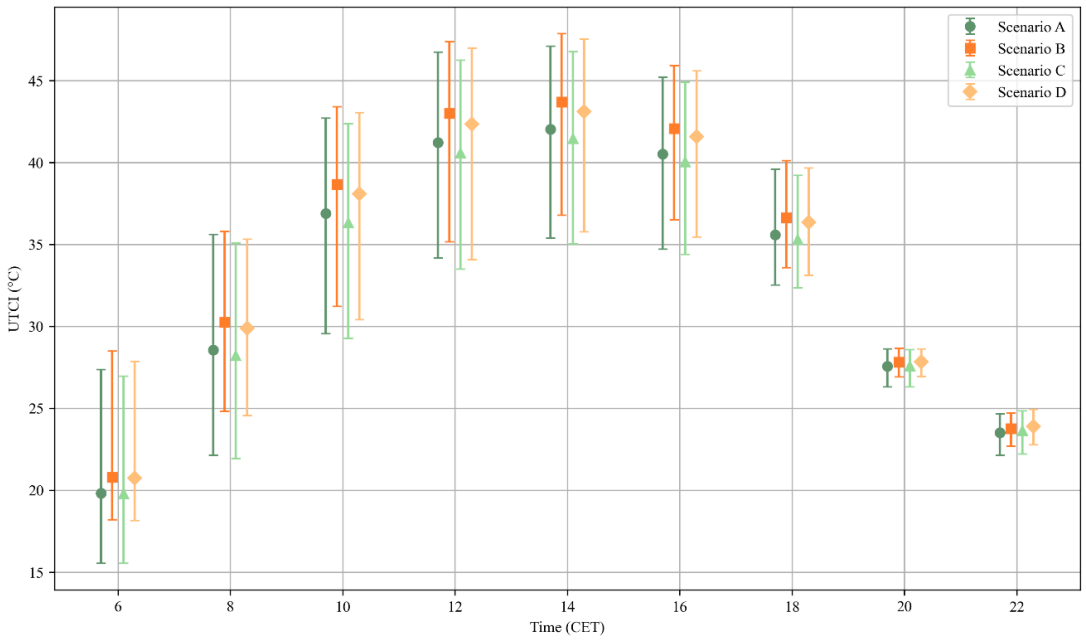


Figure 6.7 Hourly average UTCI values (06:00–22:00 CET).

Note: They across four urban design scenarios (A–D), with vertical error bars representing the minimum and maximum values across 6,032 raster cells.

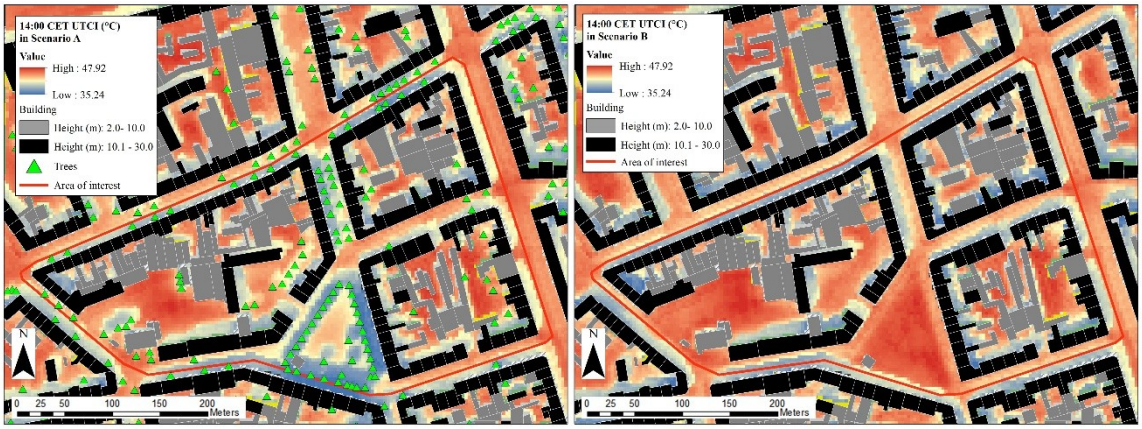


Figure 6.8 The 14:00 CET UTCI map of the study area (1.5m height) of Scenario A (left) and Scenario B (right).

Note: The trees' locations in and surrounding the study area are represented by green triangles. Solar azimuth was 189.49° and solar elevation 59.2°.

6.3.4 Scenario-specific impacts on outdoor thermal comfort

To further investigate how specific combinations of building retrofitting measures and urban green infrastructure affect localized outdoor conditions, we conducted statistical tests to compare UTCI values at 14:00 CET, the hottest period of the day. All data met the assumptions of normality and homogeneity of variances, as confirmed by the Shapiro-Wilk and Levene's tests (see Section 6.2.5). Paired t-tests were applied, and Benjamini-Hochberg correction was used to adjust for multiple comparisons.

The results (Table 6.3) indicate that all comparisons yielded statistically significant differences ($p < 0.05$ after BH correction); however, the physical relevance differed: nature-based greening produced several-degree changes in UTCI, whereas envelope-only retrofits resulted in sub-degree differences (<1 °C). Specifically, urban green significantly reduced UTCI both before and after retrofit, as seen in Scenarios A and C in Figure 6.7, which exhibited the lowest UTCI values at 14:00 CET. Even without vegetation, building retrofit (Scenario D) significantly reduced UTCI compared to the un-retrofitted, non-green Scenario B ($p < 0.05$). In this case, the average UTCI was slightly lower in Scenario D (43.11 °C) than in Scenario B (43.70 °C). However, despite its statistical significance due to consistent directional changes across the domain, this 0.6 °C reduction is physically marginal in the context of extreme heatwaves, as it fails to shift the outdoor thermal environment out of the 'very strong heat stress' category (>41°C). This should therefore be interpreted as indicating the direction and relative sensitivity of outdoor thermal stress to envelope changes, rather than as a large mitigation effect. By contrast, vegetation produces substantially stronger cooling (>5 °C), highlighting that greenery is the dominant factor for reducing outdoor heat stress in this compact neighborhood. This reduction may be attributed to the altered building envelope properties, which affect how solar radiation is absorbed and reradiated to the surroundings.

Table 6.3 Paired t-Test results for UTCI differences across urban design and retrofit scenarios at 14:00 CET, with BH correction.

Scenario Comparison	Tested Impact Factor	t-Statistic	Raw p-Value	BH Corrected p-Value	Significance level
A vs. B	Effect of greening	-5.84	0.0004	0.0008	Highly Significant ($p < 0.01$)
C vs. D	Effect of greening after retrofit	-5.88	0.0004	0.0008	Highly Significant ($p < 0.01$)
B vs. D	Effect of building renovation	3.28	0.0112	0.015	Significant ($p < 0.05$)

6.3.5 Regression analysis of climatic drivers affecting UTCI

To understand the drivers of outdoor discomfort, ridge regression was performed using the standardized predictor variables T_a, T_{mrt}, RH, and v as predictors, which described in Section 6.2.5. Table 6.4 shows the results at 14:00 CET (>37 °C), which further quantifies the influence of climatic parameters on UTCI across the four scenarios. In all cases, the models demonstrated excellent performance, with coefficients of determination (R^2) consistently above 0.995, indicating that these four parameters sufficiently capture the variance in UTCI values.

Table 6.4 Ridge regression analysis of urban design and climatic factors impacting UTCI at 14:00 CET across different scenarios.

Scenario	Parameters	R_2	Standardized Coefficient	Collinearity Statistics (VIF)	Weight (%)
A	T_{mrt}	0.996	2.580	1.231	91.7
	T_a	0.996	0.131	16.888	4.7
	RH	0.996	-0.019	17.579	0.7
	v	0.996	0.083	1.403	3
B	T_{mrt}	0.996	2.371	1.154	92.3
	T_a	0.996	0.053	8.052	2.1
	RH	0.996	-0.058	7.901	2.3
	v	0.996	0.087	1.257	3.4
C	T_{mrt}	0.996	2.608	1.280	91.6
	T_a	0.996	0.148	14.514	5.2
	RH	0.996	-0.008	14.810	0.3
	v	0.996	0.085	1.394	3
D	T_{mrt}	0.996	2.501	1.214	92.3
	T_a	0.996	0.029	2.425	1.1
	RH	0.996	-0.092	2.000	3.4
	v	0.996	0.087	1.807	3.2

Note: The α values used in the ridge regression were selected automatically through cross-validation, and were 0.201 (A), 0.050 (B), 0.175 (C), and 0.066 (D), respectively.

T_{mrt} is the dominant factor across all scenarios, with standardized coefficients ranging from 2.371 to 2.608 and accounting for over 91% of the total model weight in all cases. This confirms that radiative heat exchange, strongly influenced by surface properties and shading, is the most critical factor governing outdoor heat stress during summer heatwaves. T_a showed positive but much smaller coefficients, contributing less than 5.2% to the total model weight in all scenarios. While high T_a exacerbates thermal discomfort, its marginal effect is limited once T_{mrt} is already elevated.

RH showed weak and consistently negative coefficients. This issue is particularly evident in Scenarios A and C, where both urban green and extremely low humidity levels are present. In these scenarios, severe multicollinearity was observed between RH and

T_a, as reflected by high VIF values exceeding 14. VIF quantifies how strongly a predictor is correlated with other predictors. A high VIF indicates that the variable's coefficient may be unstable due to shared information with other variables. Here, vegetation is likely to increase RH through evapotranspiration while simultaneously reducing T_a and T_{mrt} due to shading and latent cooling, causing these variables to become highly interdependent. Furthermore, under dry atmospheric conditions, RH and T_a are naturally inversely related. Although ridge regression reduces the distortion from multicollinearity by introducing a small amount of bias into the regression coefficients (García García et al., 2022), RH's relative weight in the model remained minor, which is below 3.4% in all cases. Given the strong correlation between Ta and RH and the resulting high VIF values, the corresponding coefficients should be interpreted with caution; however, across all scenarios the dominance of T_{mrt} remains stable.

In contrast, v exhibited a small but positive association with UTCI in all scenarios, with coefficients around 0.078–0.087 and weights around 3%. This observed positive correlation aligns with physiological findings documented by Bröde and Kampmann (Bröde and Kampmann, 2023), who noted that UTCI captures both the convective and evaporative heat-transfer effects of wind and wind speed may aggravate thermal strain under extremely hot and dry conditions.

Taken together, these findings confirm that T_{mrt} is the main factor through which urban design interventions, such as tree shading or building insulation can influence outdoor comfort. The limited contribution of RH and v under the simulated conditions highlights the dominance of radiative effects over convective or latent heat exchanges during extreme afternoon heat.

To assess how these parameter-level effects translate into real-world mitigation strategies, the next section examines scenario-specific impacts on UTCI across the study area.

6.3.6 Localized impacts of microclimate variables on UTCI

To enhance our understanding of how microclimate variables influence thermal comfort at a localized level, we selected three pairs comprising a total of six observation sites (see Section 6.2.5). Each pair highlights different urban morphologies and degrees of exposure to vegetation and building shading. For each location, we analyzed UTCI and T_{mrt} at 14:00 CET, the hour of maximum thermal stress across the four design scenarios (Figure 6.9). Wind speed, while locally variable, is discussed textually due to its complex spatial dynamics and to maintain visual clarity. T_a and RH were excluded from localized graphical analysis due to their relatively low spatial and statistical variability (see Sections 6.3.4 and 6.3.5).

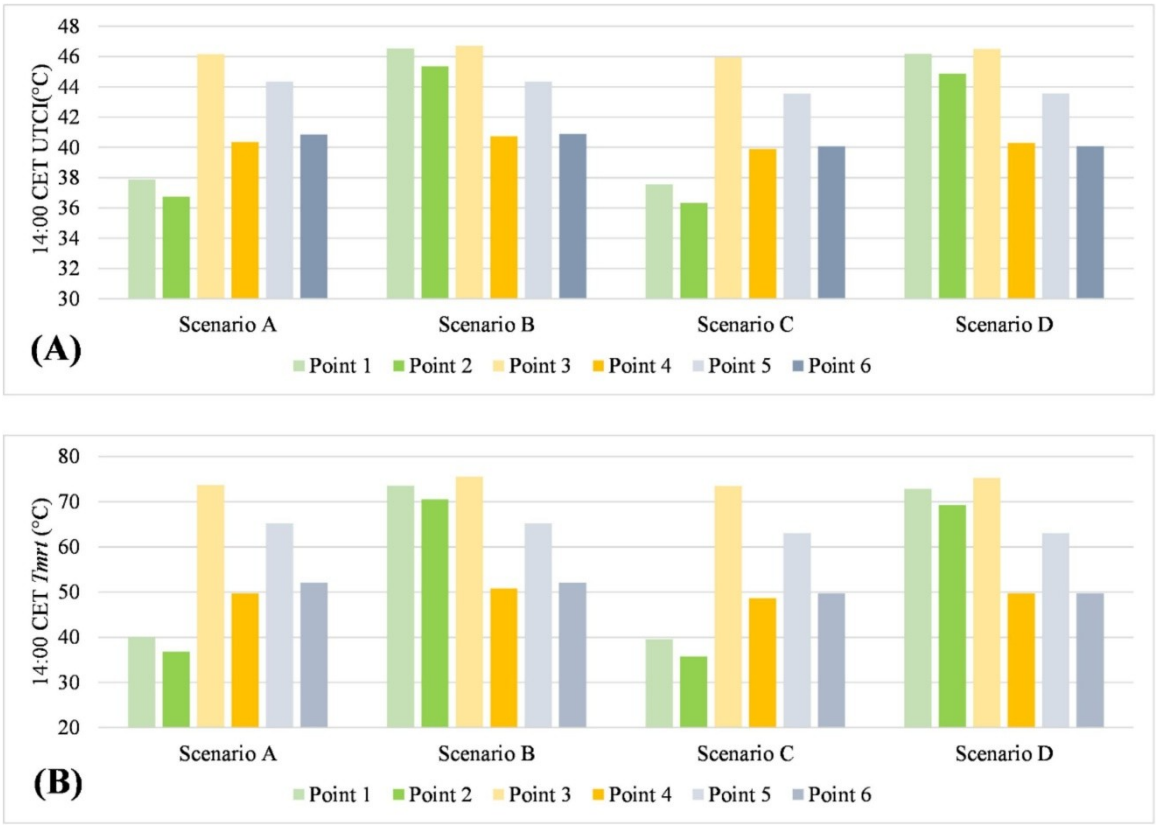


Figure 6.9 UTCI values (A) alongside variations in T_{mrt} (B) across four scenarios at 14:00 CET for six observation points within the study area.

Points 1 and 2 are located in the park area with urban green under scenarios A and C, consistently showing the lowest UTCI values. In scenarios lacking urban green (B and D), UTCI increases greatly by over 5 °C at 14:00 CET due to full solar exposure. Among these, point 2, which is slightly closer to an adjacent tall building, shows slightly lower UTCI value than point 1. Points 3 and 4 are situated within a block lacking urban green and display significant differences in UTCI values (about a 6 K difference in all scenarios). Point 3 is located in an open area without any vegetation and fully exposed to sunlight and consistently shows the highest UTCI values across all scenarios. The presence of tall buildings around point 4 casts shadows that substantially cool the area and leads to this notable difference between the two points. Points 5 and 6 are positioned on opposite sides of a street, near tall buildings with sparse vegetation. Buildings provide shading that beneficially lowers UTCI on the south side (Point 6) compared to the north side (Point 5), with a difference of approximately 3.5 °C.

Across all points, T_{mrt} closely mirrored UTCI trends, confirming the strong positive correlation observed in the ridge regression analysis (Section 3.4). Areas with effective shading from trees or building geometry exhibited significantly lower T_{mrt}, translating into better thermal comfort. Conversely, open, sun-exposed areas showed peak values for both T_{mrt} and UTCI. Meanwhile, Scenario D, only with building retrofit moderately reduces UTCI (ranging 0.24 - 0.82 °C for each Point) compared to Scenario B. While

consistent, this limited cooling effect confirms that envelope retrofits alone are insufficient to mitigate heat stress without the complementary shading provided by vegetation.

In comparison, T_a and RH showed minimal spatial variation across observation points and contributed little explanatory value. These findings are consistent with the regression results, which attributed less than 5% of model weight to T_a and under 3.4% to RH in all scenarios. v varied more noticeably among locations, with open areas such as Point 3 experiencing the highest values (>1.34 m/s), while more sheltered points (1, 2, 5, and 6) recorded the lowest. However, even in breezier areas, the dominant influence of radiation outweighed the modest cooling effect of wind under these dry, hot conditions.

These localized findings emphasize the crucial role of shading and surface radiation exchange in shaping outdoor thermal comfort, especially during heatwave conditions. They also support the broader simulation results: combining building retrofits with green infrastructure provides the most effective strategy for mitigating heat stress in urban environments.

6.4 Conclusion

This study evaluated the summer thermal implications of EU-standard residential retrofits by integrating realistic TABULA archetypes into a microclimate analysis of the peak day (19 July 2022) of the Düsseldorf heatwave. Validating the importance of envelope realism, the use of specific archetype data produced spatial UTCI differences of up to 1.5 °C compared to generic defaults. Besides, the results quantify a key trade-off between mitigation and adaptation: although green infrastructure reduced peak UTCI by up to 6.0 °C, building retrofits optimized solely for winter energy efficiency inadvertently exacerbated summer risks. Specifically, a “crossover effect” was observed, where under conservative closed window and no cooling conditions, the retrofitted building envelope reduced heating demand but increased indoor daytime peak temperatures by up to 3.8 °C. This peak exceeds heat-health guidance for safe indoor temperatures, highlighting potential risks for vulnerable occupants during heatwaves in uncooled dwellings.

These findings verify that T_{mrt}, explaining over 91% of UTCI variance, is the dominant driver of outdoor comfort. This reflects the central role of radiative processes, façade surface temperatures and shading in determining pedestrian heat stress, with trees and other vegetated elements providing both radiative shielding and latent cooling through evapotranspiration. Consequently, for municipal planners and engineers, current EU retrofit policies and practical implementation should look beyond envelope insulation and incentivize “summer-aware” packages that combine insulation with nature-based solutions and external shading, to prevent locking in indoor overheating risks.

While the proposed framework offers a potentially scalable method for bridging urban microclimate and building energy domains in other TABULA-covered cities, the results must be interpreted within specific modelling limitations. Specifically, the adopted one-way integration prioritizes passive envelope performance and does not represent anthropogenic heat feedback to the microclimate. We also acknowledge inherent limitations in the simulation engines, such as ENVI-met's known tendency to overestimate daytime T_a under stable conditions and CitySim's simplified radiation exchange. However**,** these systematic biases apply across all scenarios, ensuring that the reported relative differences remain stable. Furthermore, the indoor results represent a worst-case scenario for unventilated, uncooled spaces. Finally, since we focused on temperature and index-based indicators (T_a, T_{mrt}, UTCI and indoor temperatures) rather than on sensible and latent heat-flux budgets, a more detailed flux-based energy-balance analysis is therefore left for future work. Based on this work, future research could extend this one-way ENVI-met to CitySim workflow toward fully coupled approaches with site-specific observational validation and conduct systematic uncertainty and sensitivity analyses to refine human-centric retrofit guidelines.

Declaration of Competing Interest

The authors declare that they have no known competing financial interests or personal relationships that could have appeared to influence the work reported in this paper.

Acknowledgements

The authors would like to acknowledge funding from China Scholarship Council. The project was partly co-funded under the Excellence Strategy of the Federal Government and the Länder (Project SFBLE003 TRUKLIB).

7. Synthesis and outlook

In this chapter, the general research questions outlined in Chapter 1 are addressed and the main conclusions from the research presented in Chapters 4, 5 and 6 are summarized. Moreover, suggestions for possible and planned future research are outlined accompanied by a critical evaluation of the results of this work.

The work is based on a database-centered integration conceptin which a common urban dataset provides the shared geometric and semantic information required by both CitySim and ENVI-met. Specifically, the database integrates building geometry with archetype-based building attributes (e.g., construction properties and material parameters), which are translated into model-specific inputs for the two modelling platforms. In the Düsseldorf–Flingern case study, ENVI-met was used to represent neighborhood-scale microclimate heterogeneity under a 2022 heatwave event, while CitySim was used to assess building energy under current and future climate conditions as well as indoor comfort responses during the same heatwave event. Importantly, the implemented integration is one-way/offline: ENVI-met outputs are used to refine the

outdoor boundary conditions for CitySim indoor simulations, while the outputs from both models are subsequently linked during post-processing using persistent building identifiers and common scenario definitions where building-level correspondence is required.

7.1 Synthesis of findings against the research questions

RQ1: How can urban climate models and urban building energy models integrate through shared databases?

The dissertation Chapter 4 demonstrates that a shared, geographic archetype urban database can function as an effective intermediary layer for UCM–UBEM integration. With standardized model-ready inputs, this database can generate reproducible data for both domains. The unified building ID is central, which supports cross-model comparison and linkage. This database-centered approach also reduces repeated data preparation work across different models and improves transparency, because each model input can be traced back to a documented source and transformation step.

RQ2: How does the shared database support neighborhood residential building energy retrofit strategy?

The dissertation Chapter 5 provides a neighborhood-scale retrofit assessment aligned with EU refurbishment pathways, using archetype-based building semantics with detailed urban geometry. Unlike conventional BEMs, the UBEM framework clearly accounts for neighborhood interactions, including inter-building shading and radiative exchange. Consequently, buildings belonging to the same archetype may exhibit different energy performance depending on their position within the surrounding urban morphology. This enables a more realistic assessment of neighborhood-scale retrofit scenarios than would be possible using isolated building models.

Based on standardized TABULA refurbishment scenarios, the workflow quantifies the relative impacts of alternative retrofit options on heating demand, CO_2 emissions, and economic performance under present and future climate conditions. Rather than predicting actual retrofit outcomes within the study area, these simulations provide a consistent framework for comparing building archetypes and evaluating the influence of neighborhood context on retrofit performance. In addition, the workflow supports decision-relevant indicators, including energy savings, emissions reduction, simple payback time, and net present value under standardized assumptions.

RQ3: To what extent do retrofit measures and neighborhood greening modify outdoor heat stress and its drivers at neighborhood- scale?

Chapter 6 quantifies microclimate distribution and outdoor thermal stress under different scenario designs using ENVI-met simulation. Scenario comparisons indicate that urban greening and shading-related interventions can generate materially larger

reductions in peak outdoor thermal stress than envelope-only refurbishment measures, because the dominant driver of UTCI variability at pedestrian level is T_{mrt} rather than T_a alone. Driver attribution analyses (combining scenario contrasts, peak-hour hypothesis testing, and multivariate regression under collinearity) consistently indicate that radiative processes and shading control the peak-hour comfort outcomes, while ventilation and humidity contribute minor regulatory effects depending on local canyon geometry and surrounding vegetation.

These findings show that neighborhood-scale retrofit assessment should consider both building energy performance and outdoor thermal comfort. While envelope refurbishment effectively reduces heating demand, neighborhood greening and shading interventions have a much greater influence on pedestrian thermal stress. The complementary use of UBEM and UCM therefore provides a broader basis for evaluating climate-resilient retrofit scenarios than either modelling approach alone, even though the present dissertation adopts a one-way rather than fully coupled modelling framework.

7.2 Overall contributions

Through the three studies, the dissertation contributes in four main ways:

(1) Methodological contribution: it develops a database-centered integration workflow that harmonizes UCM and UBEM through a shared urban geographic archetype dataset, enabling reproducible multi-scenario assessments for residential building stocks supported by TABULA or comparable archetype datasets.

(2) Data contribution: it localized a georeferenced archetype dataset for Düsseldorf as a case study, showing how to build a structured pathway from urban data infrastructures to energy and climate simulations.

(3) Planning contribution: it demonstrates how this workflow can support retrofit prioritization under climate change, combining energy, emissions, and economic indicators to support municipal decarbonization planning.

(4) Climate–health contribution: specific Düsseldorf case study quantifies neighborhood-scale heat-stress impacts in different scenario designs and their drivers under heatwave conditions, highlighting the primacy of T_{mrt} for pedestrian thermal comfort and clarifying why nature-based shading interventions often outperform envelope-only measures for outdoor comfort at peak heat stress.

7.3 Limitations

Although this dissertation presents a relatively complete workflow, the findings should be interpreted in the context of several limitations:

(1) One-way (UCM→UBEM) linkage.

The implemented connection uses ENVI-met outputs to refine CitySim boundary conditions and links results offline in post-processing. It does not represent feedback from building energy use to the microclimate (e.g., anthropogenic heat emissions, HVAC waste heat, dynamically varying surface temperatures driven by indoor conditions). As a result, the current framework cannot quantify positive feedback mechanisms such as cooling-induced urban warming or the microclimatic consequences of different system choices at high temporal frequency.

(2) Lack of observational validation (outdoor and indoor).

The dissertation relies on numerical simulations and validation studies conducted in other papers and does not include dedicated Düsseldorf field measurements (e.g., T_a, T_{mrt}, solar radiation, v, surface temperatures (Ts), indoor operative temperature). Therefore, the emphasis is on relative, scenario-to-scenario differences rather than on absolute predictive accuracy at specific locations and times.

(3) Data harmonization and LoD/resolution mismatch in integrated workflows.

Although a shared database improves consistency, integrated UCM–UBEM workflows remain sensitive to (a) incomplete or inconsistent input datasets (urban morphology, meteorology, and building attributes), and (b) the mismatch in LoD and spatial resolution between climate and energy models. These issues affect how reliably UCM grid outputs can be translated into building-level boundary conditions, and how building-level results can be integrated back to climate-model scales.

(4) Model-structural limits, parameterization, and computational trade-offs.

ENVI-met and CitySim contain structural simplifications and potential systematic biases. Higher-resolution and multi-scale configurations also increase computational cost and limit scalability, often forcing simplifications (e.g., reduced-order representations, downscaling/aggregation choices) that may ignore fine building or control details relevant for microclimate feedback. While many systematic biases apply across all scenarios (supporting stable relative comparisons), they still limit absolute realism and generalizability.

(5) Boundary condition representativeness and temporal coverage.

The microclimate analysis focuses on a specific heatwave episode, and the energy analysis uses standardized climate series for future periods. Broader generalization to other years, synoptic conditions, and socio-technical futures require additional scenario sets and/or longer simulation horizons.

(6) Data privacy, access, and governance constraints (for calibration and two-way coupling).

A practical limitation for future two-way integration and calibration is that key datasets (e.g., occupancy patterns, control strategies, smart-meter or district heating records) are sensitive and often restricted. Privacy regulation and data ownership can limit access, sharing, and reproducibility, and thus constrain empirical calibration and large-scale deployment unless privacy-preserving and governance-aware approaches are adopted.

7.4 Outlook and future work

Future work should extend the dissertation in two complementary directions: (1) moving from offline, one-way linkage to true bidirectional (two-way) coupling, and (2) strengthening empirical grounding through systematic observational validation.

7.4.1 Towards bidirectional UCM–UBEM coupling

A logical next step is to establish a two-way exchange between UCM and UBEM on the basis of the shared database. Building on the bidirectional coupling concept introduced in Chapter 4, the coupling loop would comprise two complementary pathways with distinct goals.

(1) UCM → UBEM (microclimate-informed building simulation).

Localized outdoor boundary conditions (e.g., T_a, RH, v, solar radiation components) would be mapped from the UCM grid to individual building sites and façades. By representing spatially heterogeneous microclimate conditions within the UBEM, this linkage seeks to mitigate the inaccuracies typically introduced by oversimplified, uniform weather data. This integration facilitates a more accurate evaluation of building energy responses, such as cooling requirements and indoor thermal safety, while improving the characterization of heat exchange processes at the building-envelope interface.

(2) UBEM → UCM (building-physics-informed urban climate simulation).

Time-resolved anthropogenic heat emissions, especially anthropogenic heat emissions (HVAC waste heat, internal gains released outdoors) and envelope boundary conditions (surface temperature or heat flux) would be transferred from the UBEM to the UCM. This linkage ensures that anthropogenic heat emissions and envelope surface temperatures are mapped accurately back to the urban canopy layer. Consequently, it allows for a more accurate quantification of how building energy responses, specifically waste heat release and heat flux, which contributes to the spatial variability of outdoor heat stress on the neighborhood- scale.

7.4.2 Field measurement and validation work

To increase credibility and facilitate calibration, future work should add an observational experiment for both outdoor and indoor conditions.

For outdoor validation, field observation can combine a small number of fixed stations at representative street and courtyard locations with short mobile transects during heat-stress periods. Measurements should capture the key variables needed for thermal-stress assessment (e.g., air/surface temperature, humidity, wind and radiation). Particular emphasis should be placed on monitoring building envelope surface temperatures (e.g., walls and roofs), as these provide the physical interface linking outdoor microclimate conditions with indoor thermal responses.

For indoor validation, a limited set of representative archetype buildings can be monitored using temperature and humidity loggers, prioritizing units that are most prone to overheating (e.g., top-floor and courtyard-facing). Where feasible, interior surface temperatures of walls and ceilings should also be monitored to better characterize heat transfer through the building envelope. Even a relatively small observational dataset would improve calibration of key UBEM parameters, including infiltration, ventilation, and envelope thermal properties, while reducing uncertainty in simulated indoor conditions.

Given data privacy constraints, a staged strategy is recommended: start with sample data from fixed-point indoor measurement and publicly available building information and then extend calibration using sample energy-consumption data. The shared database provides a structured basis to manage metadata and data-access governance, and supports future validation and model development, including more tightly coupled UCM–UBEM workflows.

7.4.3 Broader scenario space and decision support extensions

Finally, future research should expand the proposed database-centered workflow into a practical decision-support framework for municipal planning. By combining the shared urban database with UBEM and UCM simulations, municipalities could evaluate climate mitigation (e.g., building energy demand and greenhouse-gas emissions) and climate adaptation (e.g., outdoor thermal comfort and heat exposure) within a common analytical framework. This would require integration of routinely available municipal datasets, including geospatial building inventories, archetype information, land-cover and vegetation data, and local meteorological observations. Building on this common data infrastructure, future studies could investigate a wider range of retrofit and urban-design scenarios, while extending the framework towards multi-criteria decision support that jointly considers energy, emissions, thermal comfort, economic performance, and uncertainty.

8. Danksagung/Acknowledgments

When I began this dissertation almost four years ago, the doctorate stood before me like an unclimbable mountain. I still remember the moment, nearly eight years ago, after finishing my master's degree, when my supervisor, Prof. Gerald Mills, told me that doctoral study is a long road: a demanding kind of work in which one must patiently face countless unknowns. Even so, I chose to take on that challenge. I came to Germany, often perceived as a place where earning a doctorate is especially difficult, to begin this journey.

None of what follows would have been possible without the support of the many mentors and companions who walked alongside me. If this research began in the silence of winter, overshadowed by the COVID-19 pandemic, it now draws to a close in the warm summer. The transition from winter to summer is more than a change of seasons; it has been a tempering of both mind and spirit. Throughout this journey, I have undergone a twofold growth: on an academic level, I have been honed through rigorous research; on a personal level, through quiet perseverance and nurtured hope, I have learned to coexist with the unknown and to listen to the echoes within the silence.

First and foremost, I would like to express my sincere gratitude to my doctoral supervisors, Prof. Dr. Michael Leuchner and Dr. Gunnar Ketzler, for placing their full trust in me from the very beginning, starting with my application from faraway China. As an interdisciplinary researcher whose work sits at the intersection of building energy modelling and urban climate, I have benefited a lot from their guidance and support in pursuing this ambitious research.

Prof. Dr. Michael Leuchner generously drew on his extensive network to connect me with colleagues at the Institut für Energieeffizientes Bauen E3D. Under his supervision, I was able to pursue my academic interests with real freedom, and he was always willing to listen whether my questions were scientific or administrative.

Dr. Gunnar Ketzler supported me with remarkable patience and precision, keeping help me troubleshoot and refining the weather datasets needed for the models. Beyond the technical side, he also shared his deep knowledge of the region and, through many memorable excursions around Aachen, helped me feel more connected to this place. Our conversations often reach well beyond climatology, adding warmth, perspective, and richness to my doctoral journey.

I thank Prof. Gerald Mills, who is my master supervisor and continuedly my doctoral supervisor. He leads me to the entrance of urban climate study and encourages me to continue following up in this field. My master work focused on regional scale urban climate research. Based on this, my doctoral study focused on microclimate study and linked it to relative local building energy. He extended my research work and provided me with professional guidance.

I would like to thank my dear (former) colleagues from the Physical Geography and Climatology working group, Dr. Oliver Reitz, Niels Döscher, Larissa Böhrkircher, Robin Borger, Gernot Frommelt and my office mate Erik Richter. Beyond our research collaborations, you helped me to understand and enjoy living in Germany through everyday life and different special activities, like Rosenmontag Karneval.

I must also thank my new Nigeria office mate Charles Anukwonke. I've truly learned so much about the world thanks to your fascinating office etiquette. Your utter dedication to your music and talking with friends, completely unfettered by the distraction of other people's working environment during my dissertation writing period, has been… an experience.

I would also like to express my sincere appreciation for to Mona Ziemes and Dr. Eliza Płaczkowska. Mona picked me up at the airport when I first came to Düsseldorf and kindly provided me with short-term accommodation. I could not have reached B2 level in German without her help. She and Eliza warmly welcomed me during this winter plagued by the COVID-19. And together, we embarked on a self-driving tour around Germany in the summer of 2022. Eliza took me on a tour of her hometown, Poland in 2024.

I thank my Chinese friends in Aachen, Gao Miaomiao, Jiang Qixuan, Meng hao, Wang Tianling, Ji Xianghe for their companionship and support. With you, Germany has felt less distant, and I have been fortunate to build friendships that I will always treasure. I thank my travel mate Gao Shuxian (UFZ). We travel together each year, and exchange stories shaped by different academic environments. Also, I thank my friends Ass. Prof. Jiang Yuan, Doctor Ding Mengtian and Yan Jiao (physician) in faraway China. Even though we are thousands of miles apart, we remain close friends who have stood by each other for many years.

My sincere thanks go to the China Scholarship Council (CSC) for its financial support, which gave me the opportunity to pursue advanced research in Germany. I am equally grateful to my parents for their unwavering emotional and financial support throughout my doctoral studies.

References

Abdulateef, M. F., & Al-Alwan, H. A. (2022). The effectiveness of urban green infrastructure in reducing surface urban heat island. *Ain Shams Engineering Journal, 13*(1), 101526. https://doi.org/10.1016/j.asej.2021.06.012

Aghamohammadi, N., & Santamouris, M. (2022). *Urban overheating: heat mitigation and the impact on health*. Springer. https://doi.org/10.1007/978-981-19-4707-0

Ahmadian, E., Sodagar, B., Bingham, C., Elnokaly, A., & Mills, G. (2021). Effect of urban built form and density on building energy performance in temperate climates. *Energy and Buildings, 236*, 110762. https://doi.org/10.1016/j.enbuild.2021.110762

Ang, Y. Q., Berzolla, Z. M., & Reinhart, C. F. (2020). From concept to application: A review of use cases in urban building energy modelling. *Applied Energy, 279*, 115738. https://doi.org/10.1016/j.apenergy.2020.115738

Arum, K. C., Ndukwe, S. C., Oranye, H. E., & Sule, O. B. (2025). Comparative analysis of ridge and principal component regression in addressing multicollinearity. *FUDMA Journal of Sciences, 9*(1), 240–245. https://doi.org/10.33003/fjs-2025-0901-2981

Ballester, J., Quijal-Zamorano, M., Méndez Turrubiates, R. F., Pegenaute, F., Herrmann, F. R., Robine, J. M., ... & Achebak, H. (2023). Heat-related mortality in Europe during the summer of 2022. *Nature medicine, 29*(7), 1857-1866. https://doi.org/10.1038/s41591-023-02419-z

Benjamini, Y., & Hochberg, Y. (1995). Controlling the false discovery rate: A practical and powerful approach to multiple testing. *Journal of the Royal Statistical Society: Series B (Methodological), 57*(1), 289–300. https://www.jstor.org/stable/2346101

Blazejczyk, K., Epstein, Y., Jendritzky, G., Staiger, H., & Tinz, B. (2012). Comparison of UTCI to selected thermal indices. *International journal of biometeorology, 56*, 515-535. https://doi.org/10.1007/s00484-011-0453-2

Böhringer, C., & Rutherford, T. F. (2008). Combining bottom-up and top-down. *Energy Economics, 30*(2), 574-596. https://doi.org/10.1016/j.eneco.2007.03.004

Bröde, P., & Kampmann, B. (2023). Temperature–humidity-dependent wind effects on physiological heat strain of moderately exercising individuals reproduced by the universal thermal climate index (UTCI). *Biology, 12*(6), 802. https://doi.org/10.3390/biology12060802

Bruse, M. (2004). *ENVI-met 3.0: updated model overview*. University of Bochum. Retrieved from: http://www.envi-met.com

Bundesregierung. (2024). *Federal Climate Change Act (Bundes-Klimaschutzgesetz)*

Buckley, N., Mills, G., Reinhart, C., & Berzolla, Z. M. (2021). Using urban building energy modelling (UBEM) to support the new European Union's Green Deal: Case study of Dublin Ireland. *Energy and Buildings, 247*, 111115. https://doi.org/10.1016/j.enbuild.2021.111115

Bueno, B., Norford, L., Hidalgo, J., & Pigeon, G. (2013). The urban weather generator. *Journal of Building Performance Simulation, 6*(4), 269-281. https://doi.org/10.1080/19401493.2012.718797

Cerezo, C., Sokol, J., AlKhaled, S., Reinhart, C., Al-Mumin, A., & Hajiah, A. (2017). Comparison of four building archetype characterization methods in urban

building energy modelling (UBEM): A residential case study in Kuwait City. *Energy and Buildings, 154*, 321-334. https://doi.org/10.1016/j.enbuild.2017.08.029

Chen, Y., Hong, T., Luo, X., & Hooper, B. (2019). Development of city buildings dataset for urban building energy modelling. *Energy and Buildings, 183*, 252-265. https://doi.org/10.1016/j.enbuild.2018.11.008

Chen, G., Rong, L., & Zhang, G. (2020). Comparison of urban airflow between solar-induced thermal wall and uniform wall temperature boundary conditions by coupling CitySim and CFD. *Building and Environment, 172*, 106732. https://doi.org/10.1016/j.buildenv.2020.106732

Cheng, C., Deng, X., Zhao, X., Xiong, Y., & Zhang, Y. (2023). Multi-occupant dynamic thermal comfort monitoring robot system. *Building and Environment, 234*, 110137. https://doi.org/10.1016/j.buildenv.2023.110137

Ching, J. K. (2013). A perspective on urban canopy layer modelling for weather, climate and air quality applications. *Urban Climate, 3*, 1. https://doi.org/10.1016/j.uclim.2013.02.001

City of Düsseldorf. (2022). Weather stations of the state capital Düsseldorf. Open Data Düsseldorf. https://opendata.duesseldorf.de/dataset/wetterstationen-der-landeshauptstadt-d%C3%BCsseldorf

City of Düsseldorf. (2023a). Demografiemonitoring 2013 bis 2022 (Statistische Informationen Nr. 320). https://www.duesseldorf.de/fileadmin/Amt12/statistik/stadtforschung/download/Demografiemonitoring_2023_V10_Seite_web_bf.pdf/. (accessed 13 March 2025)

City of Düsseldorf. (2023b). *Geodaten-Viewer der Landeshauptstadt Düsseldorf*. Retrieved from https://maps.duesseldorf.de/

City of Düsseldorf, Office of Economic Development. (2025a). Düsseldorf: Facts and figures. Landeshauptstadt Düsseldorf. https://www.duesseldorf.de/fileadmin/Amt80/wirtschaftsfoerderung/pdf/Daten_Fakten_e.pdf

Cleland, S. E., Steinhardt, W., Neas, L. M., West, J. J., & Rappold, A. G. (2023). Urban heat island impacts on heat-related cardiovascular morbidity: A time series analysis of older adults in US metropolitan areas. *Environment international, 178*, 108005. https://doi.org/10.1016/j.envint.2023.108005

Climate Policy Initiative. (2011). *Meeting Energy Concept Targets for Residential Retrofits in Germany*. Retrieved from https://www.climatepolicyinitiative.org/wp-content/uploads/2011/12/Costs-Benefits-and-Financial-Support-for-Thermal-Retrofit.pdf

Coates, J., Mar, K. A., Ojha, N., & Butler, T. M. (2016). The influence of temperature on ozone production under varying NO x conditions–a modelling study. *Atmospheric Chemistry and Physics, 16*(18), 11601-11615. https://doi.org/10.5194/acp-16-11601-2016

Copernicus. (2022). Copernicus: Summer 2022 Europe's hottest on record. Copernicus Climate Change Service/ECMWF. https://climate.copernicus.eu/copernicus-summer-2022-europes-hottest-record.

Crank, P. J., Middel, A., Coseo, P., & Sailor, D. J. (2023). Microclimate impacts of neighborhood redesign in a desert community using ENVI-met and MaRTy. *Urban Climate, 52*, 101702. https://doi.org/10.1016/j.uclim.2023.101702

D'Amico, A., Ciulla, G., Panno, D., & Ferrari, S. (2019). Building energy demand assessment through heating degree days: The importance of a climatic dataset. *Applied energy, 242*, 1285-1306. https://doi.org/10.1016/j.apenergy.2019.03.167

Datenblatt zum Wohnungsmarkt. (2022). Statistische InformationenNr. 318. Retrieved from https://www.duesseldorf.de/fileadmin/Amt12/statistik/stadtforschung/download/Datenblatt_Wohnungsmarkt_Duesseldorf_2022_iii.pdf.

Deutscher Wetterdienst (DWD), (2022). Surface synoptic weather map of Europe at 00 UTC on 19 July 2022. Retrieved via Wetterzentrale. Available at: https://www.wetterzentrale.de/reanalysis.php?jaar=2022&maand=7&dag=19&uur=000&var=45&map=1&model=dwd (accessed 1 August 2025).

Deutscher Wetterdienst. (n.d.). Klimadaten Deutschland: Vieljährige Mittelwerte (1991–2020). Climate Data Center (CDC). Retrieved January 8, 2026, from https://www.dwd.de/DE/leistungen/klimadatendeutschland/vielj_mittelwerte.html

Düsseldorf Census. (2020). Landeshauptstadt Düsseldorf. Retrieved from https://opendata.duesseldorf.de/dataset/bev%C3%B6lkerung-auf-ebene-der-baubl%C3%B6cke/.

DWD Climate Data Center CDC. (2019). Historical daily degree days according to VDI 3807 for Germany, Version v19.3. Retrieved from https://data.europa.eu/data/datasets/_mcloudde_historischetglichegradtagenachvdi3807frdeutschland?locale=zh.

Escandón, R., Calama-González, C. M., Alonso, A., Suárez, R., & León-Rodríguez, Á. L. (2023). How Do Different Methods for Generating Future Weather Data Affect Building Performance Simulations? A Comparative Analysis of Southern Europe. *Buildings, 13*(9), 2385. https://doi.org/10.3390/buildings13092385

Esfandi, S., Tayebi, S., Byrne, J., Taminiau, J., Giyahchi, G., & Alavi, S. A. (2024). Smart cities and urban energy planning: an advanced review of promises and challenges. *Smart Cities, 7*(1), 414-444. https://doi.org/10.3390/smartcities7010016

European Commission. (2020). *Energy statistics - cooling and heating degree days.* Retrieved from https://ec.europa.eu/eurostat/cache/metadata/en/nrg_chdd_esms.htm.

European Commission. (2021). *Proposal for a Directive of the European Parliament and of the Council on the energy performance of buildings.* Retrieved from https://eur-lex.europa.eu/resource.html?uri=cellar:c51fe6d1-5da2-11ec-9c6c-01aa75ed71a1.0001.02/DOC_1&format=PDF

European Parliament and Council. (2024). *Directive (EU) 2024/1275 of the European Parliament and of the Council of 24 April 2024 on the energy performance of buildings (recast). Official Journal of the European Union,* L Series, 2024/1275. http://data.europa.eu/eli/dir/2024/1275/oj

Eurostat. (2021a). *Energy use by businesses and households - statistics.* Retrieved from https://ec.europa.eu/eurostat/statistics-

explained/index.php?title=Energy_use_by_businesses_and_households_-_statistics/.
Eurostat. (2021b). *Energy consumption in households - Statistics Explained.* Retrieved from https://ec.europa.eu/eurostat/statistics-explained/index.php?title=Energy_consumption_in_households/.
Evins, R., Dorer, V., & Carmeliet, J. (2014). Simulating external longwave radiation exchange for buildings. *Energy and Buildings, 75*, 472-482. https://doi.org/10.1016/j.enbuild.2014.02.030
Excell, L. E., Nutkiewicz, A., & Jain, R. K. (2024). Multi-scale retrofit pathways for improving building performance and energy equity across cities: A UBEM framework. *Energy and Buildings, 324*, 114931. https://doi.org/10.1016/j.enbuild.2024.114931
Fallside, D. C., & Walmsley, P. (2004). *XML schema part 0: primer* (2nd ed.). *W3C recommendation.* Retrieved from http://www.w3.org/TR/xmlschema-0/.
Ferrando, M., Causone, F., Hong, T., & Chen, Y. (2020). Urban building energy modelling (UBEM) tools: A state-of-the-art review of bottom-up physics-based approaches. *Sustainable Cities and Society, 62*, 102408. https://doi.org/10.1016/j.scs.2020.102408
Fetting, C. (2020). The European green deal. *ESDN report, 2*(9), 53.
Federal Ministry for Economic Affairs and Climate Action. (n.d.). *Enhancing energy efficiency in buildings*. https://www.bundeswirtschaftsministerium.de/Redaktion/EN/Dossier/enhancing-energy-efficiency-in-buildings.html
Field, A. (2013). *Discovering statistics using IBM SPSS statistics* (4th ed.). Sage Publications.
Galvin, R. (2023). Policy pressure to retrofit Germany's residential buildings to higher energy efficiency standards: a cost-effective way to reduce CO2 emissions? *Building and environment, 237*, 110316. http://dx.doi.org/10.2139/ssrn.4334302
Galvin, R. (2024). Deep energy efficiency renovation of Germany’s residential buildings: is this as economically viable as Germany’s policymakers and popular promoters often claim? *Energy Efficiency, 17*(5), 47. https://doi.org/10.1007/s12053-024-10227-8
García García, C., Salmerón Gómez, R., & García Pérez, J. (2022). A review of ridge parameter selection: minimization of the mean squared error vs. *mitigation of multicollinearity. Communications in Statistics - Simulation and Computation, 53*(8), 3686–3698. https://doi.org/10.1080/03610918.2022.2110594
Garten, Friedhofs- und Fortsamt der Stadt Düsseldorf. (2010). *Grünordnungsrahmenplan für den Stadtbezirk 01.* https://www.duesseldorf.de/fileadmin/Amt68/gartenamt/pdf/gruenplanung/Bericht_01.pdf
Garuma, G. F. (2018). Review of urban surface parameterizations for numerical climate models. *Urban Climate, 24*, 830-851. https://doi.org/10.1016/j.uclim.2017.10.006
Giuzio, G. F., Russo, G., Cipolla, G., Pompei, L., Stasi, R., & Buonomano, A. (2025). User-centric urban energy modelling: A reduced order model approach based on

pre-calibrated archetypes dataset. *Energy and Buildings, 115768*. https://doi.org/10.1016/j.enbuild.2025.115768

Goerzen, A., Asmussen, C. G., & Nielsen, B. B. (2024). Global cities, the liability of foreignness, and theory on place and space in international business. *Journal of International Business Studies, 55*(1), 10-27. https://doi.org/10.1057/s41267-023-00672-5

Gröger, G., & Plümer, L. (2012). CityGML–Interoperable semantic 3D city models. *ISPRS Journal of Photogrammetry and Remote Sensing, 71*, 12-33. https://doi.org/10.1016/j.isprsjprs.2012.04.004

Guo, H., Aviv, D., Loyola, M., Teitelbaum, E., Houchois, N., & Meggers, F. (2020). On the understanding of the mean radiant temperature within both the indoor and outdoor environment, a critical review. *Renewable and Sustainable Energy Reviews*, *117*, 109207. https://doi.org/10.1016/j.rser.2019.06.014

Haneef, F., Pernigotto, G., Gasparella, A., & Kämpf, J. H. (2021). Application of urban scale energy modelling and multi-objective optimization techniques for building energy renovation at district scale. *Sustainability, 13*(20), 11554. https://doi.org/10.3390/su132011554

Hashemi, F., Mills, G., Poerschke, U., Iulo, L. D., Pavlak, G., & Kalisperis, L. (2024). A Novel Parametric Workflow for Simulating Urban Heat Island Effects on Residential Building Energy Use: Coupling Local Climate Zones with the Urban Weather Generator A Case Study of Seven US Cities. *Sustainable Cities and Society, 105568*. https://doi.org/10.1016/j.scs.2024.105568

He, B. J., Miao, C., Cheshmehzangi, A., & Mohaghegh, L. (2025). Advancement in urban climate change assessment and mitigation technologies. *International Journal of Environmental Science and Technology, 22*(12), 10979-10990. https://doi.org/10.1007/s13762-025-06679-9

Heracleous, C., Michael, A., Savvides, A., & Hayles, C. (2022). A methodology to assess energy-demand savings and cost-effectiveness of adaptation measures in educational buildings in the warm Mediterranean region. *Energy Reports, 8*, 5472-5486. https://doi.org/10.1016/j.egyr.2022.03.140

Hofmeister, B. (2003). The study of urban form in Germany. *Urban Morphology, 8*(1), 3–12. https://doi.org/10.51347/jum.v8i1.3908

Hui, Y., Tang, Y., Yang, Q., & Mochida, A. (2024). Numerical study on influence of surface vegetation on aerodynamics of high-rise buildings. *Sustainable Cities and Society, 107*, 105407. https://doi.org/10.1016/j.scs.2024.105407

Ibebuchi, C. C., & Abu, I. O. (2023). Characterization of temperature regimes in Western Europe, as regards the summer 2022 Western European heat wave. *Climate Dynamics, 61*(7), 3707-3720. https://doi.org/10.1007/s00382-023-06760-4

International Energy Agency. (2024). *Empowering Urban Energy Transitions.* https://www.iea.org/reports/empowering-urban-energy-transitions

Jackson, L. E. (2003). The relationship of urban design to human health and condition. *Landscape and urban planning, 64*(4), 191-200. https://doi.org/10.1016/S0169-2046(02)00230-X

Jareemit, D., Srivanit, M., Tanapan, S., & Limeechokchai, B. (2025). Role of urban morphology integrated building envelope materials in achieving zero emissions:

A simulation-based study in complex-shaped urban blocks. *Energy Reports, 13*, 27-39. https://doi.org/10.1016/j.egyr.2024.11.088

Jendritzky, G., De Dear, R., & Havenith, G. (2012). UTCI—why another thermal index?. *International journal of biometeorology*, *56*(3), 421-428. https://doi.org/10.1007/s00484-011-0513-7

Jiang, R., Dong, Y., Bai, L., Dong, W., & Qu, A. (2025). Predicting urban residents' climate change risk perceptions: The role of heat and green space exposure indicators in Harbin's residential environment. *Sustainable Cities and Society, 106882*. https://doi.org/10.1016/j.scs.2025.106882

Kämpf, J., Coccolo, S., Mauree, D., & Scartezzini, J. L. (2020). An integrated microclimate-energy demand simulation method for the assessment of urban districts. *Frontiers in Built Environment, 6*, 553946. https://doi.org/10.3389/fbuil.2020.553946

Kavgic, M., Mavrogianni, A., Mumovic, D., Summerfield, A., Stevanovic, Z., & Djurovic-Petrovic, M. (2010). A review of bottom-up building stock models for energy consumption in the residential sector. *Building and environment, 45*(7), 1683-1697. https://doi.org/10.1016/j.buildenv.2010.01.021

Kong, D., Cheshmehzangi, A., Zhang, Z., Ardakani, S. P., & Gu, T. (2023). Urban building energy modelling (UBEM): a systematic review of challenges and opportunities. *Energy Efficiency, 16*(6), 69. https://doi.org/10.1007/s12053-023-10147-z

Kornhuber, K., Coumou, D., Vogel, E., Lesk, C., Donges, J. F., Lehmann, J., & Horton, R. M. (2020). Amplified Rossby waves enhance risk of concurrent heatwaves in major breadbasket regions. *Nature Climate Change*, *10*(1), 48-53. https://doi.org/10.1038/s41558-019-0637-z

Kraemer, R., & Kabisch, N. (2022). Parks under stress: air temperature regulation of urban green spaces under conditions of drought and summer heat. *Frontiers in Environmental Science, 10*, 849965. https://doi.org/10.3389/fenvs.2022.849965

Landeshauptstadt Düsseldorf, Stadtplanungsamt. (2011*). Innenhofatlas Düsseldorf: Ein neues Instrument für die Stadtentwicklung. Zentral- und Landesbibliothek Berlin.* https://nbn-resolving.de/urn:nbn:de:kobv:109-opus-186300.

Landeshauptstadt Düsseldorf, Umweltamt (2022): *Baumkataster der Stadt Düsseldorf.* https://fragdenstaat.de/anfrage/baumkataster-der-stadt-dusseldorf/693246/anhang/LHD_Baumkataster_20220428_Ausgang.xlsx, 29.11.2023

Landeshauptstadt Düsseldorf. (2022). *Begründung zur Satzung zur Erhaltung baulicher Anlagen und der Eigenart von Gebieten (Erhaltungssatzung) gemäß § 172 Abs. 1 Nr. 1 BauGB Gerresheim - Dreifaltigkeitsstraße.* https://www.duesseldorf.de/fileadmin/Amt30/stadtrecht/pdf/61_119_Begruendung.pdf

Landeshauptstadt Düsseldorf. (2023). *Raumwerk D – Das städtebauliche Entwicklungskonzept für Düsseldorf.* https://www.duesseldorf.de/fileadmin/Amt61/Planung/03_Bilder_und_Plaene/Raumwerk_D/Die_sechs_Elemente/00_Raumwerk_D_barrierefrei.pdf

Levene, H. (1960). Robust tests for equality of variances. In I. Olkin (Ed.), *Contributions to Probability and Statistics: Essays in Honor of Harold Hotelling* (pp. 278–292). Stanford University Press.

Li, X., Ying, Y., Xu, X., Wang, Y., Hussain, S. A., Hong, T., & Wang, W. (2020). Identifying key determinants for building energy analysis from urban building datasets. *Building and Environment, 181*, 107114. https://doi.org/10.1016/j.buildenv.2020.107114

Lindberg, F., Holmer, B., & Thorsson, S. (2008). SOLWEIG 1.0–Modelling spatial variations of 3D radiant fluxes and mean radiant temperature in complex urban settings. *International journal of biometeorology*, *52*(7), 697-713. https://doi.org/10.1007/s00484-008-0162-7

Loga, T., Diefenbach, N., Stein, B., & Born, R. (2012). *TABULA - Scientific Report Germany: Further Development of the National Residential Building Typology*. Institut Wohnen und Umwelt. https://doi.org/10.13140/RG.2.2.16035.17445

Loga, T., Stein, B., & Diefenbach, N. (2016). TABULA building typologies in 20 European countries—Making energy-related features of residential building stocks comparable. *Energy and Buildings, 132*, 4-12. https://doi.org/10.1016/j.enbuild.2016.06.094

Ma, K., Yu, Y., Yang, B., & Yang, J. (2019). Demand-side energy management considering price oscillations for residential building heating and ventilation systems. *IEEE Transactions on Industrial Informatics, 15*(8), 4742-4752. https://doi.org/10.1109/TII.2019.2901306

Martinez, S., Machard, A., Pellegrino, A., Touili, K., Servant, L., & Bozonnet, E. (2021). A practical approach to the evaluation of local urban overheating–A coastal city case-study. *Energy and Buildings, 253*, 111522. https://doi.org/10.1016/j.enbuild.2021.111522

Masson, V., Lemonsu, A., Hidalgo, J., & Voogt, J. (2020). Urban climates and climate change. *Annual Review of Environment and Resources, 45*(1), 411-444. https://doi.org/10.1146/annurev-environ-012320-083623

Mata, E., Kalagasidis, A. S., & Johnsson, F. (2018). Contributions of building retrofitting in five member states to EU targets for energy savings. *Renewable and Sustainable Energy Reviews, 93*, 759-774. https://doi.org/10.1016/j.rser.2018.05.014

McDonald, G. C. (2009). Ridge regression. *Wiley Interdisciplinary Reviews: Computational Statistics, 1*(1), 93-100. https://doi.org/10.1002/wics.14

Miao, C., He, X., Gao, Z., Chen, W., & He, B. J. (2023). Assessing the vertical synergies between outdoor thermal comfort and air quality in an urban street canyon based on field measurements. *Building and Environment, 227*, 109810. https://doi.org/10.1016/j.buildenv.2022.109810

Miller, C., Thomas, D., Kämpf, J., & Schlueter, A. (2018). Urban and building multiscale co-simulation: case study implementations on two university campuses. *Journal of Building Performance Simulation, 11*(3), 309-321. https://doi.org/10.1080/19401493.2017.1354070

Minister für Umwelt, Raumordnung und Landwirtschaft des Landes Nordrhein-Westfalen. (1989). *Klimaatlas – NRW*.

Mohajerani, A., Bakaric, J., & Jeffrey-Bailey, T. (2017). The urban heat island effect, its causes, and mitigation, with reference to the thermal properties of asphalt concrete. *Journal of environmental management, 197*, 522-538. https://doi.org/10.1016/j.jenvman.2017.03.095

Mondal, N., Anand, P., Khan, A., Deb, C., Cheong, D., Sekhar, C., ... & Santamouris, M. (2024). Systematic review of the efficacy of data-driven urban building energy models during extreme heat in cities: Current trends and future outlook. *Building simulation.17, 695*–722. https://doi.org/10.1007/s12273-024-1112-y

Mutani, G., Coccolo, S., Jérôme, K., & Bilardo, M. (2018). *CitySim Guide: Urban Energy Modelling.*

Najafian, P., Hashemi, F., Khayatian, F., Van Tran, Q., Ochoa, E. L., & Mehta, S. (2026). The ENVI-met model for evaluating urban heat mitigation strategies in vulnerable neighborhoods: A case study of San Antonio's Historic Westside. *Urban Climate*, *67*, 102893. https://doi.org/10.1016/j.uclim.2026.102893

National Oceanic and Atmospheric Administration. (2023). *Düsseldorf climate normals (1991–2020).* Retrieved September 16, 2023, from https://www.nodc.noaa.gov/archive/arc0216/0253808/1.1/data/0-data/Region-6-WMO-Normals-9120/Germany/CSV/Duesseldorf_10400.csv

Noardo, F., Arroyo Ohori, K., Biljecki, F., Ellul, C., Harrie, L., Krijnen, T., ... & Stoter, J. (2021). Reference study of CityGML software support: The GeoBIM benchmark 2019—Part II. *Transactions in GIS, 25*(2), 842-868. https://doi.org/10.1111/tgis.12710

North Rhine-Westphalia Information and Technical Department. (2022). *OpenGeodata in NRW*. Retrieved from https://www.opengeodata.nrw.de/produkte/.

Oke, T. R., Mills, G., Christen, A., & Voogt, J. A. (2017). *Urban climates*. Cambridge university press.

Park, S., Shim, J., & Song, D. (2021). Issues in calculation of balance-point temperatures for heating degree-days for the development of building-energy policy. *Renewable and Sustainable Energy Reviews, 135*, 110211. https://doi.org/10.1016/j.rser.2020.110211

Peel, M. C., Finlayson, B. L., & McMahon, T. A. (2007). Updated world map of the Köppen-Geiger climate classification. *Hydrology and earth system sciences, 11*(5), 1633-1644. https://doi.org/10.5194/hess-11-1633-2007

Perini, K., Chokhachian, A., Dong, S., & Auer, T. (2017). Modelling and simulating urban outdoor comfort: Coupling ENVI-Met and TRNSYS by grasshopper. *Energy and Buildings, 152*, 373-384. https://doi.org/10.1016/j.enbuild.2017.07.061

Porritt, S. M., Cropper, P. C., Shao, L., & Goodier, C. I. (2012). Ranking of interventions to reduce dwelling overheating during heat waves. *Energy and buildings*, *55*, 16-27. https://10.1016/j.enbuild.2012.01.043

Piomelli, U. (1999). Large-eddy simulation: achievements and challenges. *Progress in aerospace sciences*, *35*(4), 335-362. https://doi.org/10.1016/S0376-0421(98)00014-1

Reinhart, C. F., & Davila, C. C. (2016). Urban building energy modelling–A review of a nascent field. *Building and Environment, 97*, 196-202. https://doi.org/10.1016/j.buildenv.2015.12.001

Reinhart, C (2023). Linking energy use to local climate. *Nature Energy, 8*(12), 1311-1312. https://doi.org/10.1038/s41560-023-01407-4

Remmen, P., Lauster, M., Mans, M., Fuchs, M., Osterhage, T., & Müller, D. (2018). TEASER: an open tool for urban energy modelling of building stocks. *Journal of Building Performance Simulation, 11*(1), 84-98. https://doi.org/10.1080/19401493.2017.1283539

Remund, J., Müller, S., Schmutz, M., & Graf, P. (2020). *Meteonorm version 8. METEOTEST*. http://www.meteotest.com

Robinson D., Haldi F. (2009). CitySim: Comprehensive micro-simulation of resource flows for sustainable urban planning. In *Proceedings of the 11th International IBPSA Conference* (pp. 1083–1090).

Stewart, I.D.; Mills, G. (2021). *The urban heat island: A guidebook*. Elsevier. https://doi.org/10.1016/C2017-0-02872-0

Sadineni, S. B., Madala, S., & Boehm, R. F (2011). Passive building energy savings: A review of building envelope components. *Renewable and sustainable energy reviews, 15*(8), 3617-3631. https://doi.org/10.1016/j.rser.2011.07.014

Salamanca, F. and Martilli, A. (2010). A new building energy model coupled with an urban canopy parameterization for urban climate simulations—part ii. validation with one dimension off-line simulations. *Theoretical and Applied Climatology, 99*:345–356. https://doi.org/10.1007/s00704-009-0143-8

Salamanca, F., Krpo, A., Martilli, A., and Clappier, A. (2010). A new building energy model coupled with an urban canopy parameterization for urban climate simulations— part i. formulation, verification, and sensitivity analysis of the model. *Theoretical and applied climatology, 99*:331–344. https://doi.org/10.1007/s00704-009-0142-9

Santamouris, M., & Kolokotsa, D (2013). Passive cooling dissipation techniques for buildings and other structures: The state of the art. *Energy and Buildings, 57*, 74-94. https://doi.org/10.1016/j.enbuild.2012.11.002

Santamouris, M., & Kolokotsa, D (2016). *Urban climate mitigation techniques.* Routledge. https://doi.org/10.4324/9781315765839

Santamouris, M. (2020). Recent progress on urban overheating and heat island research. Integrated assessment of the energy, environmental, vulnerability and health impact. *Synergies with the global climate change. Energy and Buildings, 207*, 109482. https://doi.org/10.1016/j.enbuild.2019.109482

Santamouris, M (2023). Urban climate change: Reasons, magnitude, impact, and mitigation. *Urban Climate Change and Heat Islands* (pp. 1-27). https://doi.org/10.1016/B978-0-12-818977-1.00002-8

Sezer, N., Yoonus, H., Zhan, D., Wang, L. L., Hassan, I. G., & Rahman, M. A (2023). Urban microclimate and building energy models: A review of the latest progress in coupling strategies. *Renewable and Sustainable Energy Reviews, 184*, 113577. https://doi.org/10.1016/j.rser.2023.113577

Shahmohamadi, P., Che-Ani, A. I., Etessam, I., Maulud, K. N. A., & Tawil, N. M. (2011). Healthy environment: the need to mitigate urban heat island effects on human

health. *Procedia Engineering, 20*, 61-70. https://doi.org/10.1016/j.proeng.2011.11.139

Shang, W., Liu, J., Meng, H., Jia, L., & Dai, X. (2025). A RL-based human behavior oriented optimal ventilation strategy for better energy efficiency and indoor air quality. *Energy and Buildings, 116072*. https://doi.org/10.1016/j.enbuild.2025.116072

Shapiro, S. S., & Wilk, M. B. (1965). An analysis of variance test for normality (complete samples). *Biometrika, 52*(3/4), 591–611. https://doi.org/10.2307/2333709

Sherif, T., Nguyen, M., Ma, N., & Rakha, T (2025). Localizing urban building energy modelling (UBEM) through inclusive microclimate and socioeconomic data. *Applied Energy, 383*, 125342. https://doi.org/10.1016/j.apenergy.2025.125342

Schöneberger, P., Sinsel, T., Ouyang, W., Zheng, T. T., Bruse, M., & Simon, H. (2025). Enhancing urban microclimate simulations: Validating ENVI-met's accuracy in modeling multi-directional radiative fluxes and mean radiant temperature in subtropical hong kong. *Building and Environment*, 113475. https://doi.org/10.1016/j.buildenv.2025.113475

Silva, T., Matias, M., Girotti, C., Vasconcelos, J., & Lopes, A. (2025). Heat stress mitigation by exploring UTCI hotspots and enhancing thermal comfort through street trees. *Theoretical and Applied Climatology, 156*(3), 162. https://doi.org/10.1007/s00704-025-05400-7

Singh, N., Singh, S., & Mall, R. K. (2020). Urban ecology and human health: implications of urban heat island, air pollution and climate change nexus. *Urban ecology* (pp. 317-334). https://doi.org/10.1016/B978-0-12-820730-7.00017-3

Song, B., Kim, S. H., Park, G., & Park, K. (2024). Comparison of urban physical environments and thermal properties extracted from unmanned aerial vehicle images and ENVI-met model simulations. *Building and Environment, 261*, 111705. https://doi.org/10.1016/j.buildenv.2024.111705

Spinoni, J., Vogt, J. V., Barbosa, P., Dosio, A., McCormick, N., Bigano, A., & Füssel, H. M. (2018). Changes of heating and cooling degree-days in Europe from 1981 to 2100. *International Journal of Climatology, 38*, e191-e208. https://doi.org/10.1002/joc.5362

Stadt Düsseldorf. (2022). *Weather stations of the state capital Düsseldorf. Open Data Düsseldorf.* https://opendata.duesseldorf.de/dataset/wetterstationen-der-landeshauptstadt-d%C3%BCsseldorf

Sufyanullah, K., Ahmad, K. A., & Ali, M. A. S. (2022). Does emission of carbon dioxide is impacted by urbanization? An empirical study of urbanization, energy consumption, economic growth and carbon emissions-Using ARDL bound testing approach. *Energy Policy, 164*, 112908. https://doi.org/10.1016/j.enpol.2022.112908

Swan, L. G., & Ugursal, V. I (2009). Modelling of end-use energy consumption in the residential sector: A review of modelling techniques. *Renewable and sustainable energy reviews, 13*(8), 1819-1835. https://doi.org/10.1016/j.rser.2008.09.033

Tabula WebTool. (2023). *Tabula WebTool*. Retrieved from https://webtool.building-typology.eu/.

Tarasova, M. A., Varentsov, M. I., & Stepanenko, V. M (2023). Parameterization of the interaction between the atmosphere and the urban surface: Current state and prospects. *Atmospheric and Oceanic Physics, 59*(2), 111-130. https://doi.org/10.1134/S0001433823020068

Teso, L., Carnieletto, L., Sun, K., Zhang, W., Gasparella, A., Romagnoni, P., ... & Hong, T (2022). Large scale energy analysis and renovation strategies for social housing in the historic city of Venice. *Sustainable Energy Technologies and Assessments, 52*, 102041. https://doi.org/10.1016/j.seta.2022.102041

The European Parliament and the Council of the European Union. (2010). *Directive 2010/31/EU of the European Parliament and of the Council of 19 May 2010 on the energy performance of buildings. Official Journal of the European Union, 53*, 13–35. Available at: http://eur-lex.europa.eu/LexUriServ/LexUriServ.do?uri=OJ:L:2010:153:0013:0035:EN:PDF

The German Federal Government. (2020). *Effectively reducing CO2 emissions.* Retrieved from https://ec.europa.eu/eurostat/cache/metadata/en/nrg_chdd_esms.htm.

Thebault, M., Govehovitch, B., Bouty, K., Caliot, C., Compagnon, R., Desthieux, G., ... & Petersen, A. J (2021). A comparative study of simulation tools to model the solar irradiation on building façades. In *ISES solar world congress 2021*. International Solar Energy Society. https://hal.science/hal-04234820

Ullah, K. R., Prodanovic, V., Pignatta, G., Deletic, A., & Santamouris, M (2024). Assessing the impact of heat mitigation measures on thermal performance and energy demand at the community level: A pathway toward designing net-zero energy communities. *Building Simulation, 17*, 1379–1400. https://doi.org/10.1007/s12273-024-1140-7

Vahid-Ghavidel, M., Jafari, M., Letellier-Duchesne, S., Berzolla, Z., Reinhart, C., & Botterud, A (2024). Integrated energy demand-supply modelling for low-carbon neighborhood planning. *Applied Energy, 358*, 122560. https://doi.org/10.1016/j.apenergy.2023.122560

Vahmani, P., Luo, X., Jones, A., & Hong, T (2022). Anthropogenic heating of the urban environment: An investigation of feedback dynamics between urban micro-climate and decomposed anthropogenic heating from buildings. *Building and Environment, 213*, 108841. https://doi.org/10.1016/j.buildenv.2022.108841

Veal, A. J. (2021). Climate change 2021: the physical science basis, 6th report. *World Leisure Journal, 63*(4), 443-444. https://doi.org/10.1080/16078055.2021.2008646

Vellei, M., Ramallo-González, A. P., Coley, D., Lee, J., Gabe-Thomas, E., Lovett, T., & Natarajan, S. (2017). Overheating in vulnerable and non-vulnerable households. Building Research & Information, 45(1-2), 102-118. https://doi.org/10.1080/09613218.2016.1222190

Vermeulen, T., Kämpf, J. H., & Beckers, B (2013). Urban form optimization for the energy performance of buildings using Citysim. *Proceedings of CISBAT 2013 cleantech for smart cities and buildings, 915*-920. https://infoscience.epfl.ch/handle/20.500.14299/99461

Verordnung über einen energiesparenden Wärmeschutz bei Gebäuden (Erste Verordnung zur Durchführung des Gesetzes zur Einsparung von Energie in Gebäuden) vom 11. August (1977). *Bundesgesetzblatt I*, 1554–1564.

Voigt, P., & von dem Bussche, A. (2017). *The EU general data protection regulation (GDPR): A practical guide.* Springer. https://doi.org/10.1007/978-3-319-57959-7

Walter, E., & Kämpf, J. H. (2015). A verification of CitySim results using the BESTEST and monitored consumption values. In *Proceedings of the 2nd Building Simulation Applications conference* (pp. 215-222). Bozen-Bolzano University Press. https://doi.org/10.5281/zenodo.3463414

Wang, W., Li, S., Guo, S., Ma, M., Feng, S., & Bao, L (2021). Benchmarking urban local weather with long-term monitoring compared with weather datasets from climate station and EnergyPlus weather (EPW) data. *Energy Reports, 7*, 6501-6514. https://doi.org/10.1016/j.egyr.2021.09.108

Wang, K., Aktas, Y. D., Malki-Epshtein, L., Wu, D., & Abdullah, M. F. A. B (2022). Mapping the city scale anthropogenic heat emissions from buildings in Kuala Lumpur through a top-down and a bottom-up approach. *Sustainable Cities and Society, 76*, 103443. https://doi.org/10.1016/j.scs.2021.103443

Wang, X., Li, H., & Sodoudi, S. (2022). The effectiveness of cool and green roofs in mitigating urban heat island and improving human thermal comfort. *Building and Environment, 217*, 109082. https://doi.org/10.1016/j.buildenv.2022.109082

Wang, J., Gao, F., Zhou, Y., Guo, Q., Tan, C. W., Song, J., & Wang, Y. (2023). Data sharing in energy systems. *Advances in Applied Energy, 10*, 100132. https://doi.org/10.1016/j.adapen.2023.100132

Wang, R., Cai, M., Shi, Y., & Ren, C (2024). Integration of LCZ to planning strategies. In C. Ren & Y. Shi (Eds.), *Local climate zone application in sustainable urban development: Experience from East and Southeast Asian high-density cities* (pp. 229–241). Springer. https://doi.org/10.1007/978-3-031-56168-9_12

Wolf, S., Teitge, J., Mielke, J., Schütze, F., & Jaeger, C (2021). The European Green Deal—more than climate neutrality. *Intereconomics, 56*, 99-107. https://doi.org/10.1007/s10272-021-0963-z

Worthy, A., Ashayeri, M., Marshall, J., & Abbasabadi, N (2025). Bridging the simulation-to-reality gap: A comprehensive review of microclimate integration in urban building energy modelling (UBEM). *Energy and Buildings, 115392*. https://doi.org/10.1016/j.enbuild.2025.115392

Xiong, J., Zhang, Y., Han, M., Wu, J., & Tian, Z. (2023). Building energy-saving mechanism for indoor cooling temperature set-point with different envelope: A case study in Guangzhou. *Journal of Chinese Architecture and Urbanism, 5*(2), 0877. https://doi.org/10.36922/jcau.0877

Xu, Y., Vahmani, P., Jones, A., & Hong, T (2024). Anthropogenic heat from buildings in Los Angeles County: A simulation framework and assessment. *Sustainable Cities and Society, 107*, 105468. https://doi.org/10.1016/j.scs.2024.105468

Yang, L., Qian, F., Song, D. X., & Zheng, K. J. (2016). Research on urban heat-island effect. *Procedia engineering, 169*, 11-18. https://doi.org/10.1016/j.proeng.2016.10.002

Yang, X., Hu, M., Tukker, A., Zhang, C., Huo, T., & Steubing, B (2022). A bottom-up dynamic building stock model for residential energy transition: A case study for the Netherlands. *Applied Energy, 306*, 118060. https://doi.org/10.1016/j.apenergy.2021.118060

Yang, S., Wang, L. L., Stathopoulos, T., & Marey, A. M (2023). Urban microclimate and its impact on built environment–a review. *Building and Environment, 238*, 110334. https://doi.org/10.1016/j.buildenv.2023.110334

Yang, M., Ren, C., Wang, H., Wang, J., Feng, Z., Kumar, P., ... & Cao, S. J (2024). Mitigating urban heat island through neighboring rural land cover. *Nature Cities, 1*-11. https://doi.org/10.1038/s44284-024-00091-z

Yang, Y., Li, X., Yao, Z., Yu, A., & Wang, M. (2025). Impact of Facade Photovoltaic Retrofit on Building Carbon Emissions for Residential *Buildings in Cold Regions. Buildings, 15*(20), 3762. https://doi.org/10.3390/buildings15203762

Yu, Q., Ketzler, G., Mills, G., et al. (2025a). Exploring the integration of urban climate models and urban building energy models through shared databases: a review. *Theoretical and Applied Climatology, 156*, 266. https://doi.org/10.1007/s00704-025-05501-3

Yu, Q., Mills, G., Ketzler, G., & Leuchner, M. (2025b). Developing an urban geographic archetype dataset to support energy retrofit strategy on residential buildings in Düsseldorf, Germany. *Energy Reports, 14*, 282-293. https://doi.org/10.1016/j.egyr.2025.06.004

Yu, Q., Mills, G., Ketzler, G., & Leuchner, M. (2026). Summer thermal consequences of EU retrofit strategies: An integrated microclimate and indoor comfort study in Düsseldorf. Energy and Buildings, 117163. https://doi.org/10.1016/j.enbuild.2026.117163

Zhang, Y., Teoh, B. K., Wu, M., Chen, J., & Zhang, L. (2023). Data-driven estimation of building energy consumption and GHG emissions using explainable artificial intelligence. *Energy, 262*, 125468. https://doi.org/10.1016/j.energy.2022.125468

Zhao, J., Chen, G., Yu, L., Ren, C., Xie, J., Chung, L., ... & Gong, P (2023). Mapping urban morphology changes in the last two decades based on local climate zone scheme: A case study of three major urban agglomerations in China. *Urban Climate, 47*, 101391. https://doi.org/10.1016/j.uclim.2022.101391

Zheng, Y., Ren, C., Shi, Y., Yim, S. H., Lai, D. Y., Xu, Y., ... & Li, W (2023). Mapping the spatial distribution of nocturnal urban heat island based on Local Climate Zone framework. *Building and Environment, 234*, 110197. https://doi.org/10.1016/j.buildenv.2023.110197

Zhong, X., Hu, M., Deetman, S., Steubing, B., Lin, H. X., Hernandez, G. A., ... & Behrens, P. (2021). Global greenhouse gas emissions from residential and commercial building materials and mitigation strategies to 2060. *Nature Communications, 12*(1), 6126. https://doi.org/10.1038/s41467-021-26212-z